Hydrothermally stable heterogeneous catalysts for biorenewable-derived molecule conversions to chemicals

by

Jason Anderson

A dissertation submitted to the graduate faculty

in partial fulfillment of the requirements for the degree of

DOCTOR OF PHILOSOPHY

Major: Chemical Engineering

Program of Study Committee:

Brent H. Shanks, Major Professor

Raj Raman

Andrew Hillier

Jean-Philippe Tessonnier

Klaus Schmidt-Rohr

Iowa State University

Ames, Iowa

2014

To my wife, who was willing to see me through all of this…

TABLE OF CONTENTS

ACKNOWLEDGEMENTS

I am thankful to my professor Brent H. Shanks, whose encouragement, supervision, and support made this thesis possible. His perspective broadened mine and allowed me to mature as a researcher. I would like to thank Klaus Schmidt-Rohr and Robert Johnson for their invaluable collaboration and wonderful ideas that without which would have not have made this work so influential. Haiyang Zhu was influencial in starting my project and his initial guidiance helped propel the research. James Anderegg helped considerably with the XPS data generation and interpretation. Stephen Veysey helped with the training and running the elemental analyzer.

I want to thank Isa Mbaraka for the mentorship when I was at ISU for an REU in 2006. The REU happened because of the encouragement of Todd Menkhaus and the excellent letter of recommendation he sent ahead of me.

I also appreciate the group members that helped refine my thoughts especially Keenan Deutsch, Tianfu Wang. The undergraduate students that helped me in this work also need great thanks from me: Molly Lohry, Cherita Young, Ashley Leitner, Karl Alderks, and Scott Nauert.

Writing and bringing together this thesis has been very difficult. I thank my friends and family, especially my wife for supporting me while I went through this time of my life. This time would have been impossible if I did not have the constant support and encouragement of my God and knowing that it was His desire for my life.

ABSTRACT

The biorenewables filed seeks to emulate the petroleum model for chemical production; from a select few chemicals a plethora of products are produced. This emulation of the modern petroleum refinery-henceforth called the biorefinery-would allow greater penetration of biorenewable feedstocks into the typically petroleum based chemicals industry. Of great important to this idea is the development of catalysts capable of handling the conditions inherent to biorenewable feedstocks. Water presents a significant challenge to today's catalysis. Using biorenewables, especially sugars, forces the processing to be in the condensed phase as they have little to no volatility. Water is the solvent of choice with most bio-based systems. In addition, the reactions desired to create the chemicals (like esterification) will also create water. This work sought to overcome this difficulty by developing new catalysts with a hydrothermally stable scaffold and active group.

From this work the development of the carbon catalyst is shown. First, I investigated of the hydrothermal stability of the current carbon catalysts in literature. Second, some model compound work showed which active site configurations, if possible, would increase the hydrothermal stability of the acid catalyst. The last two are papers developing the first and second generation of hydrothermally stable acid catalysts. This work increases the possibility of chemicals derived from biorenewables.

Hydrothermal stability of carbon based acid catalysts synthesized by sulfonating carbohydrates pyrolyzed at moderate temperatures (300-600°C) has been reported previously. To test the effect of carbon structure on hydrothermal stability, we produced catalysts by dry pyrolysis at 350ºC and 450ºC or by hydrothermal carbonization,

followed by sulfonation with fuming sulfuric acid, as well as by direct sulfonation of glucose. The catalysts were characterized by BET, titration, Raman spectroscopy, TGA, XPS, reaction testing, and ^{13}C solid state NMR. Catalysts were hydrothermally treated and then analyzed for sulfur retention and catalytic activity. The lower temperature carbon catalysts showed the best stability, however all showed significant activity loss. Solid state NMR characterized the structural details to attempt to correlate functional groups to hydrothermal stability of catalyst active sites. Structural models generated from NMR data showed that the most stable catalysts contained a significant fraction of furan rings and hardly any polycondensed aromatic rings.

Development of heterogeneous catalysts for the biorenewables industry requires catalyst materials that are resistant to hydrothermal degradation. Unlike metal oxides and silica, carbon materials are recalcitrant to hydrothermal conditions. However, for solid-acid sulfonated carbon materials, there are conflicting reports on the stability of the sulfonic-acid groups on the aromatic rings for commercial applications. Currently, incomplete understanding remains about the relationship between hydrothermal stability and the immediate electronic hybridization of the carbon atoms adjacent to the sulfonic-acid active group. To test this relation systematically, model compounds containing sulfonic acid groups linked to aromatic, alkane, or cycloalkane carbon atoms were subjected to hydrothermal conditions (100°, 130°, and 160°C DI water up to 24 h). The structural integrity of the compounds was monitored with solution NMR. While the aromatic-sulfonic compounds degrade readily, the changes in the molecules with alkyl sulfonic acid linkages are negligible. Therefore, a hydrothermally stable sulfonic-acid catalyst needs to contain the sulfur attached via alkyl linkers.

We combined research showing typical electrophilic substitution methods for sulfonated carbon catalysts to be inadequate with initial testing of model compounds and a proof of concept of glucose and taurine. This use of the Malliard reaction resulted in a catalyst stable under hydrothermal conditions but initially in colloidal form. Since this is undesireable in industrial processing, we sought to further stabilize the carbon backbone with the addition of more glucose. We found that the ratio of the glucose to the glucose taurine mixture is not as important as the ion used for the precursor. The potassium ion increased the amount of sulfur on the carbon catalyst, thereby increasing the reaction rate on a mass basis. These catalysts suffer from low surface area so we supporting them on SBA-15 and mesoporous carbon nanoparticles. With these two supports, the catalysts showed good activity on a similar sulfur basis.

From previous research the Maillard reaction was successfully used to create hydrothermally stable carbon catalysts through pyrolysis synthesis. The Maillard reaction was used to create a new catalyst through a hydrothermal synthesis. The combination of glucose and taurine in a hydrothermal synthesis creates a solid that retains the sulfur-from the active group-even better than through pyrolysis synthesis. The synthesis temperatures ranged from 200-300ºC and it was found that the most stable catalysts were synthesized at 250ºC. The catalytic activity seemed insensitive to differences in the changes of the glucose to taurine ratio from 1:1 to 2:1 at the 250ºC synthesis. At the 200ºC synthesis temperature, the activity is not stable through the hydrothermal testing and at the 300ºC synthesis temperature; the sulfur retention is not as stable as the catalysts synthesized at 250ºC.

From this work the development of the carbon catalyst is shown. First, the initial work showed the hydrothermal instability of the current carbon catalysts in literature because of their attachment of the sulfonic acid through an aromatic carbon. Second, model compounds showed an active site configuration connecting the sulfonic acid to the backbone through an aliphatic carbon, if possible, would increase the hydrothermal stability of the acid catalyst. The last two are papers developing the first and second generation of hydrothermally stable acid catalysts whereby glucose and taurine are used to make a catalyst through the Millard reaction. This work increases the possibility of chemicals derived from biorenewables.

CHAPTER 1.

INTRODUTION AND LITERATURE REVIEW

1. Sulfuric Acid as an acid catalyst

Sulfuric acid is used as an economic indicator of the United States because it exceeds consumption of 15 million tons per year [1]. Sulfur prices are projected to decrease as oil is developed from increasingly sour sources, consequently low sulfuric acid prices are also expected. However, sulfuric acid increases operation expenses because of it required separation, recycling, and waste treatment [2]. Environmental concerns about sulfuric acid abound because of its toxicity and corrosiveness leading research to focus on heterogeneous replacements [3]. These replacement solid acid catalysts would have wide applicability in the chemical industry that searches for safer means of operation and methods to reduce the use of hazardous chemicals [4]. Several catalysts have been proposed in literature and while researchers are making progress in this area, currently there lacks a heterogeneous acid catalyst that is as active, stable and inexpensive as sulfuric acid.

There are a variety of reactions catalyzed by an acid: esterification/transesterification [5-9], dehydration/hydration [10, 11], hydrolysis [8, 12], etherification [6], alkylation, acylation, condensation, oligomerization, etc. [11]. Acid catalyzed reactions generally go through a carbocation, making them prone to hydride or methyl group rearrangement. The cations are formed by hydrogen ion donation via a Brønsted acid in solution or through electrons

removed via a Lewis acid. In the condensed phase, it is difficult to determine differences in chemistry; therefore, this research seeks to investigate Brønsted chemistry. The characteristic reaction of this work will be esterification, an alcohol and a carboxylic acid combining to an ester and water, because of its sensitivity to both acid sites and strength [13, 14].

2. Heterogeneous acid response

In response to the advantages of a heterogeneous catalyst several types of catalysts supports have been used. The most common ones include: alumina [15, 16]; silica [17]; zeolites, a mixture of silica and alumina to form catalysts with well-defined structures [18-20]; resins [21, 22], carbon based polymer backbones with active sites [1, 23]; and carbon, amorphous or highly structured [24, 25]. The most frequently used in industry, zeolites, are developed around use in the petroleum industry. The petroleum industry does not operate with water in the condensed phase and silica, alumina, zeolites, and resins deactivate/collapse in subcritical water [11, 26, 27]. Carbon, therefore, remains as the support of choice for potential catalysts involving condensed phase water, either as a solvent or a product of a reaction [28].

The hydrothermal stability of a catalysts used for biorenewable conversions will be important [29]. With hydrothermally stable carbon as a support, it can satisfy two Green Chemistry directives: allowing safer solvents versus ones used currently (water versus organics) and allowing use of renewable

feedstocks. In addition, using carbon as the support limits potential deactivation of catalysts for water generating reactions. Since carbons have good water tolerance, modifiable surface functionality, and large surface area [30], it seems to be ideally suited to meet this need for hydrothermally stable catalysts [31, 32]; however, little is known about the extent of hydrothermal stability of various catalysts or what enhances stability.

To become more economically competitive, carbon derived from molecules recently converted from carbon dioxide [33] like glucose becomes more attractive. For biorenewable fuels and chemicals, catalysts need to be developed to make the conversions of lower value chemicals to higher value chemicals (e.g. glucose to ethanol or hydroxymethylfurfural). Using more environmentally conscious biorenewable resources will help combat potentially disastrous effects of our dependence on oil such as global warming.

3. Various Carbons Structures

Carbon can be categorized by how ordered they are: highly ordered carbons, semi-ordered, or amorphous. It is well known that all three of the carbon types are hydrothermally stable. However, each carbon type has advantages and disadvantages. The carbon types and their place in this work are discussed.

Highly ordered carbons are carbon nanotubes, fullerenes, and other similar molecules with extremely high carbon content (>99%) and low trace heteroatoms. The typical highly order carbon is a carbon nanotube with the fullerenes not

typically analyzed for catalytic value. Carbon nanotubes boast medium surface area and good water stability [34]. Since the carbon nanotubes are chemically and thermally stable, most are functionalized via defect formation and subsequent grafting of active groups [35, 36]. In Tessonnier's work [40], protons were extracted from the carbon nanotubes and in Villa's work, nitric acid was used to partially oxidize the nanotubes [35]. Carbon nanotubes are particularly interesting catalysts as it has been found that nanotubes may have a different environment inside the tube versus outside because of the hydrophobicity [37]. However, this can lead to undesired results: in the Villa work [35], the unwashed recycled catalyst had diffusion problems with the triglyceride after conversion and subsequently lost about half of its activity-from diffusion problems with the active sites inside the carbon nanotubes. In the papers reviewed, the attachment schemes mainly focused on electrophilic substitution of desired groups onto the delocalized pi electrons of the carbon nanotubes [38]. Carbon nanotubes have recently been explored for toxicity and data is too recent to conclude much more than carbon nanotubes can pass through human cells and accumulate in the lungs, liver, and bladder [39]. More work will need to be done to conclude whether or not these carbon supports are safe for use over the long term. Because carbon nanotubes are generally the most expensive carbon of the three choices of carbon and extensive work has been done in that area, this research will not focus on that carbon support.

Semi-ordered carbons contain mesopores and because of the macro organization boasts high surface area [11]. A typical synthesis started with a template like SBA-15 [5, 40], CMK [41], or MCM [42] to develop the stacked cylinder design typical of these mesoporous materials. The carbon material is then deposited on the cylinders and depending on the researcher, the template is either left behind or removed. Because silica is the typical template, if it is left behind it is hydrolyzed in hydrothermal conditions. However, even with the removal of the template the resulting catalysts are not expected to be stable under hydrothermal conditions because of the attachment of the sulfur to an aromatic carbon [43]. Since the semi-ordered carbons displayed minimal stability and active sites not expected to remain on the catalysts, they were not further investigated.

Amorphous carbons are the broadest grouping of carbon catalysts. They include activated, pyrolyzed, and hydrothermal carbons. Satterfield [44] describes the process activated carbons are made by first deactivating a carbonaceous material (coal, biomass, petroleum, pitch) by heating in the absence of air. This process creates a porous carbon structure as the volatile components are removed. These pockets of volatiles leave behind micropores with average pore diameter of less than 2 nm [45]. Then the carbon is selectively oxidized with steam or carbon dioxide to introduce oxygen active groups, hydroxyl, ketone, or carboxylic acid groups. Cellulosic structures develop poorly graphitized carbon versus lignin structures. With the difference in starting material, there are slight

variations in surface area but larger differences in mineral content, degree of crystallinity, and surface functionalization. With this variability, the activated carbons are not equal to one another. Commercially available activated carbons: DARCO®, NORIT®, and Vulcan are not sufficiently characterized to readily exploit these differences and this further complicates the issue of using them as supports. In addition, from literature showing functionalized activated carbon, they show low active sites per gram [32, 46] when compared to pyrolyzed carbon.

This research focuses on pyrolyzed and hydrothermally formed carbon because of the advantages this carbon offers over the other carbon types. The highly ordered carbons resembling graphite like carbon nanotubes or extremely heated carbons suffer from low activity [47]. Therefore, significant effort in the literature has focused on these carbons formed at lower temperatures. Studies have looked at a range of pyrolysis temperatures and have found that there is an "optimal" temperature for the carbon catalysts' activity and the site density and these may be characteristics that do not correlate with each other [2, 47, 48]. The ways in which they were synthesized varies as much as their starting materials and hydrothermal stability is minimally covered by any of the researchers. These will be covered in detail after a review of the general carbon chemical transformations during the pyrolysis.

Hydrothermal carbon is another carbon similar to the pyrolyzed carbon that is touted for its simple, cheap, mild, and "green" way of producing carbon supports and catalysts [49]. Studied by several researchers, hydrothermally

formed carbon promises an inexpensive way to create a carbon backbone with some tuneability [1, 50, 51]. A soluble carbon source (like glucose) is placed in a vessel with or without a sulfonating agent and heated under pressure to create an insoluble carbon support and/or catalyst. If not mixed with a sulfonating agent, the carbon is then sulfonated via typical methods: sulfuric acid, sulfur trioxide, or fuming sulfuric acid [1]. These carbons typically have a low to medium surface area with medium to high sulfonic acid sites [50]. According to some researchers, it is uncertain that hydrothermal carbon provides enough functionality to be useful as a catalyst [51]. However, other researchers disagree and their synthesis created an effective carbon catalyst similar to the critic's catalyst [1]. Hydrothermal carbon was investigated in this work because of the potential for differences versus the pyrolyzed carbons in functionality and graphitic nature.

These different types of carbons are part of the complex problem of carbon supports. The previous work in this area diminishes the role that the highly ordered carbons (nanotubes and graphite) and the extreme synthesis conditions of activated carbon play in this work. Therefore, the research presented focused on hydrothermal and pyrolyzed carbons as supports for the hydrothermally stable acid carbon catalyst.

4. History of Carbon Research

Watson's and Crick's assistant Rosalind Franklin studied pyrolyzed carbon extensively during the 1950's. She used X-ray diffraction to see the

differences of the graphitic nature of pyrolyzed carbon [52]. She noted that there are two different methods of graphitization, homogeneous and heterogeneous. The homogeneous graphitization method occurs in localized sections of minimal crosslinking and creates graphitic sheets with decreasing defects as the synthesis temperature increases. The heterogeneous graphitization takes place in localized sections with strong cross-linking and as the synthesis temperatures increases, localized crystals are formed with sections of amorphous carbon in between. This heterogeneous method of graphitization occurs in the non-graphitizing carbons. Carbons are split into hard (non-graphitizing) with mainly heterogeneous graphitization and soft (graphitizing) with mainly homogeneous graphitization, first discovered by Franklin [53]. Franklin also started the arduous process of describing and modeling the pyrolysis process. While a crude first model, it remained the only one for years that attempted to describe the differences in the carbons. This model was verified later with TEM [Figure 1] [54]; however, even now the differences between hard and soft carbons are not yet fully understood.

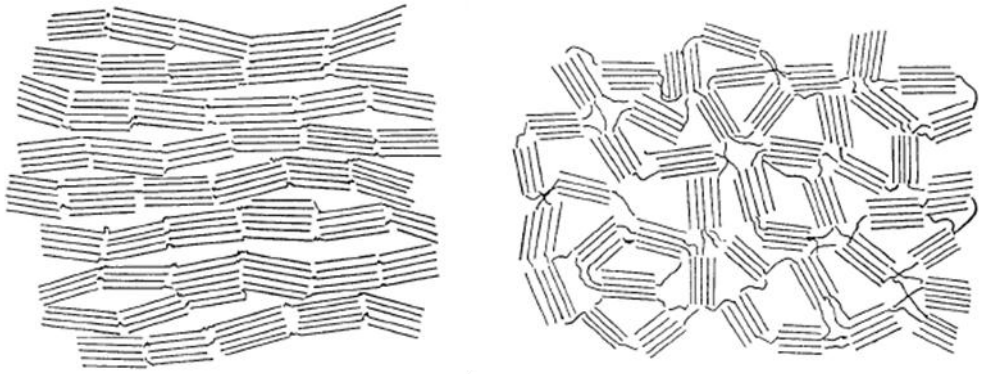

Figure 1. Franklin's first modeling of carbons pyrolyzed at 1200-3000ºC. The carbon on the left is a soft carbon, easily graphitizable whereas the right carbon is a hard carbon with many crosslinks causing it to not graphitize easily [54].

Those previous works were done with carbon at 1200-3000°C and the pyrolyzed carbon in this research mainly focuses on carbon pyrolyzed at much lower temperatures (150-450°C). At these lower temperatures the Broido mechanism is more relevant to the decomposition even though it describes cellulose, not sugar [55]. At lower temperatures cellulose decomposes to mainly char and gases with the loss of water, carbon monoxide, and carbon dioxide to leave behind carbonyl, carboxyl, lactone, and aldehyde groups. The overview of what transpires during the carbonization procedure is carefully recorded an article written by Oberlin, A., et al. [56]. The materials soften, form spheres, and those spheres end up coalescing into a larger structure.

The Boehm titration was developed as a straightforward but powerful way to characterize the carbon [57-60]. It allows the research to differentiate between different acid groups present on the surface. This allows great information to be

gleaned from a titration since these acid groups are thought to have an effect on the overall activity of the carbon catalyst [8, 9]. The Boehm titration is two indirect titrations of solid whereby from subtraction the determinations can be made of the facile titrations. These titrations have been discussed in depth and standardized as to minimize errors in the measurement [61, 62]. In this work, they allowed some conclusions to be drawn about the surface functionalities present on the surface of the carbons that was later verified with elemental analysis and solid-state NMR.

5. Carbon Materials for Catalysis

Carbon materials have been discussed at length in the literature for catalysts and catalyst supports. An excellent example is the review by Rodriguez pulling together no less than 480 references into a cohesive review [63]. Several papers talk about carbon as a catalytic material and have successfully shown these catalysts in action [46, 63-70]. The literature has even developed to the point that a textbook has been written on the subject: Carbon Materials for Catalysis [64]. These resources point to the great interest of the research community in carbon as a material and using it for catalytic applications.

An especially prolific researcher in the current carbon field is Ljubisa, Radovic. He recently won an award with the American Carbon Society (ACS) for his work and contributions to the field. He has at least 100 paper authored on the intricacies of carbon. From adsorption on carbon nanotubes [71, 72] to

simulations of carbon gasification [73-78] to supporting metals on carbon [74, 79-83], Radovic has helped the field progress. As an editor of Chemistry and Physics of Carbon, he sees the forefront in carbon research and well deserves the award from the ACS.

6. Sulfonated Carbon Catalysts

As one type of catalysts, carbons have been sulfonated in literature to create an acidic carbon catalyst. Variously the carbons have been sulfonated with sulfuric acid [84], fuming sulfuric acid [85], sulfur trioxide [86], via several chemical derivatives designed to attach the sulfonic acid group on: sulfanilic attachment [38], hydroxyethylsulfonic acid [1], aromatic sulfonic acids [1, 24, 87], and chlorosulfonic acid [23]. With all the various methods used for sulfonation, it has been chosen to use fuming sulfuric acid in this research as it was shown to have higher sulfur incorporation than sulfuric acid. The working presumption of most researchers in this field is the more sulfur incorporated into the catalyst leads to a better catalyst. Using fuming sulfuric versus regular sulfuric acid increases the amount of sulfur incorporated into the catalyst. Several research groups will be highlighted with their carbon catalyst because they pertain to this research with the hydrothermal stability of sulfonated carbon catalyst.

Similar to the hydrothermal carbon was the directly sulfonated carbon typified by the research of Valiollah Mirkhani, et al. [88]. Their most significant result is their acid site density-7.3 mmol/g, 35% of the way to the 20.4 mmol/g

acid density of sulfuric acid. During synthesis after the filtering the catalysts, it was placed in the oven to dry first at 100°C then the temperature as ramped up to 350°C to remove any trapped sulfuric acid. This heating step must have somewhat carbonized the catalyst depending on how long they left it in the oven.

One carbon worth noting from literature is the Starbon® carbon from the work of James Clark. Beginning with expanded starch, it is claimed that the properties can be tuned to form catalyst supports, and have applications in water purification and separations [45]. The carbons were used to make sulfonated carbon catalysts with low sulfur loadings on them [89]. The catalysts were tested with esterification of various compounds and alcohol acylation with microwave assist. It was claimed that the "hot filtration test" proved that the sulfur species was truly attached on the catalyst and was not leaching off.

The Clark group then turned to a more difficult reaction, preparation of amides [7]. Again, using sulfonated Starbon® material, a wide variety of compounds were synthesized and the Starbon® catalyst was better than the compared sulfuric acid and sulfonated zirconia along with the literature values from amberlyst resins and propylsulfonic supported on SBA-15. This time the catalysts were exposed to 120°-130°C in acetic acid and amine rather than 80°C water in the previous paper. There was no leaching test with this paper but from previous experience they have had with sulfonated Starbon® material, they claimed stability prior to concluding the paper.

Both the previously mentioned Clark papers used a Starbon® material called Starbon®-400, noting that it was carbonized at 400°C, because of its ideal ratio of hydrophobicity to hydrophillicity. The group investigated multiple Starbon® materials using DRIFTS to determine why this material gave them the best properties [26]. They found that there were different temperature carbons that worked best for each of the three reactions they investigated; however, no clear explanation was propsed.

Another difficult transformation of glycerol to various acetylated glycerols was investigated with Starbon® catalysts [7]. The Starbon® catalyst was used to esterify, etherify, and oxidize the glycerol with varying degrees of success. Compared to several catalysts, the Starbon®-400 with sulfonic acid groups performed better than the rest in activity. The stability testing in this article was recycling three times.

Then the Clark group proceeded with using Starbon® catalyst with esterifying succinic acid, an proposed platform chemical [90]. The Starbon®-400, expanded starch pyrolyzed at 400°C and sulfonated in sulfuric acid at 80°C, was again employed. They compared it with sulfonated DARCO® and NORIT® activated carbons and found the Starbon® carbon catalyst to be better at the esterification of succinic acid, their test reaction. When comparing sulfuric acid, they noted that the rate of formation toward the desired diester was slower than with any of the sulfonated carbons. This study was followed with a brief statement about the catalyst being reusable.

From this brief overview, three main conclusions about sulfonated carbons can be seen. First, the description of the fundamental structure of the carbon is grazed over. It is difficult to tease out the entire structure of the carbons used for catalysis because the synthesis of the carbons is typically an uncontrolled thermal reaction. Therefore many functional groups exist on the carbon [1, 30, 47], and typical methods of characterizing catalysts do not significantly not help characterize carbon (BET, XRD, XPS, Raman, etc.). Secondly, the hydrothermal stability of the carbon is rarely measured. Some experiments in literature are similar: recyclability studies [9, 91, 92], boiling in various solvents [48, 93], and leaching tests after the reactions [89]. While these tests may be similar in concept, a thorough study on hydrothermal stability in elevated temperature water for extended periods has not been done. Third, the way the sulfur attaches to the carbon has not been investigated. Combined with the first point, this leads to researchers assuming structures of carbon with large clusters of aromatic sheets [see Figure 2] and assume the sulfonic acid groups attach via electrophilic substitution. If the sulfonic acid attaches directly to the aromatic carbons, then other attachment methods should be considered for comparisons of hydrothermal stability. This work considers all three of these points to increase the fundamental knowledge of carbons catalysts.

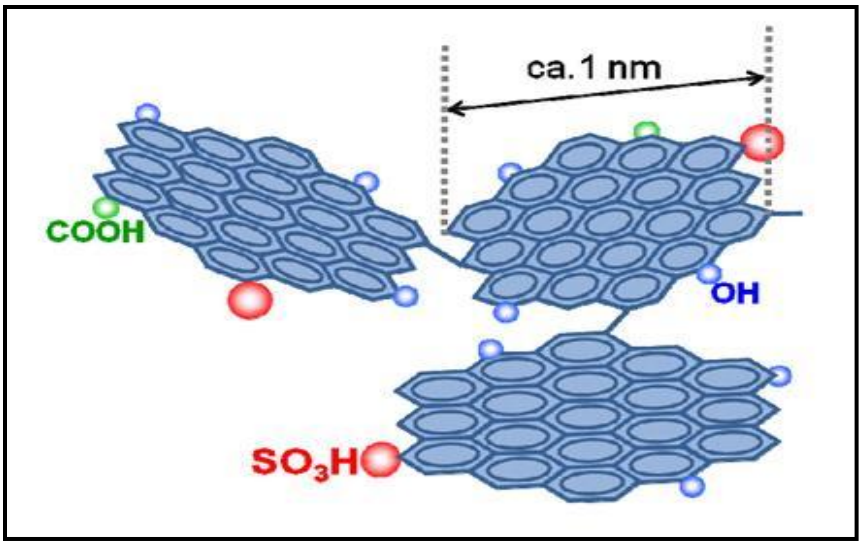

Figure 2. Model of the sulfonated 400ºC pyrolyzed glucose from Hara's work. The size of the aromatic sheets comes from Raman spectroscopy and the functional groups come from titrations and Solid-State NMR [2].

7. Carbon Research from Hara's Work

The most prolific research group in this field is Hara's group in Japan. The have currently published 30 papers about sulfonated carbons as catalysts. A select group of papers from this research is selected for further review because of their relevance to this research. There are a few specific points taken from the papers: general information about the research, starting material for the carbon because that may make a difference in the results, general activity of the catalyst, any characterization technique of note, and any stability testing. Beginning with Hara's work is beneficial because it offers many clues about what makes a hydrothermally stable catalyst, offers an easy and reproducible method for

producing the carbons, and begins to explore the structure [47]. Therefore, this series of papers is explored (in mostly chronological order) more fully than previous ones in effort to understand this touchstone to this work.

Starting in 2004, this group first published about sulfonated carbons [4]. They used naphthalene in sulfuric acid to synthesize their first catalyst. This incorporated high levels of acid density and seemed very promising since it was insoluble in the solvents they tested at room temperature (water, ethanol, methanol, benzene, and hexane). It also showed significant improvement over the other carbons they used: carbonized resin, glassy carbon, activated carbon, and natural graphite. These other forms of carbon all had limited acid density and were inactive in their catalytic testing. Hara explored this distinction between the pyrolyzed carbons and the other forms of carbon in this work.

As a starting point, the characterization techniques used on the catalysts from Hara's group [47] were considered for this research. In their research they used XRD, elemental analysis, titration, TGA, BET, catalytic activity testing with several different reactions, and Solid-State NMR. The XRD data generally showed amorphous carbon with some aromaticity via two broad peaks unless the carbon was supported on mesoporous silica or some other structure with periodicity. Because it provides more information for structured versus amorphous carbon it was not considered an effective technique for this research. Elemental analysis was used to find the bulk compositional analysis of the catalysts. Later papers use this technique to determine the number of sulfonic

acid sites [48]. It has the drawback of being unable to distinguish the surface functionalities and was used in conjunction with titrations to draw out information about the carbon. The overall composition was very useful for carbon modeling as it provided a basis for the ratios of atoms. The titrations in the paper were typical acidity measurements at first and they were used in the current research. Later papers used a more complex method for determining the number of carboxylic acid groups, phenolic hydroxyls, and sulfonic acid sites [8]. The characterization techniques of XRD, elemental analysis, and titration have various applications to this research.

Hara's research group also used TGA, BET, and catalyst reaction testing to characterize the carbon catalysts. The TGA technique is standard for catalysts characterization. It indicates the general stability of the carbon catalysts in the gaseous phase. Since the current research focused on condensed phase reactions, TGA was used to probe the thermal stability of the carbon catalysts. They also did physisorption of N_2 with the BET method to determine surface area. For catalysts, the surface area is important and must be measured. However in condensed phase with the highly mobile proton as the active species and with potential swelling of the catalyst [28], it is unclear how or if the BET surface area correlates to condensed phase conditions. BET analysis was done for this work as a comparison with other catalysts. Hara first used XRD, elemental analysis, titrations, TGA, and BET to characterize their first sulfonated carbons and represent the bulk of techniques used on carbon catalysts. The catalyst reaction

testing was prominent in all catalyst papers and was done in all papers for this work. They chose a variety of reactions to test but typically were dehydrations, esterification, or another acid catalyzed reaction.

Solid-State NMR is a potentially powerful method for carbon characterization but is hindered by resolution at natural ^{13}C abundance. Hara used Solid-State NMR in a cross-polarization mode and therefore was not quantitative since the nuclei far away from hydrogen have a greatly decreased signal versus nuclei closer to hydrogen. Since the MAS-NMR they did was neither quantitative nor enriched in ^{13}C material, it is hard to draw conclusions. Solid-state NMR used in this research utilized enriched ^{13}C precursors to allow for easier quantification by NMR. This quantification extended to advanced spectral editing that allowed for models to be developed.

In the first paper [4], Hara made some speculations about the stability of the catalysts that have guided aspects of this work. He starts with four carbons treated with sulfuric acid: carbonized resin, glassy carbon, activated carbon, and natural graphite. All the carbons had low acid site densities and the sulfonic acid sites leached off during reaction conditions and in water above 45°C. This was in contrast to the naphthalene based catalyst. The reason certain carbons leached their sulfur active groups and other carbons did not was unclear. A clear conclusion why the sulfur leached could not be drawn from the characterization done. In this paper, the first stability clue was speculated; incompletely carbonized material provided the most stable environment of the sulfonic acid

groups. Since the literature combined with the research done by myself in 2006 pointed to this incomplete carbonization as key for carbon catalysts, it was pursued for this research.

In 2008 a Chinese journal published an article of a group using Hara's sulfonated naphthalene as a catalysts for cross-aldol condensation of a wide range of ketones [94]. It does less characterization than the Hara paper: XRD, titration, BET, elemental analysis, and catalytic testing. The catalytic testing used excess of the catalyst, which minimizes the validity of the comments on catalyst stability. Overall, this paper showed the interest the literature had in the carbon catalyst and showed what other reactions it catalyzes.

Next, Hara proceeded to pyrolyzed sugar as the source for carbon [93]. As a brief communication, they describe pyrolysis of glucose or sucrose with subsequent sulfonation for synthesis of their new carbon catalyst. The main reason they diverged from the naphthalene was its tendency to lose activity via leaching when the liquid phase temperature is above 100°C or when surfactants are used. The resulting carbon was more complicated than with the naphthalene precursor since it now contained carboxylic acids and hydroxyl groups in addition to the expected sulfonic acid groups. However, it was more resistant to a wider variety of solvents under boiling conditions (water, methanol, benzene, hexane, N,N-dimethylformamide, and oleic acid). The stability experiment was reuse after decanting. Since the catalyst was in excess compared to the limiting reagent, it was difficult to draw stability conclusions from the catalyst reuse experiment.

After that paper, Hara's group proceeded to synthesize a mesoporous organosilicate catalyst by sulfonating benzene attached to the framework via two different carbons [48]. They mention that incomplete oxidation of the thiol groups could lead to leaching of the sulfonic acid groups. Because of the silicon, they were able to do solid-state NMR to investigate their catalyst more than in their previous papers. However, with the silicon incorporated into the catalyst, the catalyst backbone would dissolve in hydrothermal conditions. Therefore, this paper was helpful in its attachment of the active group to the carbon backbone, but not considered for hydrothermal testing directly.

In regards to sugar catalysts, [91] they introduced the use of X-ray photoelectron spectroscopy (XPS). The XPS investigates the oxidation state of the sulfur in the carbon catalyst. It has limited resolution, so the electronic state of a sulfur bonded to two carbon and two oxygen atoms cannot be distinguished from a sulfur atom that is bonded to one carbon and three oxygen atoms. This was a potential concern in the PNNL paper [86], but the concern for sulfones is refuted by an earlier paper [95]. The catalyst was also characterized by a complicated titration measured with UV diffuse reflectance spectroscopy. From this paper [91], the first use of fuming sulfuric acid by Hara's group is noted for the carbon catalysts. It proves to have a higher sulfur content and catalytic activity than the carbon treated with concentrated sulfuric acid. They claim this was from pushing the equilibrium of the hydrogen attached to the aromatics and sulfuric acid converting to sulfonic acid attached to aromatics and water. The

extra sulfur trioxide consumed converted water produced from the reaction to sulfuric acid and the reaction moved more to the products-sulfonic acid on the carbon catalyst. The acid strength was weaker than the Nafion catalyst they purchased. The offered explanation as to why the carbon catalyst did better than the Nafion was because of the additional acidic groups, COOH and OH, on the catalyst. This paper helped show that the acid strength of the catalyst was not the only reason that pyrolyzed carbon catalysts excel.

The next paper from the Hara groups was a paper exploring the temperature difference of the carbons and their catalytic activities [47]. Starting with glucose, it was carbonized at several different temperatures (300-550°C) and then sulfonated in concentrated sulfuric acid and fuming sulfuric acid. The highest temperature acids were found to be poor catalysts for reasons other than a decreasing amount of the sulfonic acid groups. This confirms the opposite of the previous paper and lent more credit to the other functional groups' importance as part of the catalyst. A main conclusion they had was that there is an optimal temperature for pyrolysis for carbon catalysts from glucose as a starting material. This paper is the first one to mention swelling and start with the argument that the better carbon catalysts swell and provide better access to the sulfonic acid groups than would otherwise be supposed from the BET data. The highest temperature carbon did not swell when immersed in water, methanol, ethanol, and THF and this was claimed to have an adverse effect on its catalytic activity. This paper began the argument for swelling in the pyrolyzed carbon catalysts and introduced

an upper limit on the reasonable temperatures for carbon catalysts pyrolysis temperatures.

Hara's group then introduced a couple of new characterization techniques and a different reaction for catalytic testing than in previous papers [48]. It introduces SEM pictures for the catalysts which give an indication of the size of the particles. The Solid-State NMR analysis was modified with the introduction of phosphorus for analysis of acid strength. Phosphorus' natural isotope is NMR active which allows quantification. The article came to the conclusion that the acid strength of the acid catalyst was similar to sulfuric acid. Also this article mentioned the Raman ratio of the D (defect) band (1350 cm^{-1}) to the G (graphitic) band (1600 cm^{-1}). The ratio varied for them from 0.55 to 0.68 over the temperature range they synthesized the catalysts (300-550°C). The aromatic carbon sheet size is commonly derived from this ratio in literature. Notwithstanding its use in literature, explorations by Schlögl found it to be not as indicative as previously thought in the literature [96]. The two peaks (graphite and defect) are the result of five other peaks from the multiple functionalities on the carbon, rather than a direct measurement of the ratio of sp^2 to sp^3 hybridized carbon atoms. Hara's measured stability was more rigorous than before because of the addition to the typical recycle testing, the catalysts were also exposed to steam at 127-167°C and boiling water for 24 hours each. They claimed complete preservation of the sulfonic acid groups on the catalysts. The data was similar and the catalysts were the exact same as their previous paper the year before [91].

The next paper used cellulose (Avicel) as the starting material for the carbon catalyst and the hydrolysis of cellulose as the catalytic test reaction [12]. It was a slightly higher pyrolysis temperature for the carbon than previous papers (450°C versus 400°C). This was the first paper where they described a procedure to determine the individual functional groups that are on the catalyst. The groups of interest were the carboxylic, hydroxyl, and sulfonic acid groups. The sulfonic acid groups were estimated from the elemental analysis and the carboxylic and sulfonic acid groups' total number was estimated from an acid stating titration where a sodium chloride solution was added to the catalyst and then titrated to an equivalence point. Then all the acid protons were exchanged with sodium from sodium hydroxide and titrated to determine all the functional groups of interest. An additional technique was used in this paper, FTIR, to investigate the stretching of the sulfur double bonded to oxygen. It unfortunately gave confounding results, like Raman spectroscopy, as the specific peak came out as a shoulder rather than a distinct peak. However, since they were able to see the shoulder at all, they claimed that still claim the NMR identifies the sulfonic acid group. Therefore, they claim, this as the reason carbon catalyst have a higher activity for esterification than sulfuric acid under high water concentrations. The stability analysis was extensive; they ran the reaction 25 times before claiming catalyst stability. This paper also introduced the concept of measuring the area of the pyrolyzed carbon catalyst with water vapor to see the increase surface area due to

swelling. This paper expanded on the ways Hara's group characterized their catalysts.

Hara's group proceeded to look at SBA-15 layered with glucose carbonized with sulfuric acid and heat [48]. The silica template was retained to result in a silica supported sulfonated mesoporous carbon. The characterization techniques used were all previously discussed. Since this paper used catalysts supported on retained silica versus removed silica, the expected hydrothermal stability of the catalyst would not be sufficient for this research. However, hydrophobic molecules are not the best type of molecules to use as reactants with the sulfonated carbons, but they may make exceptional products because they would release from the catalyst without proceeding further.

Developing on the carbon catalyst they made with Avicel, Hara's group proceeded to synthesize their own porous carbon from wood powder [2]. After impregnating the wood powder with zinc chloride, it was heated for an hour at various temperatures (250-600°C, 50°C step size). It was then sulfonated with sulfuric acid at 80°C. The characterization techniques were standard except for an additional pore size distribution with mercury (BJH method). This paper does well with showing the differences between the temperatures and the different functional groups on the carbons. As the temperature increased the amount of sulfonic acid groups increased and then decreased after 400°C. The catalytic results also showed significant decrease in reaction rate with the carbons exposed to temperatures higher than 450°C. The zinc chloride was found to be

instrumental in the increase of reaction rate; a sample prepared at 450°C without zinc chloride had poor acid density and reaction rate. This paper confirms the existence of optimal temperature for pyrolysis that has been seen in literature. This paper did not mention about stability of these catalysts. Potentially, the different temperatures the wood powder was exposed would change the stability of the various catalysts. The increase in the surface area with the incorporation of zinc chloride allows the surface area of these pyrolyzed materials to be greatly increased as they generally have low surface area.

The Hara group returned to Avicel because of its interesting properties as a catalyst [8]. From previous papers the optimal temperature for pyrolysis was found and used in this paper (400°C) [2]. They used fuming sulfuric as the sulfonating agent at 120°C. They used characterization results of the catalyst from the previous paper. In this paper, a schematic displaying the carbon in uniform graphene sheets is displayed. It shows only fused benzene rings and connections to the presumed carboxylic, hydroxyl, and sulfonic acid groups decorated along the outside. This highly idealized schematic does not agree with other literature depicting the carbon when it carbonizes [92]. The schematic also does not agree with the elemental analysis which then cast doubt on the accuracy of the depiction. The structure of the carbon has been controversial in literature and several models have been proposed.

In the paper they also made some further speculations on the sulfonated carbon stability in this paper. It was noted that Amberlyst-15 decreased in

activity through their catalyst recycling experiment because of loss of sulfonic acid groups through hydrolysis of the acid group. However, they could not find evidence of the same happening for their carbon catalyst and they surmised it was because of the electron withdrawing groups attached to the carbon that helped maintain the sulfonic acid sites. This seemed to be substantiated by their earlier work with naphthalene that did not contain hydroxyl groups [4, 9]. They go on to claim that since the carbon has these multiple functional groups, it could absorb β-1,4-glucan and enjoyed greater ration rates of hydrolysis of the glycosidic bond than comparable sulfonic acids: Nafion and Amberlyst-15. The stability analysis was reaction testing with five recycles. Since the yield and elemental analysis of the carbon catalyst remained unchanged, stability was claimed. This paper offered more clues on stability and the first chemical drawing of the carbon catalyst.

Hara then worked on biodiesel production with the sulfonated carbon catalysts as the workhorse for the transesterification reaction [9]. It had ~70% of the performance of sulfuric acid. The starting material for the carbon catalyst was Avicel pyrolyzed at 450°C. It was then sulfonated in fuming sulfuric acid at 80°C. The characterization techniques of the catalyst remained the same and the test reactions were esterification of oleic acid and transesterification of triolein. This article included a figure of the catalyst incorporating hydrophilic molecules including water, butanol, and cellohexaose. In the paper, the catalyst structure was proposed as pristine sheets of graphene decorated with functional groups-too

idealistic when compared to other literature and its elemental analysis [96, 97]. Interestingly, the adsorption of the hydrophilic molecules may actually be too strong; Hara noted that the activity never decreased as long as the catalyst was washed with water between recycles. Washing in methanol was noted to be detrimental for some of the activity because of methyl sulfonate formation. It was difficult to draw conclusions from the transesterification reaction data because of the confounding of variables in the testing. Hara tried to draw conclusions about what effect water has on the catalyst and the reaction concentrations were changed dramatically in addition to water addition with no further explanation. The article ends with the comment about the catalyst seeming to be more complicated than initially presumed and the extent that all the functionalities work together to create an effective catalyst is yet undiscovered.

The next paper published detailed cellulose pyrolyzed at 400°C and sulfonated with fuming sulfuric acid [28]. The characterization techniques remained the same with a different test reaction: hydrolysis of cellobiose. They did an absorbance test of the various catalysts used with a solution of cellobiose and found that the carbon catalyst was better than Amberlyst-15 and Nafion, which did not absorb any cellobiose during an exposure for 24 hours. The carbon catalyst absorbed about 7.5 moles of cellobiose per gram of catalyst which amounted for ca. 25% of the total in the solution. In contrast to cellobiose, they found the carbon catalyst does not detectably absorb any glucose. This led to the conclusion of the glycosidic bond participating in the bonding. The stability

testing was four recycles of the catalyst with fresh reactants. This paper explored the capability of the carbon catalyst to hydrolyze cellulose and showed interesting adsorption capabilities of the carbon catalysts.

After considering cellulose Hara turned to starch saccharification [98]. They used a statistical design of experiment to change the temperature, time, water concentration, stirring rate, and starch concentration. They found that the temperature, time, starch concentration, and the two-factor interaction of time and temperature were important factors while the water concentration, stirring rate, and all other two-factor interactions were not. They found that medium temperatures with short residence times retained most of the formed glucose from the starch. There was no stability analysis with this paper as it focused on optimizing the conditions of the starch saccharification. This work showed another catalytic reaction potential for the carbon catalyst.

The latest paper from Hara's group tried a new synthesis method [99]. It creates a carbon aerogel with high specific surface area and then carbonizes it through four different temperatures (300, 400, 500, 700°C). Then the char was sulfonated with fuming sulfuric acid at 80°C. The catalyst was subject to only previously mentioned characterization. The catalyst created at 500°C had the best activity. The catalyst synthesized at the lower temperatures collapsed and had poor activity. The catalyst synthesized above this temperature did not have activity even though it retained the precursor surface area. Phosphorus was used to estimate the available sulfonic acid groups and it was significantly lower than

the total estimated from elemental analysis (0.2 versus 0.9 mmols/g). This paper did not explore stability.

These papers from Hara's group better demonstrated the interest in acid carbon catalysts. Questions still remain about the fundamental chemical structure of the carbon, the hydrothermal stability of the acidic sulfonic acid carbon catalyst, and which attachment schemes for the sulfonic acid group creates the best stability.

The excellent touchstone provided by these papers was expounded upon with the addition of ^{13}C Solid-State NMR, more thorough hydrothermal testing, specific investigation on the active site, and by prescribing a hydrothermally stable synthesis method. Using labeled glucose as a starting point for this research, the general structure of these carbons could be deduced. This allowed for general structure claims to be investigated. The hydrothermal testing was more thoroughly tested with longer times and higher temperature than typically seen in literature. Then using model compounds, the actual carbon-sulfur connections were tested and subsequent attachments methods of the sulfur to the carbon were investigated. With these methods, a final synthesis method was prescribed for a hydrothermally stable carbon catalyst. From previous research efforts by the Hara group, these focus areas were straightforward continuations to help further the field of carbon catalyst research.

8. Stability of the Sulfur on the Carbon

As stated, the stability of the heterogeneous carbon catalyst is paramount. Various methods for discovering the stability of the carbon catalyst have been discussed: recycling, boiling in various solvents, and filtrate testing for leaching. While convenient, they are not industrially relevant for stability analysis. Some of the theories expounded in literature about the deactivation of sulfonated carbon catalysts include leaching and sparing solubility. The deactivation and potential mitigation strategies are discussed below.

The deactivation of the sulfonated acidic carbon catalyst may occur in several ways, but mainly manifests itself as a detectable activity change of the catalyst [5, 100]. Most researchers claim the carbon catalyst deactivates through leaching-hydrolytic removal of the active site [43, 100]; however, little proof is shown for the sulfur leaching, and no mechanism for this removal have been proposed. The desulfonation reaction was well known in the literature in 1970's [21]; however, it is poorly considered in recent research. Aromatic desulfonations are catalyzed by acid [101] and since this research considers condensed phase reactions with acidic catalysts, sulfonated aromatic carbons do not seem to be the most resilient choice versus sulfonated aliphatic carbons. Other papers emphasize that small clusters of aromatic rings are sparingly soluble in water, therefore, could leach into the water even without the carbon-sulfur bond cleaving [43, 100]. Since the proposed structure includes clusters of aromatic carbons, perhaps this is a problem [102, 103]. However, since the starting materials for the carbon

backbone are typically hard carbons unable to form graphite, the polycyclic stability may be less of an issue than the researchers convey. In this work, both active site activity measurements and post hydrothermal testing analysis is done to assess the extent of the hydrolysis of the active site.

As seen in the literature review, there have been several theories about the stability of these acid carbon catalysts put forth in the literature. With Hara's work, they claimed that aromatic bonding of the carbon to sulfur would strengthen the covalent bond [98]; however, with the previous review of desulfonation, it is evident that six carbon aromatic structure cannot be helpful to prevent the acid catalyzed desulfonation reaction. There have also been claims of the additional functional groups like COOH or OH near the sulfur group that would potentially increase the electron withdrawing nature of the bond between the carbon and the sulfur, thus increasing the stability [8]. There also seems to be a synthesis temperature of the carbons that affects its ability as a carbon catalyst that may also have something to do with the stability. However, with an incomplete understanding of the carbon, this is only speculation. With increased characterization, these claims will be systematically tested and investigated.

The carbon catalyst must be stable to be a heterogeneous catalyst. In order to prove that these catalysts are stable, testing was done before and after to investigate any changes during hydrothermal treatment. In addition, different synthesis methods and sulfonation techniques were used to discover differences of

hydrothermal stability. This will allow a better catalyst to be made that will be able to be more hydrothermally stable than current sulfonated carbon catalysts.

9. Conclusion

The papers reviewed have initiated the work of the interesting characteristics of sulfonated carbon catalysts. The hydrothermal stability is better than with typical alumina/silica catalysts. However, the fundamental knowledge of these catalysts and the variables that affect this stability is limited. Since the National Science Foundation engineering research Center for Biorenewable Chemicals (CBiRC) is researching chemical transformations of sugar to chemicals. Reactions with sugar require condensed phase processing and CBiRC has identified hydrothermal stability as a barrier to overcome. With better knowledge of the fundamentals of sulfonated carbon catalysts, the transformations CBiRC wants with sugars transformed to biorenewable chemicals are possible.

References

1. Liang, X. and J. Yang, *Synthesis of a Novel Carbon Based Strong Acid Catalyst Through Hydrothermal Carbonization.* Catal. Lett., 2009. **132**(3-4): p. 460-463.
2. Kitano, M., et al., *Preparation of a Sulfonated Porous Carbon Catalyst with High Specific Surface Area.* Catal. Lett., 2009. **131**(1-2): p. 242-249.
3. Tian, X., F. Su, and X.S. Zhao, *Sulfonated polypyrrole nanospheres as a solid acid catalyst.* Green Chem., 2008. **10**(9): p. 951-956.
4. Hara, M., et al., *A Carbon Material as a Strong Protonic Acid.* Angewandte Chemie International Edition, 2004. **43**(22): p. 2955-2958.
5. Peng, L., et al., *Preparation of sulfonated ordered mesoporous carbon and its use for the esterification of fatty acids.* Catalysis Today, 2010. **150**(1-2): p. 140-146.
6. Luque, R., et al., *Microwave-assisted preparation of amides using a stable and reusable mesoporous carbonaceous solid acid.* Green Chem., 2009. **11**(4): p. 459-461.
7. Luque, R., et al., *Glycerol transformations on polysaccharide derived mesoporous materials.* Appl. Catal., B, 2008. **82**(3-4): p. 157-162.
8. Kitano, M., et al., *Adsorption-Enhanced Hydrolysis of β-1,4-Glucan on Graphene-Based Amorphous Carbon Bearing SO3H, COOH, and OH Groups.* Langmuir, 2009. **25**(9): p. 5068-5075.

9. Hara, M., *Biodiesel Production by Amorphous Carbon Bearing SO3H, COOH and Phenolic OH Groups, a Solid Bronsted Acid Catalyst.* Top. Catal., 2010. **53**(11-12): p. 805-810.

10. Luque, R. and J.H. Clark, *Water-tolerant Ru-Starbon materials for the hydrogenation of organic acids in aqueous ethanol.* Catal. Commun., 2010. **11**(10): p. 928-931.

11. Xing, R., et al., *Active solid acid catalysts prepared by sulfonation of carbonization-controlled mesoporous carbon materials.* Microporous and Mesoporous Materials, 2007. **105**(1-2): p. 41-48.

12. Suganuma, S., et al., *Hydrolysis of cellulose by amorphous carbon bearing SO3H, COOH, and OH groups.* Journal of the American Chemical Society, 2008. **130**(38): p. 12787-12793.

13. Tang, Y., et al., *Bifunctional mesoporous organic-inorganic hybrid silica for combined one-step hydrogenation/esterification.* Appl. Catal., A, 2010. **375**(2): p. 310-317.

14. Miao, S. and B.H. Shanks, *Esterification of biomass pyrolysis model acids over sulfonic acid-functionalized mesoporous silicas.* Applied Catalysis A: General, 2009. **359**(1-2): p. 113-120.

15. Morajkar, P.P. and J.B. Fernandes, *A new facile method to synthesize mesoporous gamma -Al2O3 of high surface area and catalytic activity.* Catal. Commun., 2010. **11**(5): p. 414-418.

16. Pyatnitskii, Y., P. Strizhak, and N. Lunev, *Kinetic modeling for the conversion of synthesis gas to dimethyl ether on a mixed Cu-ZnO-Al₂O₃ catalyst with γ-Al₂O<sub>3</sub&gt.* Theoretical and Experimental Chemistry, 2009. **45**(5): p. 325-330.

17. Murkute, A.D., J.E. Jackson, and D.J. Miller, *Supported mesoporous solid base catalysts for condensation of carboxylic acids.* J. Catal., 2011. **278**(Copyright (C) 2012 American Chemical Society (ACS). All Rights Reserved.): p. 189-199.

18. Zheng, J.J., et al., *Synthesis and Catalytic Property of a Zeolite Composite for Preparation of Dimethyl Ether from Methanol Dehydration.* Catalysis Letters, 2009. **130**(3-4): p. 672-678.

19. Roh, H.-S., et al., *Superior dehydration of CH3OH over double layer bed of solid acid catalysts-A novel approach for dimethyl ether (DME) synthesis.* Chem. Lett., 2004. **33**(5): p. 598-599.

20. Hyun, S.H., et al., *Synthesis of ZSM-5 zeolite composite membranes for CO2 separation.* J. Mater. Sci., 1999. **34**(Copyright (C) 2012 American Chemical Society (ACS). All Rights Reserved.): p. 3095-3103.

21. Kapura, J.M. and B.C. Gates, *Sulfonated polymers as alkylation catalysts.* Ind. Eng. Chem., Prod. Res. Develop., 1973. **12**(Copyright (C) 2012 American Chemical Society (ACS). All Rights Reserved.): p. 62-7.

22. Turbak, A.F., *Sulfonation with organic phosphorus compound-sulfur trioxide adducts*. 1963, Esso Research and Engineering Co. . p. 6 pp.

23. Shaabani, A., A. Rahmati, and Z. Badri, *Sulfonated cellulose and starch: New biodegradable and renewable solid acid catalysts for efficient synthesis of quinolines.* Catalysis Communications, 2008. **9**(1): p. 13-16.

24. Zhao, Y., et al., *Preparation of a novel sulfonated carbon catalyst for the etherification of isopentene with methanol to produce tert-amyl methyl ether.* Catal. Commun., 2010. **11**(9): p. 824-828.

25. Tan, X.J., et al., *Thermoelectric Properties of Ultrasmall Single-Wall Carbon Nanotubes.* J. Phys. Chem. C, 2011. **115**(Copyright (C) 2012 American Chemical Society (ACS). All Rights Reserved.): p. 21996-22001.

26. Budarin, V.L., et al., *Tunable mesoporous materials optimized for aqueous phase esterifications.* Green Chem., 2007. **9**(9): p. 992-995.

27. Petrus, L., E.J. Stamhuis, and G.E.H. Joosten, *Thermal deactivation of strong-acid ion-exchange resins in water.* Industrial & Engineering Chemistry Product Research and Development, 1981. **20**(2): p. 366-371.

28. Suganuma, S., et al., *Synthesis and acid catalysis of cellulose-derived carbon-based solid acid.* Solid State Sciences, 2010. **12**(6): p. 1029-1034.

29. Li, H. and A. Adronov, *Water-soluble SWCNTs from sulfonation of nanotube-bound polystyrene.* Carbon, 2007. **45**(5): p. 984-990.

30. Yang, Y., K. Chiang, and N. Burke, *Porous carbon-supported catalysts for energy and environmental applications: A short review.* Catal. Today, 2011. **178**(Copyright (C) 2012 American Chemical Society (ACS). All Rights Reserved.): p. 197-205.

31. Zaiku, X.i.e., Xie, and Z. Xie, *An overview of recent development in composite catalysts from porous materials for various reactions and processes.* International journal of molecular sciences, 2010. **11**(5): p. 2152.

32. Onda, A., T. Ochi, and K. Yanagisawa, *Hydrolysis of Cellulose Selectively into Glucose Over Sulfonated Activated-Carbon Catalyst Under Hydrothermal Conditions.* Top. Catal., 2009. **52**(6-7): p. 801-807.

33. Brown, R.C., *Biorenewable Resources: Engineering New Products from Agriculture*. 2003: Blackwell Publishing.

34. Yang, S., et al., *Catalytic activity, stability and structure of multi-walled carbon nanotubes in the wet air oxidation of phenol.* Carbon, 2008. **46**(3): p. 445-452.

35. Villa, A., et al., *Transesterification of Triglycerides Using Nitrogen-Functionalized Carbon Nanotubes.* Chemsuschem, 2010. **3**(2): p. 241-245.

36. Tessonnier, J.-P., et al., *Defect-Mediated Functionalization of Carbon Nanotubes as a Route to Design Single-Site Basic Heterogeneous Catalysts for Biomass Conversion.* Angewandte Chemie International Edition, 2009. **48**(35): p. 6543-6546.

37. Hummer, G., J.C. Rasaiah, and J.P. Noworyta, *Water conduction through the hydrophobic channel of a carbon nanotube.* Nature, 2001. **414**(6860): p. 188-190.

38. Bahr, J.L., et al., *Functionalization of Carbon Nanotubes by Electrochemical Reduction of Aryl Diazonium Salts: A Bucky Paper Electrode.* Journal of the American Chemical Society, 2001. **123**(27): p. 6536-6542.

39. Simate Gs Fau - Iyuke, S.E., et al., *Human health effects of residual carbon nanotubes and traditional water treatment chemicals in drinking water*. (1873-6750 (Electronic)).

40. Liu, R., et al., *Sulfonated ordered mesoporous carbon for catalytic preparation of biodiesel.* Carbon, 2008. **46**(13): p. 1664-1669.

41. Wang, X., et al., *Sulfonated Ordered Mesoporous Carbon as a Stable and Highly Active Protonic Acid Catalyst.* Chemistry of Materials, 2007. **19**(10): p. 2395-2397.

42. Liu, Y., et al., *Preparation and properties of sulfonated carbon-silica composites from sucrose dispersed on MCM-48.* Chemical Engineering Journal, 2009. **148**(1): p. 201-206.

43. Mo, X., et al., *Activation and deactivation characteristics of sulfonated carbon catalysts.* J. Catal., 2008. **254**(2): p. 332-338.

44. Satterfield, C.N., *Heterogeneous Catalysis in Industrial Practice. 2nd Ed*. 1991. 554 pp.

45. White Robin, J., et al., *Tuneable porous carbonaceous materials from renewable resources.* Chemical Society Reviews, 2009. **38**(12): p. 3401-18.

46. Sun, J., et al., *Catalytic Performance of Activated Carbon Supported Tungsten Carbide for Hydrazine Decomposition.* Catalysis Letters, 2008. **123**(1): p. 150-155.

47. Hara, M., et al., *Sulfonated incompletely carbonized glucose as strong Bronsted acid catalyst.* Stud. Surf. Sci. Catal., 2007. **172**(Science and Technology in Catalysis 2006): p. 405-408.

48. Nakajima, K., et al., *Amorphous Carbon Bearing Sulfonic Acid Groups in Mesoporous Silica as a Selective Catalyst.* Chemistry of Materials, 2008. **21**(1): p. 186-193.

49. Hu, B., et al., *Functional carbonaceous materials from hydrothermal carbonization of biomass: an effective chemical process.* Dalton Trans., 2008(40): p. 5414-5423.

50. Zhang, W., et al., *One-pot synthesis of carbonaceous monolith with surface sulfonic groups and its carbonization/activation.* Carbon, 2011. **49**(6): p. 1811-1820.

51. Xiao, H., et al., *One-step synthesis of novel biacidic carbon via hydrothermal carbonization.* Journal of Solid State Chemistry, 2010. **183**(7): p. 1721-1725.

52. Franklin, R.E., *Homogeneous and heterogeneous graphitization of carbon.* Nature (London, U. K.), 1956. **177**: p. 239.

53. Harris, P.J.F., *Rosalind Franklin's work on coal, carbon, and graphite.* Interdisciplinary Science Reviews, 2001. **26**(3): p. 204-209.

54. Harris, P.J.F., *New Perspectives on the Structure of Graphitic Carbons.* Critical Reviews in Solid State and Materials Sciences, 2005. **30**(4): p. 235-253.

55. Radlein, D., J. Piskorz, and D.S. Scott, *Fast pyrolysis of natural polysaccharides as a potential industrial process.* J. Anal. Appl. Pyrolysis, 1991. **19**: p. 41-63.

56. Oberlin, A., *Carbonization and graphitization.* Carbon, 1984. **22**(6): p. 521-41.

57. Boehm, H.P., *Carbon surface chemistry.* World Carbon, 2001. **1**(Graphite and Precursors): p. 141-178.

58. Boehm, H.P., *Chemical identification of surface groups.* Advan. Catalysis, 1966. **16**: p. 179-274.

59. Boehm, H.P., *Some aspects of the surface chemistry of carbon blacks and other carbons.* Carbon, 1994. **32**(5): p. 759-69.

60. Boehm, H.-P., *Surface chemical characterization of carbons from adsorption studies.* Adsorpt. Carbons, 2008: p. 301-327.

61. Goertzen, S.L., et al., *Standardization of the Boehm titration. Part I. CO2 expulsion and endpoint determination.* Carbon, 2010. **48**(4): p. 1252-1261.

62. Oickle, A.M., et al., *Standardization of the Boehm titration: Part II. Method of agitation, effect of filtering and dilute titrant.* Carbon, 2010. **48**(12): p. 3313-3322.

63. Radovic, L.R. and F. Rodriguez-Reinoso, *Carbon materials in catalysis.* Chem. Phys. Carbon, 1997. **25**: p. 243-358.

64. Serp, P., J.L. Figueiredo, and Editors, *Carbon Materials For Catalysis*. 2009: John Wiley & Sons, Inc. 579 pp.

65. Su, D.S., S. Perathoner, and G. Centi, *Catalysis on nano-carbon materials: Going where to?* Catal. Today, 2012. **186**(1): p. 1-6.

66. Hu, B., et al., *Engineering Carbon Materials from the Hydrothermal Carbonization Process of Biomass.* Adv. Mater. (Weinheim, Ger.), 2010. **22**(7): p. 813-828.

67. Titirici, M.-M., *Hydrothermal carbons: synthesis, characterization, and applications.* Novel Carbon Adsorbents, 2012: p. 351-399.

68. Dai, S., *Self-assembly synthesis and functionalization of mesoporous carbon materials for catalysis and energy applications.* Prepr. Symp. - Am. Chem. Soc., Div. Fuel Chem., 2009. **54**(1): p. 379.

69. Rodriguez, F., et al., *Synthesis of hierarchical porous carbons and hybrid materials by dual block copolymer/nanoparticles templating method.* Pacifichem 2010, International Chemical Congress of Pacific Basin Societies, Honolulu, HI, United States, December 15-20, 2010, 2010: p. MATNANO-619.

70. Dai, S., *Tailoring mesoporous carbons and related materials for energy applications.* Abstracts of Papers, 246th ACS National Meeting & Exposition, Indianapolis, IN, United States, September 8-12, 2013, 2013: p. ENFL-30.

71. Inagaki, M. and L.R. Radovic, *Nanocarbons.* Carbon, 2002. **40**(12): p. 2279-2282.

72. Silva-Tapia, A.B., X. Garcia-Carmona, and L.R. Radovic, *Similarities and differences in O2 chemisorption on graphene nanoribbon vs. carbon nanotube.* Carbon, 2012. **50**(3): p. 1152-1162.

73. Radovic, L.R., *Catalysis in coal and carbon gasification.* Handb. Heterog. Catal. (2nd Ed.), 2008. **6**: p. 3037-3045.

74. Kyotani, T., et al., *Inhibiting effect of coexisting gas on CO2 gasification of Ca-loaded coal char.* Nippon Enerugi Gakkaishi, 1994. **73**(11): p. 1005-12.

75. Kyotani, T., et al., *Monte Carlo simulation of carbon gasification using molecular orbital theory.* AIChE J., 1996. **42**(8): p. 2303-2307.

76. Lizzio, A.A., H. Jiang, and L.R. Radovic, *On the kinetics of carbon (char) gasification: reconciling models with experiments.* Carbon, 1990. **28**(1): p. 7-19.

77. Kyotani, T., y.L.C.A. Leon, and L.R. Radovic, *Simulation of carbon gasification kinetics using an edge recession model.* AIChE J., 1993. **39**(7): p. 1178-85.

78. Ito, K.-i., et al., *Simulation of carbon gasification using computer.* Sekitan Kagaku Kaigi Happyo Ronbunshu, 1992. **29TH**: p. 126-9.

79. Nowack, K.O., et al., *A commentary on "effect of metal additives on the physico-chemical characteristics of activated carbon exemplified by benzene and acetic acid adsorption".* Carbon, 2001. **39**(6): p. 951-953.

80. Leon, y.L.C.A. and L.R. Radovic, *Influence of oxygen functional groups on the performance of carbon-supported catalysts.* Prepr. Pap. - Am. Chem. Soc., Div. Fuel Chem., 1991. **36**(3): p. 1007-14.

81. Lopez-Ramon, V., et al., *Ionic strength effects in aqueous phase adsorption of metal ions on activated carbons.* Carbon, 2003. **41**(10): p. 2020-2022.

82. Radovic, L.R., *A landmark paper on carbon-supported catalysts: the real story revealed by the Science Citation Index.* Prepr. Symp. - Am. Chem. Soc., Div. Fuel Chem., 2000. **45**(4): p. 845-849.

83. Illan-Gomez, M.J., et al., *NO reduction by activated carbons. Some mechanistic aspects of uncatalyzed and catalyzed reaction.* Coal Sci. Technol., 1995. **24**(Coal Science, Vol. 2): p. 1799-802.

84. Boonoun, P., et al., *Application of Sulfonated Carbon-Based Catalyst for Reactive Extraction of 1,3-Propanediol from Model Fermentation Mixture.* Industrial & Engineering Chemistry Research, 2010. **49**(24): p. 12352-12357.

85. Yu, J.T., A.M. Dehkhoda, and N. Ellis, *Development of Biochar-based Catalyst for Transesterification of Canola Oil.* Energy Fuels, 2011. **25**(1): p. 337-344.

86. Yantasee, W., et al., *Electrophilic Aromatic Substitutions of Amine and Sulfonate onto Fine-Grained Activated Carbon for Aqueous-Phase Metal Ion Removal.* Sep. Sci. Technol., 2004. **39**(14): p. 3263-3279.

87. Zhang, B., et al., *Novel sulfonated carbonaceous materials from p-toluenesulfonic acid/glucose as a high-performance solid-acid catalyst.* Catal. Commun., 2010. **11**(7): p. 629-632.

88. Mirkhani, V., et al., *Preparation of an improved sulfonated carbon-based solid acid as a novel, efficient, and reusable catalyst for chemoselective synthesis of 2-oxazolines and bis-oxazolines.* Monatsh. Chem., 2009. **140**(12): p. 1489-1494.

89. Budarin Vitaly, L., et al., *Versatile mesoporous carbonaceous materials for acid catalysis.* Chem Commun (Camb), 2007(6): p. 634-6.

90. Clark, J.H., et al., *Catalytic performance of carbonaceous materials in the esterification of succinic acid.* Catalysis Communications, 2008. **9**(8): p. 1709-1714.

91. Takagaki, A., et al., *Esterification of higher fatty acids by a novel strong solid acid.* Catalysis Today, 2006. **116**(2): p. 157-161.

92. Titirici, M.-M. and M. Antonietti, *Chemistry and materials options of sustainable carbon materials made by hydrothermal carbonization.* Chemical Society Reviews, 2010. **39**(1): p. 103-116.

93. Toda, M., et al., *Green chemistry: Biodiesel made with sugar catalyst.* Nature, 2005. **438**(7065): p. 178-178.

94. Zali, A., et al., *Carbon-Based Solid Acid as an Efficient and Reusable Catalyst for Cross-Aldol Condensation of Ketones with Aromatic Aldehydes under Solvent-Free Conditions.* Chinese Journal of Catalysis, 2008. **29**(7): p. 602-606.

95. Hawash, S., et al., *Kinetic study of naphthalene sulfonation reaction.* Industrial & Engineering Chemistry Research, 1993. **32**(6): p. 1066-1070.

96. Knauer, M., et al., *Soot Structure and Reactivity Analysis by Raman Microspectroscopy, Temperature-Programmed Oxidation, and High-Resolution Transmission Electron Microscopy.* The Journal of Physical Chemistry A, 2009. **113**(50): p. 13871-13880.

97. Titirici, M.M., et al., *A Direct Synthesis of Mesoporous Carbons with Bicontinuous Pore Morphology from Crude Plant Material by Hydrothermal Carbonization.* Chemistry of Materials, 2007. **19**(17): p. 4205-4212.

98. Yamaguchi, D. and M. Hara, *Starch saccharification by carbon-based solid acid catalyst.* Solid State Sciences, 2010. **12**(6): p. 1018-1023.

99. Suganuma, S., et al., *SO3H-bearing mesoporous carbon with highly selective catalysis.* Microporous and Mesoporous Materials, 2011. **143**(2–3): p. 443-450.

100. Mo, X., et al., *A Novel Sulfonated Carbon Composite Solid Acid Catalyst for Biodiesel Synthesis.* Catal. Lett., 2008. **123**(1-2): p. 1-6.

101. Cerfontain, H., *Mechanistic Aspects in Aromatic Sulfonation and Desulfonation*. Interscience Monographs on Organic Chemistry, ed. G. Olah. 1968, New York: Interscience Publishers.

102. Karásek, P., J. Planeta, and M. Roth, *Solubility of Solid Polycyclic Aromatic Hydrocarbons in Pressurized Hot Water: Correlation with Pure Component Properties.* Industrial & Engineering Chemistry Research, 2006. **45**(12): p. 4454-4460.

103. Karásek, P., J. Planeta, and M. Roth, *Solubility of Solid Polycyclic Aromatic Hydrocarbons in Pressurized Hot Water at Temperatures from 313 K to the Melting Point.* Journal of Chemical & Engineering Data, 2006. **51**(2): p. 616-622.

CHAPTER 2.

CHEMICAL STRUCTURE AND HYDROTHERMAL DEACTIVATION OF MODERATE-TEMPERATURE CARBON MATERIALS WITH ACIDIC SO_3H SITES

A paper submitted to Carbon

Jason M. Anderson, Robert L. Johnson, Klaus Schmidt-Rohr, and Brent H. Shanks

Abstract

Hydrothermal stability of carbon based acid catalysts synthesized by sulfonating carbohydrates pyrolyzed at moderate temperatures (300-600°C) has been reported previously. To test the effect of carbon structure on hydrothermal stability, we produced catalysts by dry pyrolysis at 350ºC and 450ºC or by hydrothermal carbonization, followed by sulfonation with fuming sulfuric acid, as well as by direct sulfonation of glucose. The catalysts were characterized by BET, titration, Raman spectroscopy, TGA, XPS, reaction testing, and ^{13}C solid state NMR. Catalysts were hydrothermally treated and then analyzed for sulfur retention and catalytic activity. The lower temperature carbon catalysts showed the best stability, however all showed significant activity loss. Solid state NMR characterized the structural details to attempt to correlate functional groups to hydrothermal stability of catalyst active sites. Structural models generated from

NMR data showed that the most stable catalysts contained a significant fraction of furan rings and hardly any polycondensed aromatic rings.

1. Introduction

Acid catalysts promote a variety of important reactions: esterification/transesterification [1-5], dehydration/hydration [6, 7], hydrolysis [4, 8], etherification [2], alkylation, acylation, condensation, oligomerization, etc. [7]. These reactions generally proceed through a carbocation intermediate, generated either by protonation of a Brønsted acid or through abstraction of electrons by a Lewis acid. Brønsted acids are ubiquitous in the chemical industry in homogeneously and heterogeneously catalyzed systems. Industry uses sulfuric acid for a myriad of reactions [9] and while it is inexpensive and highly active, it requires separation, recycling, and waste treatment, which are energy inefficient [10, 11]. Therefore, significant incentive exists for the development of heterogeneous acid catalysts to replace sulfuric acid thereby reducing costs and minimizing environmental impacts [12].

In general, industry would prefer to utilize solid acid catalysts, and for predominantly gas phase or non-aqueous processing, heterogeneous Brønsted acid catalysts with alumina, silica, zeolites, or resins supports have proven effective. However, the development of heterogeneous acid catalysts functional and stable in aqueous systems, which is a research target for utilization of bio-based

feedstocks, has been significantly more challenging. Many common support materials including alumina, silica, and zeolites degrade readily in subcritical water [7, 13, 14]. Recently, promising sulfonated carbon catalysts with improved hydrothermal stability have been reported [15, 16]. While these materials are quite interesting, no systematic experimental testing for the hydrothermal stability of the solid acid catalysts and importantly little correlation of stability to the structure and chemistry of the carbon support has been reported.

The deactivation of sulfonated carbon catalysts may occur in several ways, but is primarily explored through changes in the catalyst activity [1, 17]. Several researchers have explained the decrease in catalyst activity in terms of hydrolysis of the carbon-sulfur bond and then loss of a sulfate group (SO_4) [17, 18] although no definitive experimental evidence was shown of sulfur leaching as the primary deactivation pathway. Yamaguchi and Hara suggested that adjacent electron-withdrawing groups on the arene sheets composing the carbon support improved the strength of the sulfur-carbon bond [19] and thereby reduced hydrolysis of the active site. The current work seeks to explore this hypothesis by producing supports with varying degrees of aromaticity and oxygen-containing functional groups. The sulfonated carbon materials examined include alteration of the balance between the arene and furan aromatic rings as well as the number of carboxylate and phenolic functional groups.

A number of strategies have been used to produce carbons, which are subsequently sulfonated for use as catalyst to transform fatty acids into biodiesel

[20]. While there is general agreement that processing temperature is a critical parameter governing the amount of hetero atoms remaining in the final carbon materials, understanding of the transformation from the carbohydrate starting material to carbon remains limited [21, 22]. To provide a more direct basis for comparison, the sulfonated carbon materials examined were similar to those reported previously including pyrolyzed carbons [10], hydrothermal carbon [9, 23, 24], direct sulfonation of a carbohydrate [25], and sulfonation via electrophilically substituting benzene sulfonic acid as shown for carbon nanotubes [26]. Since increasing carbonization temperature decreases the amount of oxygen present in the carbon material, the oxygen functionality should be the most extensive for low synthesis temperature. The expected order from high to low oxygen content of the materials synthesized would be the directly sulfonated carbon (150°C), the hydrothermal carbon (200°C), and the pyrolyzed carbons (350°C and 450°C synthesis temperatures). The structure and chemical composition of the different materials were determined using solid-state NMR. Quantitative NMR spectra with a chemical shift-modeling algorithm were used to determine structural models of the materials through iterative comparisons between measured and simulated spectra. These models summarize the structural insights from NMR and enable direct assessment of the effect of the carbon structure on hydrothermal stability.

To measure the stability of the sulfonate groups under hydrothermal conditions, the various sulfonated carbon materials are subjected to extended

hydrothermal conditions and the retained sulfur content was measured using elemental analysis. Furthermore, the catalytic activity of the materials both freshly produced and after having been subjected to successive hydrothermal treatments is tested via the esterification of acetic acid and methanol, which is quite sensitive to both the number and pK_a of the acid sites present [27].

2. Experimental

2.1. Materials and Synthesis

Glucose, sodium chloride, sodium hydroxide, glacial acetic acid, dimethylsulfoxide (DMSO), sodium hydroxide, and methanol were purchased from Fisher Scientific and methyl acetate, 1,4-dioxane, isoamyl nitrite, and sulfur trioxide were purchased from Sigma-Aldrich. Glucose enriched with ^{13}C was purchased from Cambridge Isotopes. All chemicals were used without further purification. Nitrogen (99.995%) was obtained from Airgas. The fuming sulfuric acid (~20-30 mol% excess SO_3) used for sulfonation was created using a mixture of sulfuric acid with sulfur trioxide.

2.2. Pyrolyzed Carbon Preparation

Glucose (~15g) was pyrolyzed at either 350 or 450 °C in a horizontal tube furnace, for one hour after a temperature ramp (10°C min^{-1})from room temperature in flowing nitrogen (about 1L min^{-1}) and then cooled and

homogenized through grinding with a mortar and pestle. Next, the char was subjected to additional reaction time of 9 hours in nitrogen after the temperature ramp to ensure uniform composition (verified by NMR-data not shown). The ramp rate in the tube furnace was 10°C min^{-1}.

2.3. Hydrothermal Carbon Preparation

In a stainless steel Parr reactor, glucose (5 g) was dissolved in deionized (DI) water (50 mL) and then nitrogen flushed three times. The vessel was then pressurized to 500 psi and heated to 200 °C with a ramp rate of 10ºC min^{-1} and then held for ~18.5 hours. The resulting insoluble carbon material was filtered (4.5-5µm Buchner funnel) and washed with DI water and dried overnight at 100 °C within an air atmosphere in an oven.

2.4. Sulfonation of the Carbon by Fuming Sulfuric Acid

The pyrolytic carbons (350°C & 450°C), and hydrothermal ("Hydro") carbons were individually sulfonated with fuming sulfuric acid. In an Erlenmeyer flask, carbon (~5 g) was placed in fuming sulfuric acid (150 mL of 30% excess of SO_3) made from sulfuric acid and sulfur trioxide, and then heated to 150 °C. The carbon material was allowed to react for 2 hours at 150 °C and then was cooled to room temperature. The resulting solid material was filtered (4.5-5 µm Buchner funnel) and washed with ~2-3 L of DI water until the effluent was clear and colorless. Measurement of sulfate ions in the filtrate was accomplished by

precipitation with barium chloride. The catalyst was dried overnight in an oven at 100ºC.

2.5. Preparation of "Direct" Sulfonated Carbon

Glucose will also dehydrate in concentrated sulfuric acid to a char similar in appearance to the pyrolytic carbons. This direct dehydration provided the highest sulfur incorporation seen in the literature for these catalysts [28]. In an Erlenmeyer flask, glucose (~5 g) was placed in fuming sulfuric acid (150 mL of 30% excess of SO_3). It was heated to 150ºC and allowed to react for 2 hours. The resulting solid was washed and filtered (4.5-5 µm Buchner funnel) with DI water (~2-3 L) until the solution was clear and colorless and no sulfate ions were detected with barium chloride. The final material was dried overnight at 100ºC.

2.6. Preparation of "Chem" Sample Using Sulfanilic Acid

For comparison, hydrothermal carbon was also sulfonated using an alternative method with sulfanilic acid that was adapted from the literature [26]. Briefly, sulfanilic acid (6 g), isoamyl nitrite (15 mL), and hydrothermal carbon (2 g) were added to DMSO solvent (30 mL) in a stainless steel Parr reactor. The reactor headspace was flushed with nitrogen (pressurized to 750 psi, vented to 100 psi) three times before heating the reactor to 70°C for 2 hours. The resulting slurry was first filtered (4.5-5µm Buchner funnel) with toluene to remove any residual organics, with NaOH (1M) to remove remaining sulfanilic acid, with HCl (0.05M) to reacidify the catalyst for storage, and lastly with DI (2-3 L) water to

remove as many ions as possible. The final material was dried overnight at 100ºC.

A summary of the materials produced for the study with their synthesis conditions are given in Table 1. The synthesized materials were labeled either with the pyrolysis temperature (350°C or 450°C) or the unique synthesis step: Hydro, Direct, or Chem. Each sample preparation was duplicated to demonstrate reproducibility, so the sample names were annotated with #1 or #2 such as Chem#1 or 350°C#2.

Table 1. Carbon Samples Synthesis Parameters.

Pyrolysis		Direct	Hydro	Chem	350°C	450°C
Temp	°C	N/A	200	200	350	450
Media		N/A	Water	water	nitrogen	nitrogen
Time	hr	N/A	18.5	18.5	1+9.33	1+9.33
Sulfonation						
Temp	°C	150	150	70	150	150
Media		fuming H_2SO_4	fuming H_2SO_4	DMSO	fuming H_2SO_4	fuming H_2SO_4
Time	hr	2	2	2	2	2

2.7. Catalyst Characterization

The carbon materials were imaged with scanning electron microscopy (FEI Quanta-250 SEM), to compare their morphologies with carbons generated by similar synthesis methods in the literature. Surface area characterization was performed by physisorption using Kr as the adsorbing gas in a Micromeritics ASAP 2020. Analysis of the materials with a Perkin Elmer STA 6000 Simultaneous Thermal Analyzer (TGA), using a ramp rate of 10°C in flowing air was performed. Elemental analysis results for the carbon, hydrogen, nitrogen, and sulfur (CHNS) were acquired using a PE 2100 Series II combustion analyzer (Perkin Elmer Inc., Waltham, MA). The chemical state of sulfur was analyzed using a Physical Electronics 550 Multitechnique XPS system employing a standard Al electron source. The samples were run at 10^{-9} Torr and mounted on double-sided tape. Charging was corrected for by adjusting the carbon peak to 284 eV. Ion exchange titrations were run to measure the number of acidic groups present on the sulfonated carbons. The number of sulfonic acid ($R\text{-}SO_3H$), carboxylic acid, and phenolic hydroxyl groups were measured using the titration method reported by Suganuma et al. [29]. One back titration measured all the acidic functionalities. It used a known amount of NaOH (~0.1g) dissolved in water with the catalytic material using sufficient time (~2 hours) to exchange the sodium ions with all the hydrogen ions from the acid groups on the material. Then, a simple acid titration using sodium hydroxide was used to exchange the acidic protons from the sulfonic acid and carboxylic acid groups. It was assumed

that the sulfonic acid, carboxylic acid, and hydroxyl groups were measured. The sulfonic acid groups were measured by the elemental analysis of the sulfur and the other groups were determined by subtraction of these measurements. As presented previously by Suganuma, Raman spectroscopy was used to determine the ratio of defect to graphitic carbon [8]. The spectra were obtained on a Renishaw InVia Raman spectrometer using a 488 nm laser and wave numbers from 500 to 2500 and measured at two different locations with three scans each.

2.8. Solid State NMR and Structure Simulations

The ^{13}C NMR was performed at a resonance of 100 MHz on ^{13}C-enriched samples using a Bruker DSX400 spectrometer, magic angle spinning at 14 kHz, and high power ^{1}H decoupling. The 90° ^{13}C pulse-length was 4.5 μs. Quantitative ^{13}C spectra were measured using direct polarization (DP) magic-angle spinning (MAS) and a Hahn echo with high-power decoupling, with recycle delays of 30 s (> 5 T_1), and spectra of nonprotonated carbons (and mobile segments) were obtained after recoupled ^{13}C-^{1}H dipolar dephasing [30]. Sufficiently strong ^{1}H decoupling at $\gamma B_1/ 2\pi$ = 72 kHz with the two-pulse phase-modulated (TPPM) scheme was applied during an acquisition time of 3 ms. Chemical shifts were referenced to neat TMS using the resonance of $^{13}C1$-labeled glycine with a chemical shift of 176.46 ppm as a secondary reference.

Two-dimensional (2D) NMR spectra to identify nonprotonated C near CH in the Hydro sample were measured by 2D exchange NMR after short (0.07 ms) cross-polarization and with dipolar dephasing before detection (exchange with

protonated and nonprotonated spectral editing, EXPANSE NMR). Dipolar assisted rotary recoupling (DARR) [31] was applied during the mixing time of 10 ms. Details of this new combination of spectral editing with 2D ^{13}C-^{13}C NMR are described in ref. [32]. 2D NMR correlation spectra showing selectively peaks from pairs of nonprotonated carbons in the Hydro sample were obtained by dipolar dephasing of double-quantum coherence in a double-quantum/single-quantum (DQ/SQ) correlation experiment, with a total of 0.57 ms of SPC5 [33] homonuclear dipolar recoupling [32]. The initial magnetization was generated by a combination of cross polarization and direct polarization, followed by 100 ms of spin diffusion [32]. The DQ/SQ spectrum was sheared for direct comparison with the EXPANSE spectrum [32]. Both 2D spectra were recorded at a magic-angle spinning frequency of ν_r = 14 kHz. To convert the COOH to COOLi groups, which have characteristic ^{13}C NMR chemical shifts, the Hydro and 350^oC materials were treated with 0.1 M LiOH, which was titrated to a pH of 9.0 to ensure exchange of H on COO groups but not phenols. The materials (~100 mg) were washed three times with 1 mL of the LiOH solution and pelleted by centrifugation. After washing with DI water the materials were freeze dried. Structural models were generated for each of the sulfonated carbon materials based on the quantitative 1D and spectrally edited 2D ^{13}C NMR spectra as well as elemental analysis (C, H, N, S, and then O by difference), which provide relative amounts of key structural fragments and atomic compositions and thus greatly constrain the possible structures. Integration of the one-dimensional ^{13}C NMR

spectra directly provided quantitative amounts of major functional groups present, including alkyls, ketones, carboxylic acids, aromatic carbons bonded to O or two bonds from oxygen, protonated and nonprotonated aromatic C, and alkyl C, see Table 2. The spectrally edited two-dimensional NMR experiments [32] were used to identify the predominant linkage patterns of the aromatic subunits and the ketones.

Table 2. Carbon fractions (in atomic %) in functional groups for four ^{13}C-enriched sulfonated carbon materials from quantitative ^{13}C NMR and spectral editing. Error margins: ±1% for large, ±0.5% for small (<10%) signals. For the 350°C and 450°C samples, the C=O/COO and $C_{nonp}O/C_{nonp}$ boundaries were shifted to 175 and 147 ppm, respectively. The percentages can be changed into mmol g^{-1} by multiplication with a factor of 0.67 (1 g ≙ [1/15] mol = 68 mmol; 1 mmol g^{-1} ≙ 1/68 = 1.5%; so 1% ≙ 0.67 mmol g^{-1}) for the low-T and by a factor of 0.77 for the ≥ 350°C materials.

			Aromatic					
Functional Group	C=O	COO	$C_{nonp}O$	C_{nonp}	CH	OCH_n	CH_2+CH	CH_3
Chemical Shift	224-180	180-162	162-142	142-90	162-90	90-52	52-28	28-6

Sample								
Direct	6.6	11.4	24	34	17	2.1	2.9	1.2
Hydro	5.8	11.4	23	44	12	1.7	0.9	0.6
350°C	7.4	10.3	15	51	13	1.7	0.9	0.6
450°C	2.5	1.3	8	65	21	1.0	0.9	0.4

The models were refined by calculating 1D ^{13}C NMR spectra, both for all C and for C not bonded to H, using chemical shifts from the empirical chemical-shift prediction program ACD. These data were input to a MatLab program that converted them into spectra with a Gaussian line broadening of ca. 14 ppm full width at half maximum applied to all peaks. The structural model was optimized iteratively by small modifications of the structures until the simulated and experimental spectra were in good agreement. The structural models presented should be thought of as average structures containing all of the key chemical features of these materials. The inhomogeneous broadening of all resonance lines indicates the presence of many slightly different structures.

2.9. Reaction and Stability Testing

Esterification of acetic acid with methanol was used as the test reaction since it is sensitive to the number of acid sites and their pK_a [27]. The reactions were performed at 40 °C in an Alltech 10 mL reactor vial loaded (total volume 7

mL) with methanol (6 M)and acetic acid (3 M) in dioxane with the respective sulfonated carbon (10 mg). The reactions were run at low conversions (<5%) to allow comparison of initial rates. The reaction testing was performed at a range of stir rates so that it was determined that no mass transfer effects occurred as long as the stirring rate was above 200 rpm. The reaction product samples were analyzed on an Agilent 7890A GC equipped with a flame ionization detector. The sulfonated carbons were compared in terms of activity per mass of catalyst, with units of mmol acetate formed min^{-1} (g catalyst)$^{-1}$.

After full characterization of the fresh materials, the catalysts were subjected to hydrothermal treatment. The treatment involved the catalyst material (0.5 g) stirred in DI water (7 mL) at 160°C in the Alltech reactors under autogenous pressure for 24 hours. The solid material was separated from the water with the water subsequently measured for sulfur content using ICP analysis. After the initial separation, the samples were washed copiously (generally about 0.5 L of DI water) until the filtrate was clear and colorless. The hydrothermally treated sulfonated carbon was then characterized and subjected to two more hydrothermal treatments following the same protocol as the first treatment.

3. Results and Discussion

Characterization results of the samples produced in the current study provide good evidence that the materials were representative of the carbon-based

materials studied in previous publications. The SEM images of the hydrothermal carbon, see Figure 1, showed the same clusters of nearly uniform spheres of about 0.5-1 μm diameter that have been reported by other groups [34, 35]. The sulfonation of the hydrothermal carbon via fuming sulfuric acid did not affect the spherical morphology. However, the morphology of the spheres changed significantly when modified with sulfanilic acid as they changed from well-defined spheres to pitted amorphous shapes only vaguely reminiscent of the original spherical morphology (see Figure 2). The other materials (Direct, 350°C, and 450°C) exhibited shapes resembling shards of glass of ca. 10-150 μm in size with amorphous characteristics (see Figure 3), also consistent with previous literature [36, 37]. The samples all had low BET surface areas of 0.22 ± 0.11 m^2 g^{-1}, except for the Hydro samples, which had 1.6 m^2 g^{-1}, in agreement with standard values found in literature [34, 37]. After sulfonation, the materials retained the same BET surface areas. The results can be found in the supplemental information (Table S1).

The TGA results demonstrated that all of the materials were thermally stable in air up to 300°C and with the 450°C material up to 400°C. The sulfonated carbons lost about 10% of their mass, presumably water, before reaching their highest stable temperature. After the noted stable temperature, the materials quickly decomposed, presumably due to oxidation.

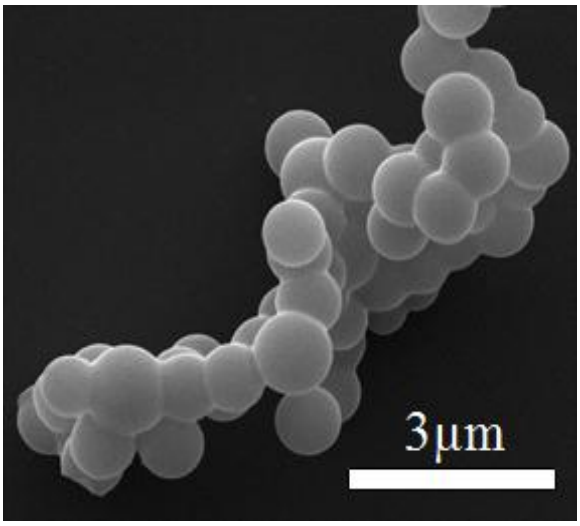

Figure 1. Scanning electron micrograph of hydrothermal carbon before sulfonation.

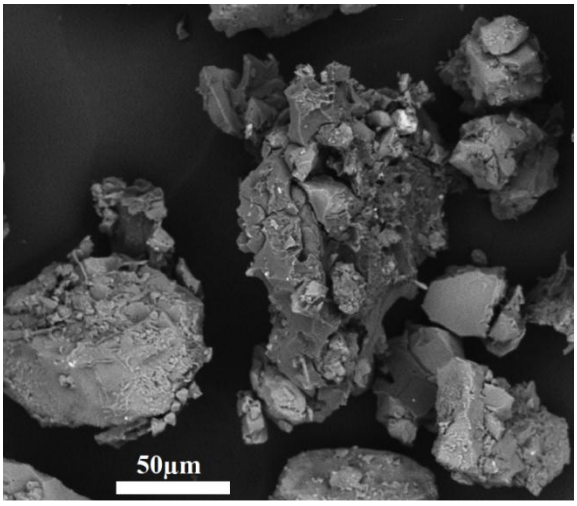

Figure 2. Scanning electron micrograph of hydrothermal carbon after sulfanilic acid sulfonation.

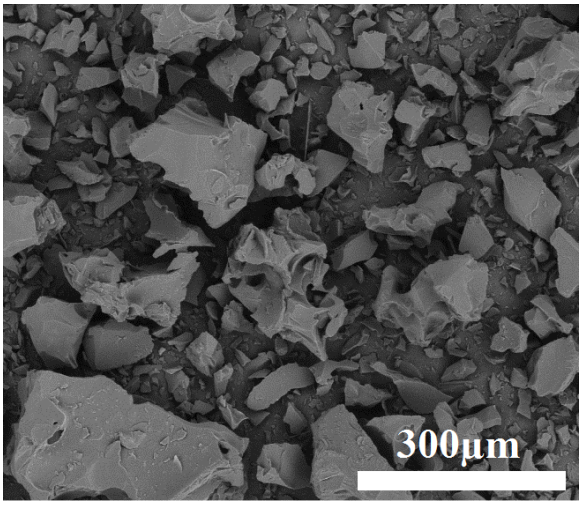

Figure 3. Scanning electron micrograph of 450°C carbon before sulfonation.

The Raman ratio of the D ("defect") and G ("graphitic") bands, commonly used in this research area, failed to provide any differentiation of structure for testing hydrothermal stability. The ratio of the defect to the graphitic peak area for all the materials was 0.7 ± 0.15, similar to literature values [38]. Figure 4, however, shows the poor peak separation, unlike pristine carbon nanotubes, which limits the information available from this commonly used ratio [39]. It has been shown that these two peaks in lower temperature char are confounded by other phenomena and cannot be strictly delineated as graphene core and edge carbons, respectively [40]. NMR (see below) shows no graphene core for the Hydro and Direct materials, and this is supported by their low C : (O+H) atomic ratios of about 0.8 : 1. Even this range of synthesis temperatures, the materials fail to show significant differences with Raman spectroscopy.

Literature reports show examples of using IR for these types of materials generated from pyrolysis [8] or hydrothermal synthesis [41]. The IR spectra show

peaks relating to OH stretching, C=O bending, OH bending, O=S=O bending, and SO_3 stretching. Unlike the NMR peak areas, the area under the IR bands are not quantitative, i.e., their area fractions do not quantitatively correspond to the fraction of the individual functional groups, since IR band intensities are distorted by variable transition-matrix elements [42]. As a result, the quantitative amount of the functional groups cannot be determined from IR spectra without extensive calibrations using reference materials. In addition, the complexity of the fingerprint region between 1500 and 500 cm^{-1} makes it difficult even to unambiguously identify oxygen-bonded aromatic C (especially when it is not protonated) or oxygen-bonded alkyl CH, OCH_3, or C-CH_3 groups, while this can be done based on ^{13}C NMR spectra, particularly when using spectra editing. Furthermore, clusters of fused aromatic rings, which are particularly relevant in carbon materials, do not show specific IR bands, whereas 1D and 2D ^{13}C NMR spectra exhibit a characteristic narrow band of nonprotonated interior aromatic carbons near 130 ppm. In a previous spectroscopic study of chars [43], IR spectra suggested that some of the materials retained a significant fraction of lignocellulosic functional groups, while quantitative ^{13}C NMR spectra, validated by large C:O ratios from elemental analysis, showed that none of the chars contained more than a few percent of carbohydrates. Therefore, the use of solid-state NMR for characterization allowed more in-depth analysis of the quantitative amounts of the functional groups than could be achieved with IR.

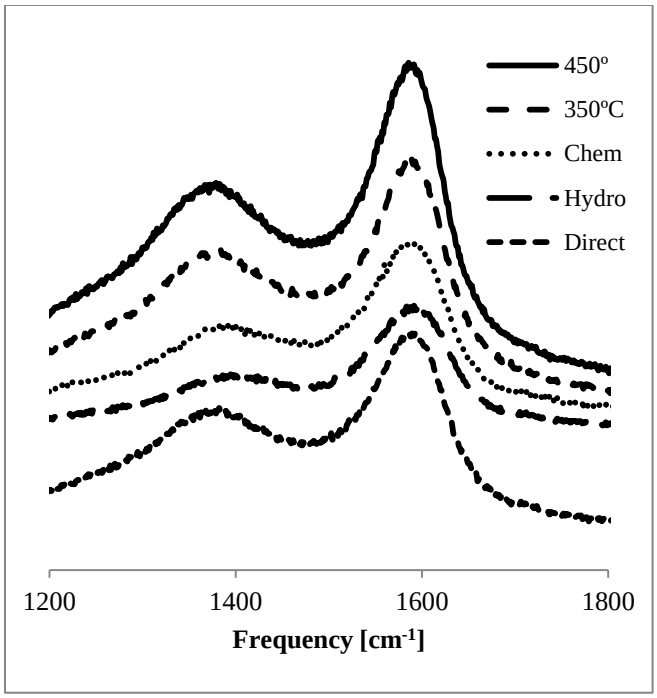

Figure 4. Stacked Raman spectra of the sulfonated carbon materials. The ratio of the peak area of the defect peak (1375 cm^{-1}) versus the graphitic peak (1575 cm^{-1}) for all materials was 0.7+/- 0.15.

The initial elemental analysis of the materials, see Figure 5, resembled the reported results for both the pyrolyzed carbon material [12] and the hydrothermal carbon [35]. The sulfonated carbons only contained C, H, N, S, and O, with the oxygen determined by difference, and carbon was the most abundant element in all samples. Figure 5 shows a general trend of decreasing oxygen content with increasing treatment temperature; in particular, the 450°C material clearly had the least oxygen. However, the Hydro materials contained slightly more oxygen than the Direct material. The synthesis used for the Chem materials resulted in significant incorporation of oxygen-free aromatic rings, which gave an overall

decrease in the weight fraction of oxygen in the resulting material. This hypothesis was confirmed by NMR spectra, which showed a substantial increase in the intensity of the 127 ppm resonance, typical of fused benzene rings. The Chem samples were the only ones with significant amounts of nitrogen, as expected from the synthesis technique. The XPS data showed the sulfur groups on all the materials to be in the reduced chemical state corresponding to the sulfonic acid group, at ca. 168 eV [44]. This value agreed satisfactorily with the sulfur peak of sulfanilic acid.

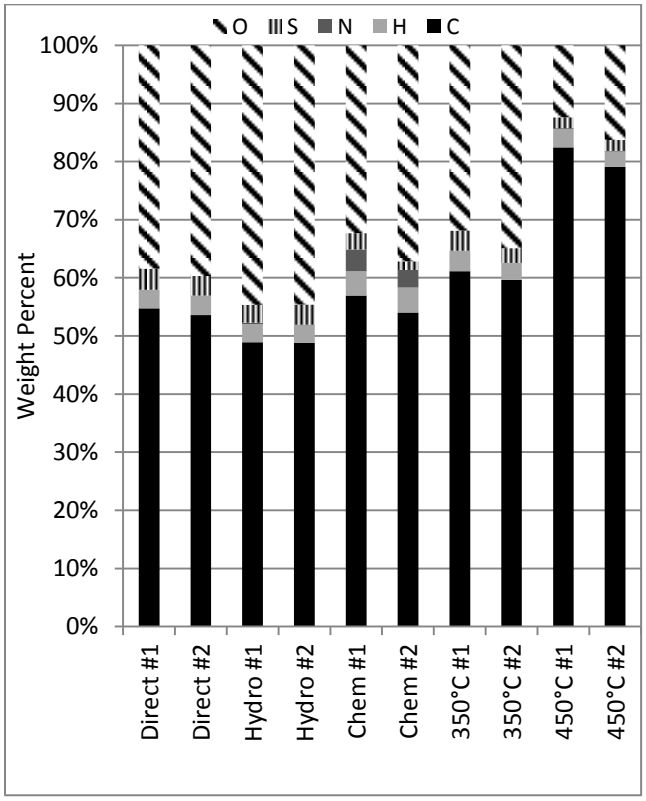

Figure 5. Initial elemental analysis of the sulfonated carbon materials.

Figure 6 shows the sulfonated carbons exhibited different amounts of acidic functional groups. Duplicate syntheses showed good reproducibility with the amount of sulfonic acid groups per gram remaining consistent. The temperature of synthesis roughly correlated with the amount of hydroxyls on the carbons: Direct < Chem ≈ Hydro ≈ 350°C < 450°C. The trend for the carboxylic acid generally followed the same trend. Consistent with the elemental analysis, the 450°C samples possessed less oxygen than the lower-temperature materials. However, comparison of the oxygen atoms in the acidic functional groups with the elemental analysis, showed that oxygen bound in acidic groups comprised only 30-50% of the total oxygen in the 450°C carbon. The Direct samples were the most similar in oxygen balance with >67% of the total oxygen accounted for by the acidic functionalities. The numbers of SO_3H groups and the COOH groups agree with other literature for the sulfonated pyrolyzed carbons [4, 29], while the number of OH groups reported in the literature was more than three times larger [4, 29] than the number of phenolic OH groups measured here. Overall, the preliminary characterization of the carbons suggested they share similarities with materials described in the recent literature.

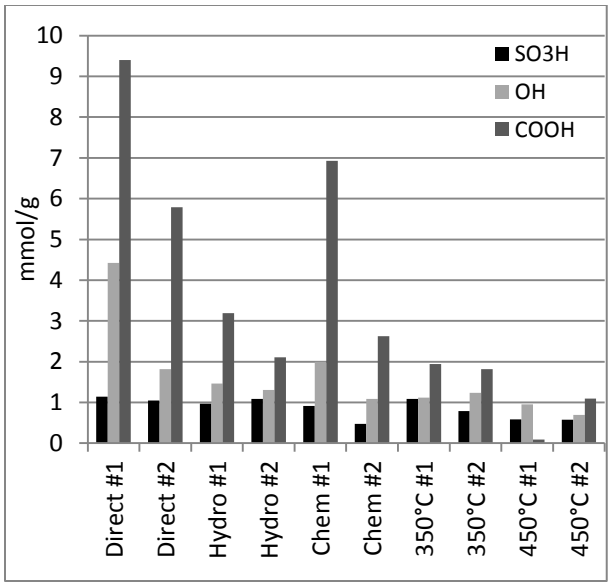

Figure 6. The acidic groups on the sulfonated carbon materials, determined by back titration.

3.1. Solid-State NMR

One-dimensional ^{13}C NMR spectra of the four sulfonated carbon materials are presented in Figure 7 and Figure 8 (the Chem samples were not characterized with NMR since their activity in reaction testing was extremely poor). Shown are quantitative (direct-polarization) ^{13}C NMR spectra of all carbons (thick line) and selective spectra of only nonprotonated carbons and CH_3 groups (thin line) in each of the sulfonated materials. In all samples, the dominant signals, observed between 100 and 155 ppm, are from aromatic carbons. Peaks of alkyl OCH groups, which resonate near 70 ppm, are not observed, indicating that complete transformation of the precursor sugar molecules has occurred as a result of both heat treatment and sulfonation. The materials show only minor signals (< 8%)

from other alkyl carbons, which demonstrates that sulfonation has effectively removed any small molecules resulting from fragmentation of furan rings, such as levulinic acid [45]. The large fraction of nonprotonated aromatic carbons (~85% of all aromatic C) revealed by the small difference between the spectra without and with dipolar dephasing indicates ample substitutions of, and linkages between, the aromatic rings. The substituents include ketones (C=O), which can resonate between 210 and 165 ppm, and COO groups (180-162 ppm). The relatively low chemical shifts of both ketones and carboxylic acids in the Direct and Hydro samples confirm that these groups are linkers and substituents on aromatic rings [45].

The lower temperature materials show a broad range of chemical shifts in the aromatic region characteristic of oxygen bonded to aromatic carbons, e.g. in phenols or furans. Oxygen not only induces a significant increase in chemical shift of the directly bonded aromatic carbon, to 140-162 ppm, but also shifts the signal of the next carbon (i.e., separated from O by two bonds) down to 95-130 ppm [34, 46]. Since all the carbons in furan rings are bonded to O (α-carbons) or two bonds from O (β-carbons), furans show only two main resonances, near 150 ppm and near 120 ppm, in 1:1 ratios. This has been nicely demonstrated on polyfurans, where the two peaks are baseline-resolved [46]. It is also confirmed in the simulated spectra of the furan components in our low-temperature samples, see bottom half of Figure 7(c) and (d); here, even with a multitude of different substituents on the furan rings, whose effects on chemical shifts can be

complicated, the two peaks are clearly resolved. The absence of a deep intensity minimum near 135 ppm in the measured spectra of our materials must be attributed to the presence of six-membered aromatic rings (termed arenes in the following), which resonate between 120 and 145 ppm.

Spectrally edited two-dimensional ^{13}C-^{13}C NMR spectra [32] shown in Figure 9 provide proof of arene rings and characterize the linkages between the aromatic rings in the Hydro sample. Figure 9(a) is a spectrum correlating signals of CH in the vertical dimensional with signals of nearby nonprotonated-C in the horizontal dimension, while Figure 9(b) shows the spectrum of directly bonded nonprotonated carbons [32]. Several characteristic peaks, in particular those of arene rings in Figure 9(a), are labeled in the spectra. Cross sections from the spectrum in Figure 9(a) are shown in Figure 10.

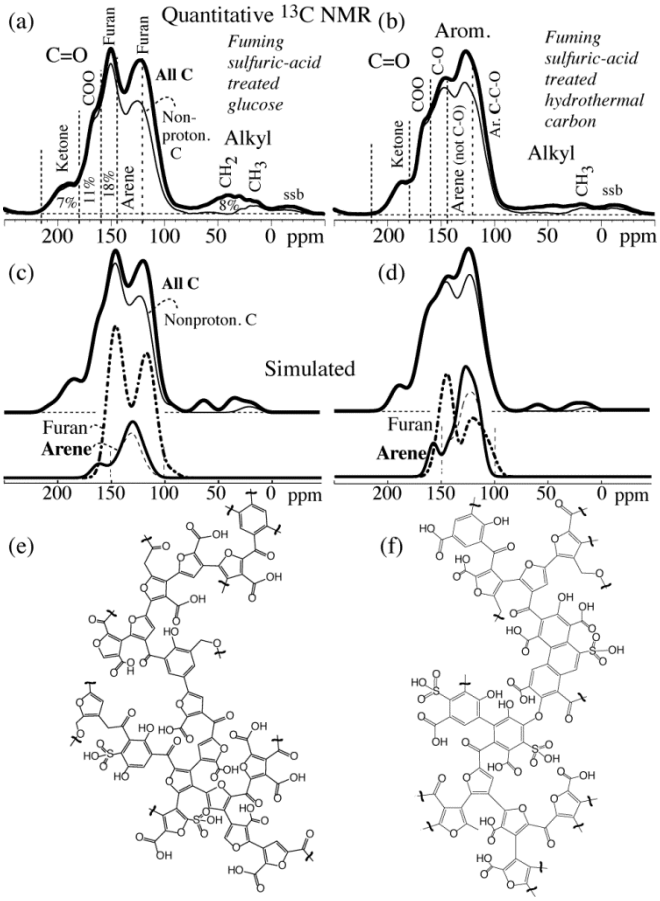

Figure 7. Quantitative ^{13}C NMR spectra of sulfonated carbon materials made from ^{13}C-enriched glucose at low temperatures. Thick line: all C; thin line: nonprotonated C as well as CH_3. "ssb": spinning sideband (14-kHz MAS). (a) Direct, (b) hydrothermal synthesis. (c, d) Corresponding simulated spectra from the structural models shown in (e, f). In (c) and (d), below the full spectra, the contributions from furan carbons (dash-dotted line), arene carbons (thick black line), and nonprotonated arene carbons (dashed lines) are also shown separately. Furan rings exhibit two peaks of similar integrated intensity at 145 and 120 ppm,

while arenes display a main peak near 130 ppm; also, the average chemical shifts of C-O in furan (147 ppm) and phenol (158 ppm) are distinctly different.

The selective 2D spectrum of nonprotonated carbons shown in Figure 9(b) exhibits the signals of linkages between aromatic rings, which must show up here since they always involve directly bonded nonprotonated carbons. The intensity distribution shows evidence for many different inter-aromatic linkages, including furan Cα-Cβ and Cβ-Cβ, and of some substitution by C=O and COO groups. The most pronounced peak is from substituted furan Cα connected to substituted furan Cα, which highlights that both sites are heavily substituted. This is also required by the large fraction of nonprotonated Cα (145-155 ppm) and Cβ (in the region < 125 ppm) detected in the quantitative spectra of Figure 7(b). These signals support the presence of the multiple types of linkages seen in the model of Figure 7(f).

Figure 9(c) shows a DQ/SQ NMR spectrum of the nonprotonated carbons in the 450^{o}C material. By far the most intense peak is observed at 130 ppm on the diagonal. It must be assigned to pairs of nonprotonated carbons (the C-CH signals have been suppressed by ^{1}H-^{13}C dipolar dephasing of ^{13}C-^{13}C double-quantum coherence [32]) in the interior of clusters of fused aromatic rings, while pairs of nonprotonated aromatic carbons connected by a single bond would resonate near 140 ppm [47]. The characteristic 130-ppm diagonal signal of polycondensed

aromatic rings is barely discernible in the corresponding spectra of the lower-temperature materials [32], see for instance Figure 9(b).

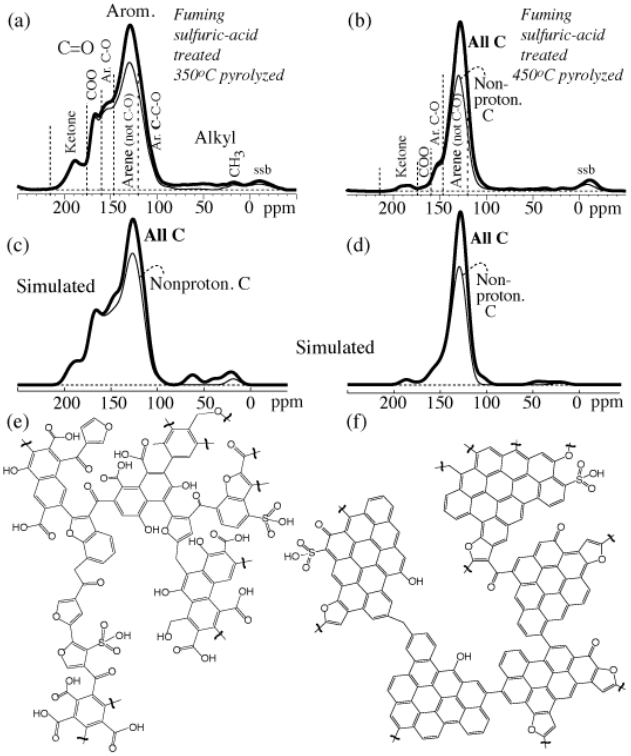

Figure 8. Quantitative ^{13}C NMR spectra of sulfonated carbon materials made from ^{13}C-enriched glucose at higher temperatures. Thick line: all C; thin line: nonprotonated C as well as CH_3. "ssb": spinning sideband (14-kHz MAS). (a) 350°C, (b) 450°C synthesis temperature. (c, d) Corresponding simulated spectra from the structural models shown in (e, f).

The carbon materials pyrolyzed above 300°C exhibit a main maximum near 130 ppm in their ^{13}C NMR spectra, see Figure 8, indicative of arene rings. In

the material pyrolyzed at 450^{o}C, this is by far the most intense peak. The low chemical shift of the nonprotonated carbons, near 130 ppm, indicates polycondensation, which is confirmed by the strong diagonal peak at 130 ppm from pairs of nonprotonated carbons in fused aromatic rings seen in the dipolar dephased DQ/SQ spectrum of Figure 9(c). Due to its higher degree of polycondensation, the 450°C material contains only a low concentration of edge sites that can easily undergo oxidation, resulting in only relatively minor changes in the backbone structure resulting from the sulfonation procedure.

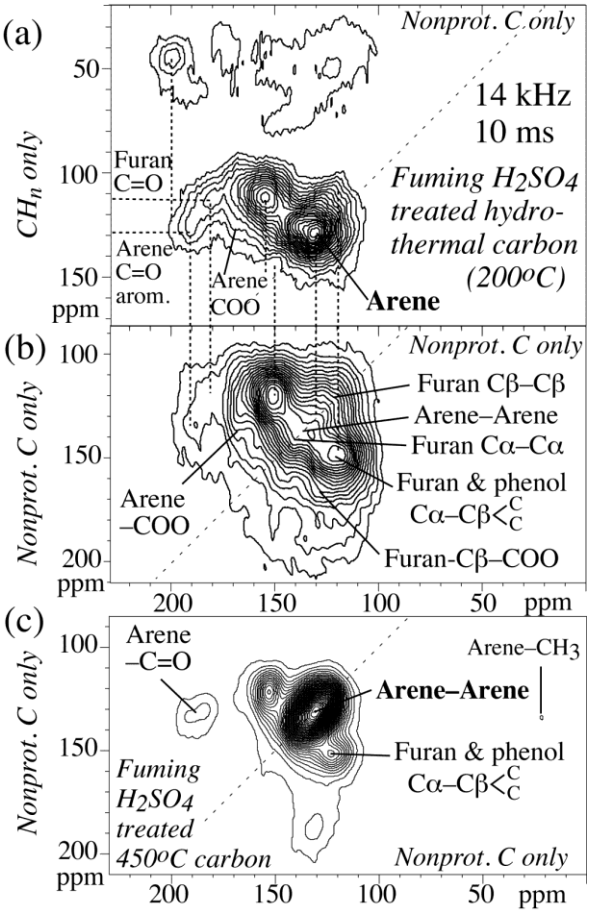

Figure 9. Two-dimensional ^{13}C-^{13}C NMR spectra with spectral editing, of (a, b) the ^{13}C-enriched Hydro material, used to identify structural units and establish their connectivities. (a) Exchange with protonated and nonprotonated spectral editing (EXPANSE) spectrum with a spin-diffusion time of 10 ms, correlating signals of CH (vertical axis) and nonprotonated C (horizontal axis). (b) Sheared dipolar-dephased double-quantum/single-quantum NMR spectrum, showing cross peaks exclusively from pairs of directly bonded nonprotonated carbons. The diagonal in the spectra (at $\omega_2 = \omega_1$) is marked by a dashed line. (c) Same as (b) for the ^{13}C-enriched sulfonated 450^{o}C material, with a dominant peak characteristic of nonprotonated carbons in polycondensed aromatic rings.

In the quantitative ^{13}C NMR spectra of Figure 7 and 8, many peaks are merged into broad spectral bands. In order to prove that our interpretation of the various shoulders and components of these broad bands is correct, selective spectra of the four materials obtained by spectral editing and 2D NMR are displayed in Figures 10, 11, S1, and S2 (see Supporting Information). For each sample, these show half a dozen peaks that are only visible as shoulders in the unselective spectrum. Peaks resolved in this way include signals from: aromatic C-H; COO (shifted by +7 ppm after Li binding); furan-bonded vs. arene-bonded vs. alkyl-bonded C=O (from EXPANSE or DQ/SQ ^{13}C-^{13}C spectra); aromatic C-O (from EXPANSE or DQ/SQ spectra); nonprotonated arene C (bonded to

protonated arene C, from EXPANSE spectrum); and CH_2-bonded arene (from EXPANSE spectrum).

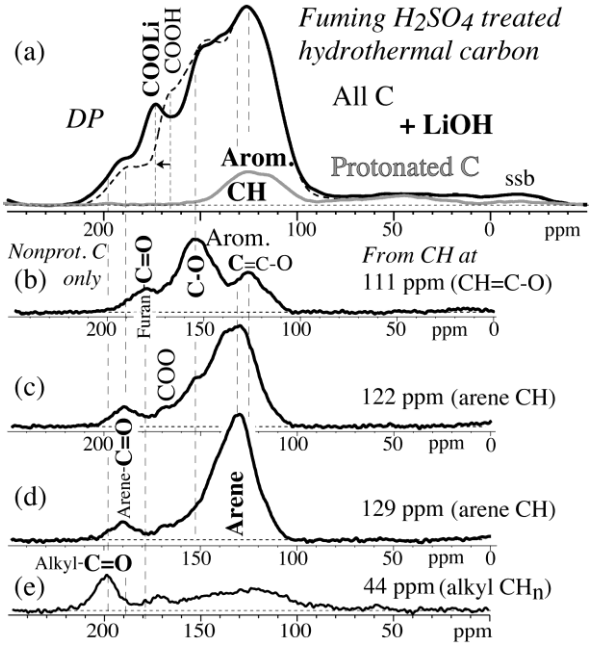

Figure 10. Selective ^{13}C NMR spectra of the ^{13}C-enriched Hydro material. (a) Full quantitative spectrum (dashed line, for reference) with corresponding selective quantitative spectrum of protonated C (gray line), obtained by dipolar-dephasing difference, and (full line) spectrum after treatment of the material with LiOH; the signal of COOLi groups is shifted by +7 ppm from that of COOH and is thus better resolved. "ssb": spinning side band. (b-e) Horizontal cross section from the 2D ^{13}C-^{13}C EXPANSE spectrum in Figure 9(a), with signals of (b) aromatic C-O bonded to aromatic CH and C=O bonded to a furan ring; (c, d) nonprotonated arene C bonded to arene CH; a peak of C=O bonded to an arene ring is also detected; and (e) C=O and other sp^2-hybridized C bonded to alkyl C.

The spectra in Figure 10(c, d), obtained as cross sections from EXPANSE ^{13}C-^{13}C spectra, show a particularly distinct peak of arene rings: CH carbons with a maximum near 127 ppm exhibit a strong correlation with nonprotonated C resonating around 131 ppm. These chemical shifts are very rare in furans, where CH usually resonates near 115 or 145 ppm and nonprotonated C near 120 or 147 ppm, but they are typical of arene rings, in particular with COO substitution. The corresponding spectra of the other materials, see Figures S1(c, d) and S2(c, d), also exhibit this arene peak, while it is completely overlapped by the furan signals in the unselective ^{13}C NMR spectra of Figure 8(a, b). In addition, the spectra show cross peaks of C=O near 190 ppm with aromatic C near 130 ppm; both chemical shifts are characteristic of arene-bonded C=O [32], confirming the presence of arene rings.

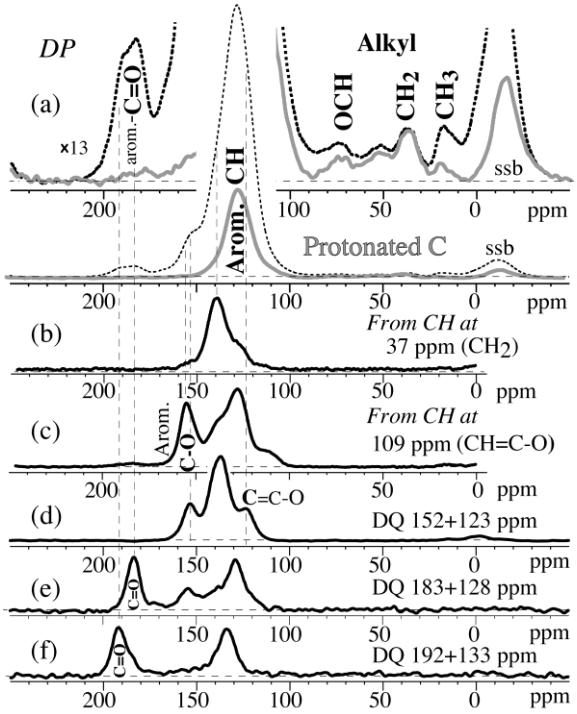

Figure 11. Selective ^{13}C NMR spectra of the ^{13}C-enriched sulfonated 450^{o}C material. (a) Full quantitative spectrum (dashed line, for reference) with corresponding selective quantitative spectrum of protonated C (gray line), obtained by dipolar-dephasing difference; the top traces show the spectra vertically expanded by a factor of 13. "ssb": spinning side band. (b, c) Horizontal cross sections from 2D ^{13}C-^{13}C EXPANSE spectrum, with signals of (b) 140-ppm arene C bonded to CH_2 resonating at 37 ppm, and (c) aromatic C-O bonded to aromatic CH. (d-f) Horizontal cross sections from a dipolar-dephased DQ/SQ ^{13}C-^{13}C correlation spectrum (not sheared), with signals of (d) aromatic C-O and neighboring nonprotonated aromatic C; (e) C=O at 183 ppm and its bonded aromatic C at 128 ppm; and (f) C=O at 192 ppm and its bonded aromatic C at 133 ppm.

Based on the NMR-derived percentages of the carbons in the various functional groups compiled in Table 2 and taking into account the elemental composition as well as linkages established by 2D NMR, structural models have been generated, see Figure 7(e, f) and Figure 8(e, f). The structures have been adjusted such that the corresponding simulated spectra, see Figure 7(c, d) and Figure 8(c, d), match the main features of the quantitative ^{13}C NMR spectra. As expected given the pronounced differences between the experimental spectra in Figure 7 and Figure 8, the models show significant differences in the molecular structures comprising this suite of materials. The arene:furan ratios and degree of condensation (aromatization) increase with processing temperature, and functional group substitutions also change.

The sulfonated glucose (Direct sample) contains predominantly furan rings, as proved by (i) strong cross peaks between protonated alkyl carbon and aromatic C-O, [32] which are impossible in phenols or arene ethers; (ii) the similar intensity of the pair of peaks at 150 and 123 ppm in Figure 7a, while the intensity at 150 ppm would be lower in phenols; and (iii) the low chemical shifts of C=O (<195 ppm) and COO (<165 ppm) groups, which are characteristic of bonding to furan [32]. The furan rings are linked via direct C_α-C_β, C_α-C_α, and C_β-C_β bonds, as well as ketones and a few alkyls. The furan rings are also heavily substituted with carboxylic acids. Some arene formation has also occurred but to a rather limited extent. The characteristic signal of interior carbons in

polycondensed arene rings is not observed in the selective 2D spectrum of nonprotonated C [32].

The structure in Figure 7(e), with a large fraction of ketone and acid groups linked directly to furan rings, has not been often reported in the literature and seems to be characteristic of a carbohydrate subjected to oxidation by hot, concentrated fuming sulfuric acid. Without NMR, this highly aromatic material might appear as consisting of polycondensed aromatic rings substituted with SO_3H groups [28] as well as many electron-withdrawing OH, –O–, COOH, and C=O moieties. This model can be directly refuted, even without detailed chemical-shift and cross-peak analysis, based on the large fractions of edge carbons that are aromatic and bonded to H, O, COO, C=O, SO_3, or to alkyl C, which account for 17, 24, >10, >5, >3, and >2%, respectively (see Table 2). The total of these carbons that cannot be in the interior of a polycondensed aromatic cluster is >61%, to be compared with <17% of other aromatic carbons that could be in the interior of a cluster (or linked to another aromatic C through a single bond). Such a small fraction of interior carbons does not permit construction of polycondensed clusters of significant size.

Sulfonation of hydrothermal carbon produces a material with a larger arene:furan ratio, which is nearly 1:1 on a carbon-atom basis. The arene groups, proved by the spectra in Figure 9(a) and 10(c, d), are linked individual rings and have not polycondensed to a significant degree. This is proved by the absence of a strong peak at 130 ppm near the diagonal in the 2D spectrum of nonprotonated

carbons, Figure 9b. Our model incorporates the arene with the furan rings, which is contrary to models proposed in a previous publication for hydrothermal char without sulfonation [45]. This conclusion is further supported by 2D exchange NMR spectra with long mixing times that show no domain separation (data not shown). Similarly as in the Direct sample, numerous ketone linkers, with characteristic NMR signals, connect arene and furan aromatic rings, and these rings are heavily substituted with carboxylic acid groups. While the fuming sulfuric acid treatments result in nearly complete conversion of carbohydrates to aromatic carbons, it does not catalyze the polycondensation of the aromatic rings, which is only achieved by higher-temperature treatment.

Our sulfonated 350°C carbon model in Figure 8(e), although more condensed than that of the Hydro material, does not contain large polycondensed aromatic sheets, again supported by the absence of a strong peak at 130 ppm near the diagonal in the spectrum of nonprotonated carbons [32]. Instead, it is mainly composed of naphthalene units, benzofurans, arenes, and a small fraction of individual furan rings. The abundance of ketone linkers and carboxylic acid groups, directly based on NMR peak areas, is reduced compared to either the Direct or the Hydro material, which can be attributed to a lower amount of sites that are susceptible to oxidation in the precursor material. Our analysis shows that polycondensation does not occur to a significant extent until above 350°C.

Models containing large (>5 rings) polycondensed aromatic units, as proposed in the literature even for materials heated to only 350^{o}C [48], are

plausible only for carbohydrate materials heated to significantly higher temperatures. For instance, the model in reference [48] with more than a dozen fused aromatic rings corresponds to elemental ratios of C:H:O:S = 1 : 0.32 : 0.12 : 0.02, completely inconsistent with the measured elemental compositions [48] of C:H:O:S = 1 : 0.71 : 0.58 : 0.011 at 300^{o}C and 1 : 0.45 : 0.39 : 0.014 at 400^{o}C.

At higher temperatures, the structures of the materials begin to appear like those postulated in literature. In the sulfonated 450°C carbon, the aromatic rings have undergone polycondensation reactions to a significant extent, nearly all furan rings have been removed, and virtually no carboxylic acid groups have been introduced from the sulfonation procedure. These data show that the suite of materials produced here contain substantially different structures, and they indicate that while fuming sulfuric acid treatment produces five- and six-membered aromatic rings, thermal treatment at > 350^{o}C is required to induce significant polycondensation of aromatic rings. This data complements the existing knowledge about carbons and their structure, especially filling in details about the structures resulting from lower temperature pyrolysis.

Additionally, we were able to use the NMR-based structural analysis to test the utility of less involved methods such as Raman spectroscopy. Our structural analysis shows that the Raman methods used to indicate the graphitic character and defect sites of high temperature carbons are not reliable for low temperature materials. Raman analysis would lead to grossly incorrect conclusions about the material structure. The Direct sample shows a strong peak

at 1575 cm^{-1}, see Figure 4, which is usually taken to indicate a highly graphitic character. In contrast, NMR clearly shows that this material is predominantly furanic with only minor fraction of arene rings, which is supported by the relatively low C:(O+H) atomic ratio. On the other hand, the NMR spectra clearly identify polycondensed aromatic rings in the 450^{o}C sample. Advanced solid-state NMR techniques can achieve a level of detail unmatched by conventional characterization methods.

3.2 Hydrothermal Treatment and Reaction Testing

The sulfonated carbons were tested for their hydrothermal stability using the protocol given in the Experimental section. Shown in Figure 12 is the elemental analysis for the sulfonated carbons through the progression of stability testing. As demonstrated by the NMR characterization, the overall chemical structures for these materials were quite different. Despite the range of structures, the differences in hydrothermal stability for the range of sulfonated materials were relatively small. The first hydrothermal treatment (24 hr at 160°C) significantly reduced the sulfur content for all of the sulfonated carbons. As clearly demonstrated from elemental analysis, the sulfonic groups could not withstand extended exposure to condensed-phase water at 160°C. With subsequent treatments, the sulfur content continued to diminish significantly in all the materials never asymptoting to a stable value. The least stable material, the 450°C carbon, lost >90% of its original sulfur content. The other catalysts,

Hydro, Direct, 350°C, and Chem, retained similar percentages of original sulfur 50% ±20%. Most of the sulfur was lost in the first hydrothermal treatment and less was generally lost in subsequent treatments. The carbon structures with more furan rings (Direct & Hydro) retained slightly more sulfur than the carbon structures with more arene rings (350º & 450º). The well-known equilibrium incorporating sulfate groups on the aromatic rings, which was strongly favored by the excess sulfur acid present during the synthesis worked in reverse under the harsh hydrothermal conditions. The ICP results for the water phase after hydrothermal treatment (data not shown) validated the considerable leaching seen with all of the sulfonated carbons. While literature reports have suggested enhanced stability based on less severe hydrothermal treatments, the carbon sulfur bond produced from electrophilic substitution on a double bond undoubtedly hydrolyzes in 160ºC condensed-phase water to release the sulfur independently of the overall amount of substitution on the arene carbons.

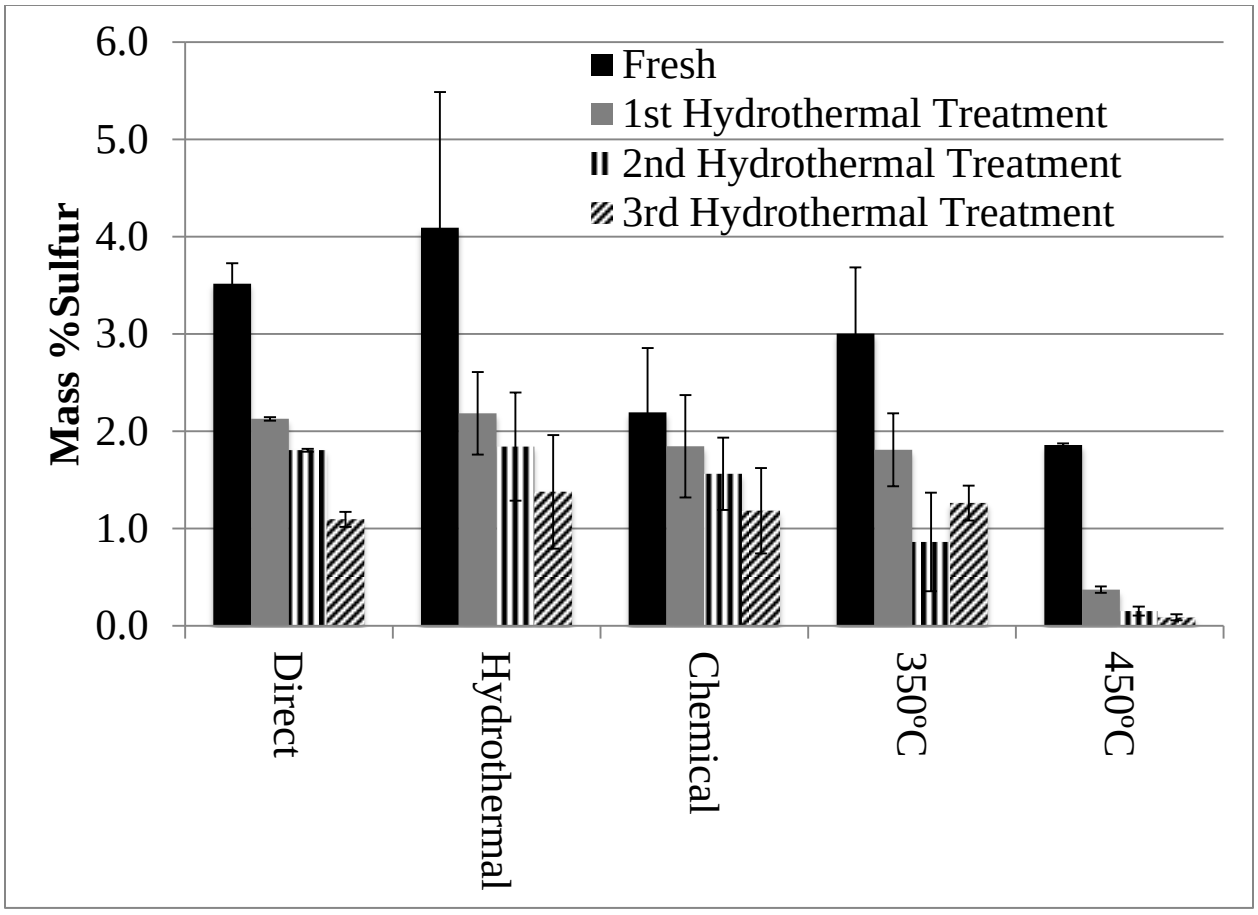

Figure 12. Sulfur elemental analysis of the sulfonated carbons throughout the hydrothermal testing. Hydrothermal testing was 160ºC in liquid water (autogenous pressure) for 24 hours.

Results for reaction testing of the sulfonated carbons are summarized in Figure 13. A preferred carbonization temperature, which has been a phenomenon reported in the literature,[21] was observed for the lower synthesis temperatures in this work as the 350°C, Hydro, and Direct (200°C and 150°C synthesis) materials had much better reaction rates than the 450°C or Chem samples. After hydrothermal treatment, however, even these catalysts did not retain significant

activity nor did they plateau to a consistent value after three treatments. The Chem catalysts, while synthesized from the hydrothermally created carbon, did not share the same reaction rates as the Hydro catalysts even though the Chem catalysts retained sulfur reasonably well. In the supplemental information (Figure S3), the calculated turnover frequency based on the number of acid sites is shown. The trend for the materials was consistent with the overall reaction rates given in Figure 12. As can be seen from the data, the sulfonated carbons performed poorly after hydrothermal treatment, which further validated the poor stability of all these materials under aggressive hydrothermal conditions.

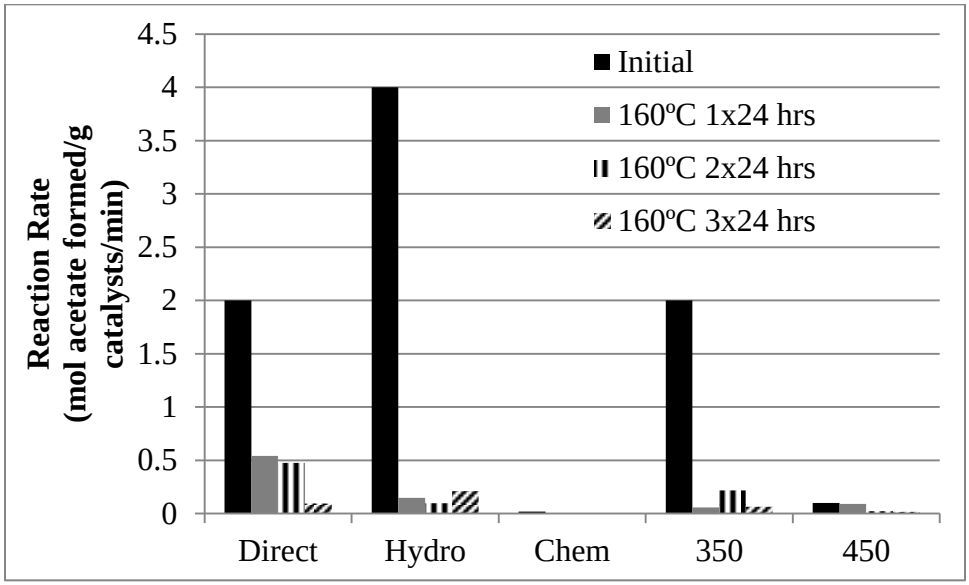

Figure 13. Reaction rate data throughout the hydrothermal treatments.

4. Conclusions

Hydrothermal-stability testing of sulfonated carbon catalysts from glucose, synthesized analogously to materials reported recently, showed that these catalysts do not appear to be industrially viable above 160°C, as the sulfonic groups continue to leach after exposure to condensed water. By analyzing a suite of materials with different structures, we tested how their structure, characterized in detail by quantitative ^{13}C NMR with spectral simulations, affects the hydrothermal stability. Structures ranged from tightly linked individual furan and arene rings, to fused aromatic clusters of about 1 nm diameter. The results showed that differences in the aromatic structures had only a small effect on the stability of these materials and all the sulfonated carbons proved to be unsuitable under extended hydrothermal testing at 160°C. The carbon supports with greater content of oxygen and furan rings fared somewhat better through the hydrothermal treatments suggesting that furan-carbon–sulfur bonds are slightly less susceptible to hydrolysis than are arene carbon–sulfur bonds. Nevertheless, all the catalysts lost significant amounts of their sulfur (>90%) making their utilization ultimately problematic. The sulfur loss itself was expected from the reversible reaction, however the amounts were not known up until this study. The rate of sulfur loss for the sulfonated carbons was considerable during the initial water exposure and then generally slowed with successive treatments, but it showed no sign of reaching an asymptotic limit. The lower temperature chars (Direct & Hydro) retained a slightly higher percentage of sulfur than the higher

temperature chars (350º & 450º) leading to the postulate that sulfur might be slightly better retained in the more furanic structures present in the lower temperature chars versus the arene structures of the higher temperature chars. Importantly, the sulfur loss from the sulfonated carbons never reached a plateau. Subsequent research is needed to determine if a different chemical attachment of the sulfonic acid groups can lead to a truly hydrothermally stable sulfonated carbon catalyst.

5. Acknowledgements

The authors would like to acknowledge NSF Award number EEC-0813570 for generously supporting this work. Purchase of the Perkin Elmer 2100 Series II CHN/S analyzer used to obtain results included in this publication was supported in part by the National Science Foundation under Grant No. DBI 9413969. We wish to thank ISU Chemical Instrumentation Facility staff members Stephen Veysey for training and assistance pertaining to the PE 2100 CHN/S elemental analysis. Keith Fritzsching developed the coding for transferring ACD NMR chemical shifts into MatLab. The authors would like to acknowledge undergraduates that worked on the project: Molly Lohry, Cherita Young, Ashley Leitner, and Scott Nauert. Jim Anderegg graciously ran and expertly helped interpret the XPS results. Any opinions, findings, and conclusions, or

recommendations expressed herein are those of the authors and do not necessarily reflect the views of the National Science Foundation.

References

[1] Peng L, Philippaerts A, Ke X, Van Noyen J, De Clippel F, Van Tendeloo G, et al. Preparation of sulfonated ordered mesoporous carbon and its use for the esterification of fatty acids. Catalysis Today. 2010;150(1-2):140-6.

[2] Luque R, Budarin V, Clark JH, Macquarrie DJ. Microwave-assisted preparation of amides using a stable and reusable mesoporous carbonaceous solid acid. Green Chemistry. 2009;11(4):459-61.

[3] Luque R, Budarin V, Clark JH, Macquarrie DJ. Glycerol transformations on polysaccharide derived mesoporous materials. Applied Catalysis, B: Environmental. 2008;82(3-4):157-62.

[4] Kitano M, Yamaguchi D, Suganuma S, Nakajima K, Kato H, Hayashi S, et al. Adsorption-Enhanced Hydrolysis of β-1,4-Glucan on Graphene-Based Amorphous Carbon Bearing SO3H, COOH, and OH Groups. Langmuir. 2009;25(9):5068-75.

[5] Hara M. Biodiesel Production by Amorphous Carbon Bearing SO3H, COOH and Phenolic OH Groups, a Solid Bronsted Acid Catalyst. Topics in Catalysis. 2010;53(11-12):805-10.

[6] Luque R, Clark JH. Water-tolerant Ru-Starbon materials for the hydrogenation of organic acids in aqueous ethanol. Catalysis Communications. 2010;11(10):928-31.

[7] Xing R, Liu Y, Wang Y, Chen L, Wu H, Jiang Y, et al. Active solid acid catalysts prepared by sulfonation of carbonization-controlled mesoporous

carbon materials. Microporous and Mesoporous Materials. 2007;105(1-2):41-8.

[8] Suganuma S, Nakajima K, Kitano M, Yamaguchi D, Kato H, Hayashi S, et al. Hydrolysis of cellulose by amorphous carbon bearing SO3H, COOH, and OH groups. Journal of the American Chemical Society. 2008;130(38):12787-93.

[9] Liang X, Yang J. Synthesis of a Novel Carbon Based Strong Acid Catalyst Through Hydrothermal Carbonization. Catalysis Letters. 2009;132(3-4):460-3.

[10] Kitano M, Arai K, Kodama A, Kousaka T, Nakajima K, Hayashi S, et al. Preparation of a Sulfonated Porous Carbon Catalyst with High Specific Surface Area. Catalysis Letters. 2009;131(1-2):242-9.

[11] Tian X, Su F, Zhao XS. Sulfonated polypyrrole nanospheres as a solid acid catalyst. Green Chemistry. 2008;10(9):951-6.

[12] Hara M, Yoshida T, Takagaki A, Takata T, Kondo JN, Hayashi S, et al. A Carbon Material as a Strong Protonic Acid. Angewandte Chemie International Edition. 2004;43(22):2955-8.

[13] Budarin VL, Clark JH, Luque R, Macquarrie DJ, Koutinas A, Webb C. Tunable mesoporous materials optimized for aqueous phase esterifications. Green Chemistry. 2007;9(9):992-5.

[14] Petrus L, Stamhuis EJ, Joosten GEH. Thermal deactivation of strong-acid ion-exchange resins in water. Industrial & Engineering Chemistry Product Research and Development. 1981;20(2):366-71.

[15] Zaiku Xie, Xie, Xie Z. An overview of recent development in composite catalysts from porous materials for various reactions and processes. International journal of molecular sciences. 2010;11(5):2152.

[16] Onda A, Ochi T, Yanagisawa K. Hydrolysis of Cellulose Selectively into Glucose Over Sulfonated Activated-Carbon Catalyst Under Hydrothermal Conditions. Topics in Catalysis. 2009;52(6-7):801-7.

[17] Mo X, Lotero E, Lu C, Liu Y, Goodwin JG. A Novel Sulfonated Carbon Composite Solid Acid Catalyst for Biodiesel Synthesis. Catalysis Letters. 2008;123(1-2):1-6.

[18] Mo X, Lopez DE, Suwannakarn K, Liu Y, Lotero E, Goodwin JG, Jr., et al. Activation and deactivation characteristics of sulfonated carbon catalysts. Journal of Catalysis. 2008;254(2):332-8.

[19] Yamaguchi D, Hara M. Starch saccharification by carbon-based solid acid catalyst. Solid State Sciences. 2010;12(6):1018-23.

[20] Lou W-Y, Guo Q, Chen W-J, Zong M-H, Wu H, Smith TJ. A Highly Active Bagasse-Derived Solid Acid Catalyst with Properties Suitable for Production of Biodiesel. ChemSusChem. 2012;5(8):1533-41.

[21] Hara M, Okamura M, Toda M, Kondo JN, Takagaki A, Domen K, et al. Sulfonated incompletely carbonized glucose as strong Bronsted acid

catalyst. Studies in Surface Science and Catalysis. 2007;172(Science and Technology in Catalysis 2006):405-8.

[22] Franklin RE. Homogeneous and heterogeneous graphitization of carbon. Nature (London, United Kingdom). 1956;177:239.

[23] Zhang B, Ren J, Liu X, Guo Y, Guo Y, Lu G, et al. Novel sulfonated carbonaceous materials from p-toluenesulfonic acid/glucose as a high-performance solid-acid catalyst. Catalysis Communications. 2010;11(7):629-32.

[24] Xiao H, Guo Y, Liang X, Qi C. One-step synthesis of novel biacidic carbon via hydrothermal carbonization. J Solid State Chem. 2010;183(7):1721-5.

[25] Boonoun P, Laosiripojana N, Muangnapoh C, Jongsomjit B, Panpranot J, Mekasuwandumrong O, et al. Application of Sulfonated Carbon-Based Catalyst for Reactive Extraction of 1,3-Propanediol from Model Fermentation Mixture. Ind Eng Chem Res. 2010;49(24):12352-7.

[26] Bahr JL, Yang J, Kosynkin DV, Bronikowski MJ, Smalley RE, Tour JM. Functionalization of Carbon Nanotubes by Electrochemical Reduction of Aryl Diazonium Salts: A Bucky Paper Electrode. Journal of the American Chemical Society. 2001;123(27):6536-42.

[27] Miao S, Shanks BH. Esterification of biomass pyrolysis model acids over sulfonic acid-functionalized mesoporous silicas. Applied Catalysis A: General. 2009;359(1-2):113-20.

[28] Mirkhani V, Moghadam M, Tangestaninejad S, Mohammadpoor-Baltork I, Mahdavi M. Preparation of an improved sulfonated carbon-based solid acid as a novel, efficient, and reusable catalyst for chemoselective synthesis of 2-oxazolines and bis-oxazolines. Monatshefte fuer Chemie. 2009;140(12):1489-94.

[29] Suganuma S, Nakajima K, Kitano M, Yamaguchi D, Kato H, Hayashi S, et al. Synthesis and acid catalysis of cellulose-derived carbon-based solid acid. Solid State Sciences. 2010;12(6):1029-34.

[30] Mao JD, Schmidt-Rohr K. Accurate Quantification of Aromaticity and Nonprotonated Aromatic Carbon Fraction in Natural Organic Matter by 13C Solid-State Nuclear Magnetic Resonance. Environmental Science & Technology. 2004;38(9):2680-4.

[31] Takegoshi K, Nakamura S, Terao T. C13-H1 dipolar-assisted rotational resonance in magic-angle spinning NMR. Chem Phys Lett. 2001;344:631-7.

[32] Johnson RL, Anderson JM, Shanks BH, Fang X, Hong M, Schmidt-Rohr K. Spectrally edited 2D 13C13C NMR spectra without diagonal ridge for characterizing 13C-enriched low-temperature carbon materials. J Magn Reson. 2013;234:112-24.

[33] Hohwy M, Rienstra CM, Jaroniec CP, Griffin RG. Fivefold symmetric homonuclear dipolar recoupling in rotating solids: Application to double quantum spectroscopy. J Chem Phys. 1999;110:7983-92.

[34] Demir-Cakan R, Baccile N, Antonietti M, Titirici M-M. Carboxylate-Rich Carbonaceous Materials via One-Step Hydrothermal Carbonization of Glucose in the Presence of Acrylic Acid. Chemistry of Materials. 2009;21(3):484-90.

[35] Sevilla M, Fuertes AB. The production of carbon materials by hydrothermal carbonization of cellulose. Carbon. 2009;47(9):2281-9.

[36] Torri C, Samorì C, Adamiano A, Fabbri D, Faraloni C, Torzillo G. Preliminary investigation on the production of fuels and bio-char from Chlamydomonas reinhardtii biomass residue after bio-hydrogen production. Bioresource Technology. 2011;102(18):8707-13.

[37] Takagaki A, Toda M, Okamura M, Kondo JN, Hayashi S, Domen K, et al. Esterification of higher fatty acids by a novel strong solid acid. Catalysis Today. 2006;116(2):157-61.

[38] Nakajima K, Okamura M, Kondo JN, Domen K, Tatsumi T, Hayashi S, et al. Amorphous Carbon Bearing Sulfonic Acid Groups in Mesoporous Silica as a Selective Catalyst. Chemistry of Materials. 2008;21(1):186-93.

[39] Yun S, Heo Y, Im H, Kim J. Sulfonated multiwalled carbon nanotube/sulfonated poly(ether sulfone) composite membrane with low methanol permeability for direct methanol fuel cells. Journal of Applied Polymer Science. 2012;126(S2):E513-E21.

[40] Knauer M, Schuster ME, Su D, Schlögl R, Niessner R, Ivleva NP. Soot Structure and Reactivity Analysis by Raman Microspectroscopy,

Temperature-Programmed Oxidation, and High-Resolution Transmission Electron Microscopy. The Journal of Physical Chemistry A. 2009;113(50):13871-80.

[41] Kang S, Ye J, Zhang Y, Chang J. Preparation of biomass hydrochar derived sulfonated catalysts and their catalytic effects for 5-hydroxymethylfurfural production. RSC Advances. 2013;3(20):7360-6.

[42] Levine IN. Molecular Spectroscopy: Wiley-Interscience; 1975.

[43] Brewer CE, Schmidt-Rohr K, Satrio JA, Brown RC. Characterization of biochar from fast pyrolysis and gasification systems. Environ Prog Sustainable Energy. 2009;28(3):386-96.

[44] Shu Q, Gao J, Nawaz Z, Liao Y, Wang D, Wang J. Synthesis of biodiesel from waste vegetable oil with large amounts of free fatty acids using a carbon-based solid acid catalyst. Applied Energy. 2010;87(8):2589-96.

[45] Baccile N, Laurent G, Babonneau F, Fayon F, Titirici M-M, Antonietti M. Structural Characterization of Hydrothermal Carbon Spheres by Advanced Solid-State MAS 13C NMR Investigations. The Journal of Physical Chemistry C. 2009;113(22):9644-54.

[46] Burket CL, Rajagopalan R, Marencic AP, Dronvajjala K, Foley HC. Genesis of porosity in polyfurfuryl alcohol derived nanoporous carbon. Carbon. 2006;44(14):2957-63.

[47] Ewing DF. Carbon-13 substituent effects in monosubstituted benzenes. Org Magn Reson. 1979;12(9):499-524.

[48] Okamura M, Takagaki A, Toda M, Kondo JN, Domen K, Tatsumi T, et al. Acid-Catalyzed Reactions on Flexible Polycyclic Aromatic Carbon in Amorphous Carbon. Chemistry of Materials. 2006;18(13):3039-45.

CHAPTER 3.

HYDROTHERMAL DEGRADATION OF MODEL SULFONIC ACID COMPOUNDS: PROBING THE RELATIVE SULFUR–CARBON BOND STRENGTH IN WATER

A paper to be submitted to Catalysis Communications

Jason M Anderson, Robert L Johnson, Klaus Schmidt-Rohr, Brent H Shanks

Abstract

Development of heterogeneous catalysts for the biorenewables industry requires catalyst materials that are resistant to hydrothermal degradation. Unlike metal oxides and silica, carbon materials are recalcitrant to hydrothermal conditions. However, for solid-acid sulfonated carbon materials, there are conflicting reports on the stability of the sulfonic-acid groups on the aromatic rings for commercial applications. Currently, incomplete understanding remains about the relationship between hydrothermal stability and the immediate electronic hybridization of the carbon atoms adjacent to the sulfonic-acid active group. To test this relation systematically, model compounds containing sulfonic acid groups linked to aromatic, alkane, or cycloalkane carbon atoms were subjected to hydrothermal conditions (100°, 130°, and 160°C DI water up to 24

h). The structural integrity of the compounds was monitored with solution NMR. While the aromatic-sulfonic compounds degrade readily, the changes in the molecules with alkyl sulfonic acid linkages are negligible. Therefore, a hydrothermally stable sulfonic-acid catalyst needs to contain the sulfur attached via alkyl linkers.

1. Introduction

Development of heterogeneous catalysts for transforming carbohydrate and other bio-derived feedstocks into higher-value chemicals will require catalyst materials that are stable in condensed phase. Carbohydrates are quite reactive compared to hydrocarbons, and using catalysts in gas phase reactors results in poor selectivity and rapid coke formation [1, 2]. Water under hydrothermal conditions (typically pressurized at 120-250^{o}C) [3, 4] is physically destructive to a large number of materials, including silica, metal oxides such as gamma alumina, and numerous functionalized polymers [5-7]. Metal oxides are by far the most widely used support materials in the petroleum industry, while silica, carbon, and polymer resins have found only limited applications. Carbon is quite resistant to hydrothermal breakdown and shows promise to be viable support and catalyst for hydrothermal reactors. It can be produced at relatively low cost from a wide variety of feedstocks including lignocellulosic materials and carbohydrates.

The use of solid carbon-based acid catalysts with sulfonic acid functionality is a promising approach to replace sulfuric acid used in numerous

applications including cellulose hydrolysis, sugar dehydration, and transesterification of biodiesel. These materials can be produced in a simple two-step process using glucose pyrolysis at temperatures ranging from 350-550^{o}C followed by sulfonation [8, 9] with fuming sulfuric acid, or sulfur trioxide. Electrophilic aromatic substitution is the predominant mechanism forming the C-SO_3 bond and these treatments result in nearly complete removal of alkyl carbons, and minor additional polycondensation [10, 11]. Sulfonated carbon materials produced using this method have sulfonic-acid groups linked to aromatic carbons, and are highly acidic due to the electronegativity of the aromatic system [10, 11]. These materials are highly active, but their hydrothermal stability is not certain. A spectrum of carbon materials, produced at a range of temperatures, were sulfonated, and tested for hydrothermal stability. All readily lost activity through hydrolysis and leaching of sulfur [10], which indicates that these materials are likely not suitable for commercial applications [11]. Given the difficulty of characterizing the location of sulfur in the chemical structure, it was not possible to draw conclusions about the effects of the local structure on sulfonate stability, including the influence of adjacent groups and carbon hybridization, and temperature at which degradation occurred [12, 13]. The literature suggests that bonding of S to aliphatic C would be more stable [14] but a systematic comparison of hydrothermal stability has not been published. This current work seeks to investigate these effects by using model compounds that simulate various active sites on a carbon surface.

The molecule types chosen for stability analysis included sulfonic-acid groups bonded to aromatic, saturated cyclic, and straight chain aliphatic structures. It has been proposed in the literature that an increase in electron-withdrawing functional groups near an aromatic-bound sulfonic acid would lead to increased stability of the carbon–sulfur bond [15]. To test this hypothesis, we compare trimethylbenzene sulfonic acid, trinitrosulfonic acid, and benzenesulfonic acid, which represent electron donation, withdrawal, and the control case, respectively. To compare alicyclic versus aromatic rings, cyclohexane and benzene sulfonic acid were included in the study. Linear aliphatic compounds were also investigated. The chain length dependence, important for silica attachments [16, 17], was explored with methane sulfonic acid, butane sulfonic acid, and octane sulfonic acid. The study of the degradation behavior of all these sulfonic acids enable us to make specific comparisons about stability of the carbon-sulfur bond and its dependence on its immediate chemical environment.

2. Experimental

2.1 Materials

The trimethylbenzene sulfonic acid, trinitrosulfonic acid, benzenesulfonic acid, cyclohexane sulfonic acid, sodium butane sulfonate, sodium octane sulfonate, and deuterium oxide were purchased from Sigma Aldrich. Hydrochloric acid was purchased from Fisher Scientific. All chemical were used

without further purification. The chemical was acidified if it was in the salt form by adding an equivalent molar amount of HCl to the salt.

2.2 Methods

Each sulfonic acid was placed into a Parr reactor at 160ºC at a 100 mmol/g concentration in D_2O for initial hydrothermal treatment and it also was used to verify safety of the chemical (some compounds created significant pressures when heated). The trinitrobenezensulfonic acid caused the greatest safety concerns as it needed to be vented during the hydrothermal testing to ensure safe operating conditions. If the compound did not generate pressure, it was subsequently placed in Altech glass vials for the 130ºC and 100ºC testing. In this way, all the compounds were tested at the three different temperatures. Samples were taken at time points of 0 (when the Parr reactor was up to temperature, ramp rate of 10ºC/min), 1, 6, 12, 18, and 24 hours. Solution NMR was used for species identification.

Since the sulfonic acids with a benzene backbone generated a solid via carbonization, elemental analysis was done on both the liquid filtrate and the solid to determine the amount of sulfur in each. To prevent the solids from interfering with solution NMR, the resulting sample was filtered with a 0.2 µm filter before analysis. The filtrate and solids were analyzed via elemental analysis, ICP-AES, and XPS to determine the amount and oxidation number of sulfur left in each phase.

3. Characterization

^{1}H and ^{13}C solution NMR spectroscopy was used to monitor the structures of the various sulfonic acids resulting from hydrothermal treatment, using a Bruker Biospin spectrometer with a 14.1 T magnet and TopSpin processing software. For both ^{1}H and ^{13}C, spectra were acquired with excitation pulses of 30^{o} flip angle (with durations of 3.3 and 4 □s, respectively) to reduce the time required for relaxation between scans. Proton spectra were acquired at 600 MHz with 16 scans and a 1-s recycle delay. Carbon spectra were acquired at 150 MHz with a power gated decoupling scheme during acquisition (WALTZ16), 1024 scans, and a 2-second recycle delay. The compound stability was evident from the loss or retention of signals after subsequent hydrothermal treatments.

The chemical state of sulfur in the remaining solids was analyzed using a Physical Electronics 550 Multitechnique XPS system employing a standard Al electron source. The samples were run at 10^{-9} Torr and mounted on double-sided tape. Charging was corrected for by adjusting the carbon peak to 284 eV. The solids underwent elemental analysis for carbon, hydrogen, nitrogen, and sulfur (CHNS) using a PE 2100 Series II combustion analyzer (Perkin Elmer Inc., Waltham, MA). Atomic emission spectra were obtained using an ICP-AES Spectro CCD. Argon was used as a monitor line and 1 ppm scandium for reference line (internal standard).

4. Results and Discussion

4.1 Hydrolysis and NMR characterization.

The ^{13}C NMR of the materials, see Fig. 1, showed that sulfonated aliphatic molecules remained intact in the solution phase to a far greater extent than sulfonated aromatic rings (Fig. 1 d-f). The most unstable molecules were the substituted aromatics. Both the tri-nitro (electron-withdrawing), and trimethyl (electron-donating) sulfonated benzene had lost signal at the mild 130ºC condition, and formed a solid precipitate (not visible in solution NMR) (Fig. 1 a,b). Benzenesulfonic acid was the most stable of the aromatic molecules, but did form a solid after 24 h at 160°C (fig X c). It was surprising that no significant degradation was observed for 18 h, given that the literature described facile desulfonation of aromatic sulfonic acids [18, 19]. The data show that substitution of aromatic systems only serves to weaken the carbon sulfur linkage. The stability of the model compounds decreased from aliphatic to unsubstituted aromatic to substituted aromatic compounds.

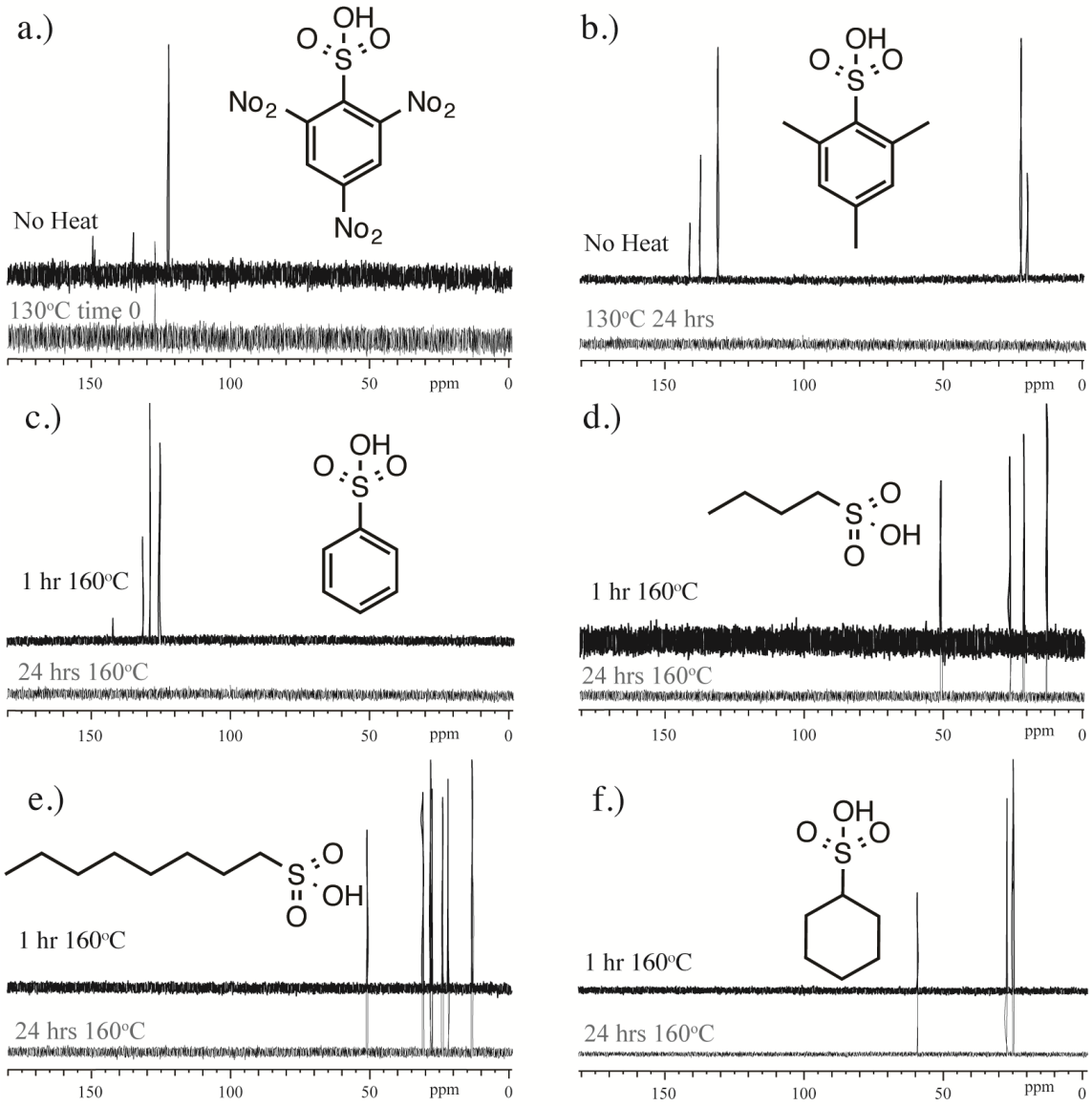

Figure 1. Solution ^{13}C NMR spectra of (a-c) aromatic sulfonic acid compounds and alkyl sulfonic acid molecules (d-f). The black spectrum (top) is from the un-transformed molecule and the red (bottom) is the spectrum showing breakdown at the mildest condition (if any).

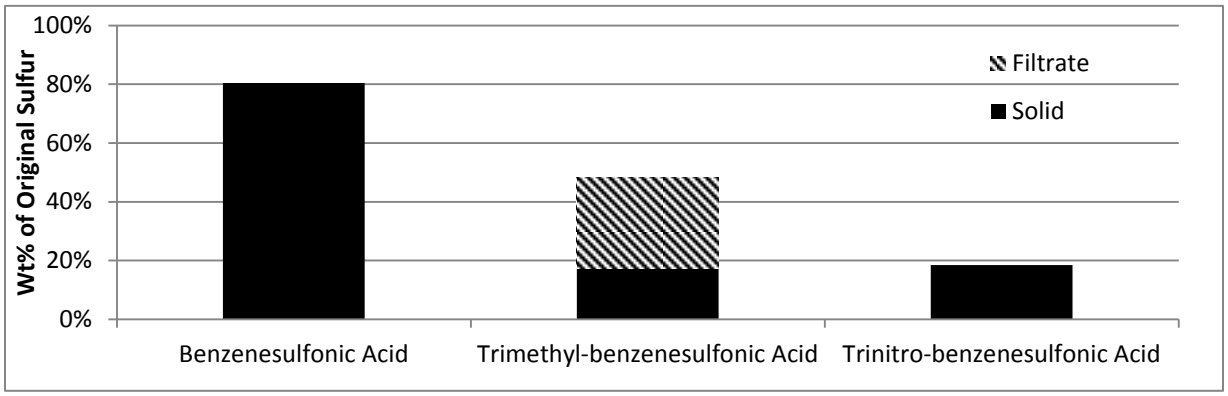

Figure 2. Mass balance, from elemental analysis, after 24-hour hydrothermal treatment for the aromatic sulfonic acids (benzenesulfonic acid, trimethylsulfonic acid, and trinitrosulfonic acid), relative to the initial sulfur content. These materials tended to carbonize and separate into a solid and liquid phase. These two phases were dried and analyzed via CHNS.

4.2 Chemical transformations of the sulfonic-acid groups.

The ^{13}C NMR spectra showed the aromatic sulfonic acids readily condensed forming solids during hydrothermal treatment. Solution NMR was not able to characterize this solid material, and therefore it was unclear if the condensation process involved the cleavage of the carbon sulfur bond. To probe

the fate of sulfur, the resulting solid and filtrate was analyzed using elemental analysis, XPS, and ICP-AES.

Figure 2 shows the sulfur weight fractions, determined by elemental analysis, after hydrothermal treatment for 24 h, in both the solution phase and the solid precipitate formed. The data show that the total sulfur balance never reached 100%. It is presumed the missing sulfur went into the gas phase. The solid phase of the unsubstituted benzenesulfonic acid preserved the most (80%), the trinitrobenzenesulfonic acid and the trimethylbenzenesulfonic acid the least (18% each) sulfur on the solid. This confirms that the relative strength of the carbon–sulfur bond for the unsubstituted benzene ring is greater than for the substituted rings. In addition, since the mass balance is not 100% and some was detected in the liquid phase, it is a good indication that cleavage of the carbon sulfur bond occurred to a certain extent for all the aromatic molecules tested.

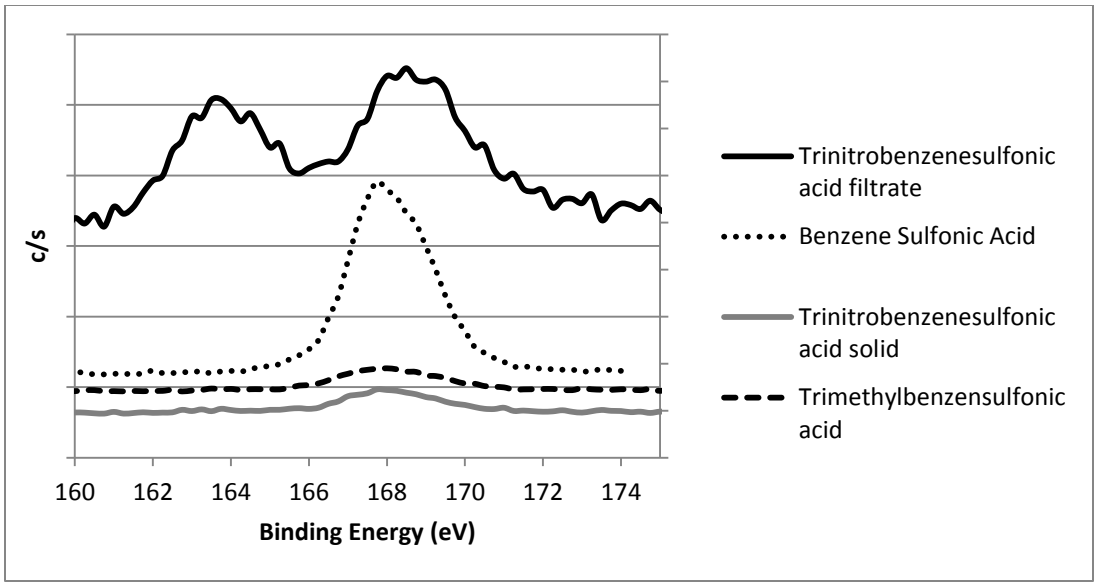

Figure 3. Sulfur XPS data from the solids recovered after filtration and the dissolved material in the filtrate after drying. The other samples are all three of the solids recovered from filtration; they are qualitatively the same. This also matches up with the curve for a reference compound with aromatic sulfanilic attachment.

The recovered precipitated solids were also subjected to XPS analysis, to give an indication about what happens to the sulfur as a result of the hydrothermal treatment. The qualitative XPS data of the solids recovered from the aromatics showed they all retained the expected S2p peak at 168 eV (see Figure 3). Interestingly, the S2p peak with the filtrate of the trimethylbenzenesulfonic acid after 24 hours at 160^{o}C split into two peaks (see Figure 3), one around 168 and another at 164 eV, indicating the expected sulfonic acid [20, 21] and a reduced sulfur form, respectively. The latter is perhaps thiophene or a similar molecule

containing organic sulfur [22]. Since XPS is qualitative, it was not possible to determine relative amounts of the sulfur species present. Regardless of the specific molecular form, since the sulfur peak shifted, some of the initial surrounding oxygen atoms bonded to the sulfur atom must have been lost. This reduces the acidity on any attached proton(s). In other words, the hydrothermal treatment not only removed sulfur from the trimethylbenzenesulfonic acid, but the sulfur was also transformed into an unusable product. Since this occurred in the liquid phase, it would indicate carbon sulfur–bond breakage. This highlights our finding that the aromatic sulfonic acids, in particular the substituted ones, were unable to fully retain their sulfur during the hydrothermal treatments. Especially when compared to their alkyl counterparts, the aromatic sulfonic acids are less hydrothermally stable (see Fig. 4).

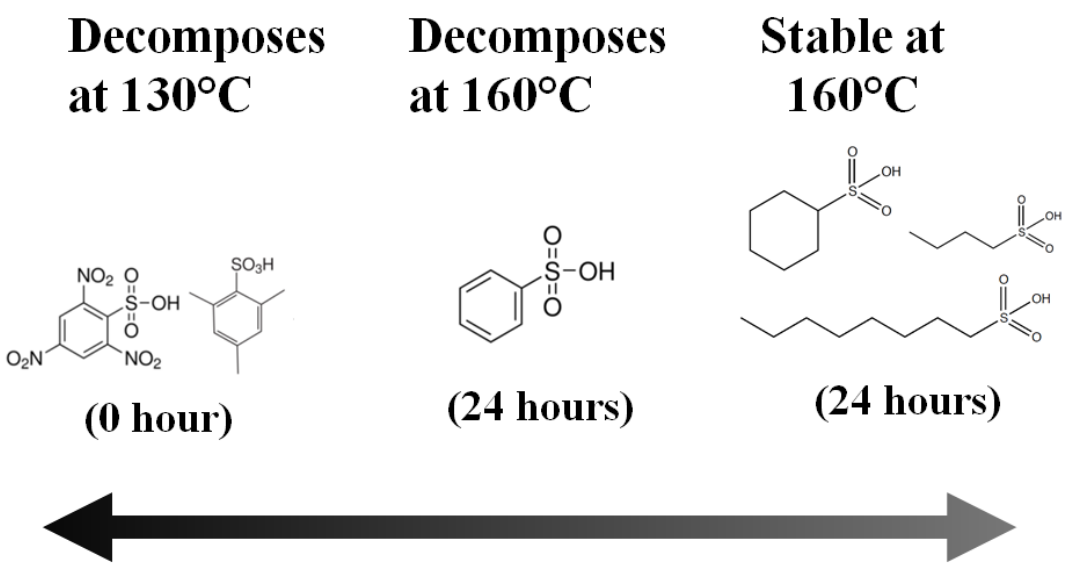

Figure 4. Summary of the results with the least stable sulfonic-acid model compounds on the left and the most stable ones on the right

5. Conclusions

Six sulfonic-acid model compounds were tested for hydrothermal stability and characterized by solution NMR, ICP-AES, XPS, and elemental analysis to determine hydrothermal stability over time. The aromatic compounds tended to carbonize and form an insoluble solid and were subsequently analyzed by CHNS elemental analysis, XPS of the solid, and ICP-AES of the liquid filtrate to determine the fate of the sulfur. The least stable compounds were the trisubstituted benzenesulfonic acids, which condensed into insoluble materials even when treated at mild temperature (130°C). The solids from these materials retained only about 18% of the original sulfur. The benzenesulfonic acid

remained detectable via NMR until 24 h at 160°C. When the benzensulfonic acid degraded, only 80% of the sulfur could be accounted for. The alkanes and the saturated cyclic compounds did not degrade even after 24 h at 160° C. From this, the relative carbon-sulfur bond strength in the hydrothermal environment can be inferred to be substituted aromatic < non-substituted aromatic < alkanes. Therefore, in sulfonated acid catalysts designed to withstand hydrothermal conditions, sulfonic-acid groups should be attached to sp^3-hybridized carbons. This could be accomplished with the use of aliphatic linkers that connect sulfonic acid groups to an aromatic carbon scaffold. Materials designed according to this principle may provide a path to greater hydrothermal stability than achieved previously using aromatic substitution reactions. The pKa values of benzene- and methanesulfonic acid are -2.8 and -1.9, respectively.[23] Thus, there is only a slight trade-off between hydrothermal stability and acid strength.

Acknowledgements

The authors would like to acknowledge NSF Award number EEC-0813570 for generously supporting this work in the framework of the Center for Biorenewable Chemicals (CBiRC). We wish to thank ISU Chemical Instrumentation Facility staff member Sarah Cady for training and assistance pertaining to solution NMR. We would also like to thank two undergraduate students, Karl Alderks and Ashley Leitner, who worked on this project. Purchase

of the Perkin Elmer 2100 Series II CHN/S analyzer used to obtain results included in this publication was supported in part by the National Science Foundation under Grant No. DBI 9413969. We wish to thank ISU Chemical Instrumentation Facility staff members Stephen Veysey for training and assistance pertaining to the PE 2100 CHN/S elemental analysis. Jim Anderegg graciously ran and expertly helped interpret the XPS results. Any opinions, findings, and conclusions, or recommendations expressed herein are those of the authors and do not necessarily reflect the views of the National Science Foundation.

References

1. Akbar, J., et al., *Kinetics and mechanism of thermal degradation of pentose- and hexose-based carbohydrate polymers.* Carbohydrate Polymers, 2012. **90**(3): p. 1386-1393.
2. Zamora, F., et al., *Hydrolytic degradation of carbohydrate-based aromatic homo- and co-polyesters analogous to PET and PEI.* Polymer Degradation and Stability, 2006. **91**(11): p. 2654-2659.
3. Funke, A. and F. Ziegler, *Hydrothermal carbonization of biomass: A summary and discussion of chemical mechanisms for process engineering.* Biofuels Bioproducts & Biorefining-biofpr, 2010. **4**(2): p. 160-177.
4. Hickel, B. and K. Sehested, *Reaction of hydroxyl radicals with ammonia in liquid water at elevated temperatures.* Radiation Physics and Chemistry, 1992. **39**(4): p. 355-357.
5. Xiong, H., H.N. Pham, and A.K. Datye, *A facile approach for the synthesis of niobia/carbon composites having improved hydrothermal stability for aqueous-phase reactions.* Journal of Catalysis, 2013. **302**(0): p. 93-100.
6. Pham, H.N., et al., *Improved Hydrothermal Stability of Mesoporous Oxides for Reactions in the Aqueous Phase.* Angewandte Chemie International Edition, 2012. **51**(52): p. 13163-13167.
7. DeLaRiva, A.T., et al., *In situ Transmission Electron Microscopy of catalyst sintering.* Journal of Catalysis, (0).

8. Zaiku, X. and X. Z, *An overview of recent development in composite catalysts from porous materials for various reactions and processes.* International journal of molecular sciences, 2010. **11**(5).

9. Onda, A., T. Ochi, and K. Yanagisawa, *Hydrolysis of Cellulose Selectively into Glucose Over Sulfonated Activated-Carbon Catalyst Under Hydrothermal Conditions.* Top. Catal., 2009. **52**(6-7): p. 801-807.

10. Johnson, R.L., et al., *Spectrally edited 2D 13C13C NMR spectra without diagonal ridge for characterizing 13C-enriched low-temperature carbon materials.* J. Magn. Reson., 2013. **234**: p. 112-124.

11. Anderson, J., et al., *Chemical Structure and Hydrothermal Deactivation of Moderate-Temperature Carbon Materials with Acidic SO_3H Sites.* Carbon *Submitted*, 2014.

12. Cerfontain, H., *Mechanistic Aspects in Aromatic Sulfonation and Desulfonation*. 1968: John Wiley & Sons, Inc.

13. Krylov, E.N., *Aromatic desulfonation: analysis in terms of acid-base interaction.* Russ. J. Gen. Chem., 1997. **67**(10): p. 1624-1627.

14. Wagner, F.C. and E.E. Reid, *Stability of the carbon-sulfur bond in some aliphatic sulfonic acids.* J. Am. Chem. Soc., 1931. **53**: p. 3407-13.

15. Yamaguchi, D. and M. Hara, *Starch saccharification by carbon-based solid acid catalyst.* Solid State Sciences, 2010. **12**(6): p. 1018-1023.

16. Jenkins, M.L., R.H. Dauskardt, and J.C. Bravman, *Important factors for silane adhesion promoter efficacy: Surface coverage, functionality and chain length.* J. Adhes. Sci. Technol., 2004. **18**(13): p. 1497-1516.

17. Staub, H., F. Kleitz, and F.-G. Fontaine, *Confinement of the Grubbs catalyst in alkene-functionalized mesoporous silica.* Microporous Mesoporous Mater., 2013. **175**: p. 170-177.

18. Graybill, B.M., *Synthesis of aryl sulfones.* The Journal of Organic Chemistry, 1967. **32**(9): p. 2931-2933.

19. Setzkorn, E.A. and A.B. Carel, *The analysis of alkyl aryl sulfonates by micro desulfonation and gas chromatography.* Journal of the American Oil Chemists' Society, 1963. **40**(2): p. 57-59.

20. Takagaki, A., et al., *Esterification of higher fatty acids by a novel strong solid acid.* Catalysis Today, 2006. **116**(2): p. 157-161.

21. Shu, Q., et al., *Synthesis of biodiesel from waste vegetable oil with large amounts of free fatty acids using a carbon-based solid acid catalyst.* Applied Energy, 2010. **87**(8): p. 2589-2596.

22. *NIST X-ray Photoelectron Spectroscopy Database, Version 4.1 (National Institute of Standards and Technology, Gaithersburg, 2012); http://srdata.nist.gov/xps/.*

23. Guthrie, J.P., *Hydrolysis of esters of oxy acids: pKa values for strong acids; Brønsted relationship for attack of water at methyl; free energies of hydrolysis of esters of oxy acids; and a linear relationship between free*

energy of hydrolysis and pKa holding over a range of 20 pK units. Canadian Journal of Chemistry, 1978. **56**(17): p. 2342-2354.

CHAPTER 4.

ENGINEERING OF CARBON MATERIALS PRODUCED FROM THE MAILLARD REACTION TO PRODUCE HYDROTHERMALLY STABLE ACID CATALYST

A Paper to be submitted to Carbon

Jason M Anderson, Robert L Johnson, Tianfu Wang, Klaus Schmidt-Rohr, Brent H Shanks

Abstract

We combined research showing typical electrophilic substitution methods for sulfonated carbon catalysts to be inadequate with initial testing of model compounds and a proof of concept of glucose and taurine. This use of the Malliard reaction resulted in a catalyst stable under hydrothermal conditions but initially in colloidal form. Since this is undesireable in industrial processing, we sought to further stabilize the carbon backbone with the addition of more glucose. We found that the ratio of the glucose to the glucose taurine mixture is not as important as the ion used for the precursor. The potassium ion increased the amount of sulfur on the carbon catalyst, thereby increasing the reaction rate on a mass basis. These catalysts suffer from low surface area so we supporting them on SBA-15 and mesoporous carbon nanoparticles. With these two supports, the catalysts showed good activity on a similar sulfur basis.

1. Introduction

Homogeneous acid consumption of sulfuric acid exceeds 15 million tons per year [1]. It is used in a variety of different industries and can be used as an industrial economic indicator in the US. However, sulfuric acid is difficult to separate from the reaction and must be treated prior to discharging to the environment [2, 3]. Therefore researchers are interested in discovering a heterogeneous catalyst that is similar in price and activity as sulfuric acid. One such solid acid that is a logical replacement for sulfuric acid is a sulfonic acid tethered to a carbon support. We have discovered that the linker plays an important role in the hydrothermal stability. This research further developed a new method for creating solid acid catalysts as described in a previous paper [4].

Acid catalysts are important in a number of different reactions: esterification, dehydration, etherification, [5-12]. Typically the reactions proceed through a carbocation intermediate. These reactions transform the simple commodity chemicals to the ones more typically seen by consumers. By using acid catalysts, the chemical industry transforms a handful of chemicals to the thousands used in today's society. The characteristic reaction of this work will be esterification, an alcohol and a carboxylic acid combining to an ester and water, because of its sensitivity to both acid sites and strength [13, 14].

Typical catalyst supports used in the petroleum industry include alumina and zeolites. However, as oil and non-renewable resources become expensive, interest grows in using renewable resources. Typically carbohydrates like glucose are the primary feedstock [15]. This feedstock cannot be chemically transformed in the gas phase like the petroleum products can as they degrade long before they are volatile [16-18]. The catalyst supports used in the petroleum industry degrade under hot water conditions and therefore cannot be used with biorenewable processing. New catalysts must be created to have the hydrothermal stability needed to withstand condensed phase processing.

Carbon may be one support with hydrothermal stability and sulfonated carbon provides one logical replacement scheme for sulfuric acid in acid catalyzed reactions. Work on sulfonated carbons has been numerous. Previous research has created a various varieties of sulfonated carbon catalysts and variously tested those catalysts for their stability [12, 19-26]. From the literature some pyrolyzed [8, 11, 27] and hydrothermally [28-30] synthesized catalysts were systematically tested for stability to determine differences between the carbons [31]. It was shown that overall these materials could not handle the harshness of 160°C liquid water for several cycles however significant strides were made in characterizing these difficult carbons [31, 32]. Further research was done to probe the immediate chemical nature of the active site with model compounds [33]. It was found that the carbons nearby the carbon linking the sulfur group to the backbone must be alkane to ensure the most hydrothermal stability. From

research on the Malliard reaction [34-37] a unique synthesis method was developed to create these alkane linkages desired in the catalyst [4]. This has led to more hydrothermally stable carbon catalysts.

In this research the glucose-taurine (GT) colloid is expanded to be a more heterogeneous catalyst. There is disagreement in the literature if attachments made via Maillard reactions retain the functionalities attached to the amine precursor [38]. In our research, we found the functionality remains mostly intact via extensive NMR data [4, 34]. At a 1:1 molar ratio, the catalyst is a colloid and does not have the expected hydrothermal stability nor the handling characteristics inherent of a typical heterogeneous catalyst [4]. Developed in this research are the changes inherent in the GT catalyst with the addition of more glucose to increase the carbon backbone. Further NMR characterization shows the differences between the carbons and which ratio imparts the most hydrothermal stability.

This research also includes additional improvements on surface area. As shown from previous research, coating a silica surface with carbon improves it hydrothermal stability [39]. We improved the surface areas with SBA-15 mesoporous silica. With the sufficient surface area, the reaction rates should be improved. Then using the technique for coating the silica, it could be protected against hydrothermal conditions.

2. Experimental

2.1 Materials and synthesis

The sucrose, glucose, tetamethoxy silane, sulfuric acid, and taurine were purchased from Fisher and used without prior purification. The ^{13}C uniformly labeled glucose was purchased from Cambridge Isotopes. Nitrogen (99.995%) was obtained from Airgas. The surfactant P123 was purchased from BASF.

2.2 Bulk GT synthesis

Mixtures of glucose taurine and base were co-precipitated with equal molar ratios of taurine and base (either sodium hydroxide or potassium hydroxide). The resulting material was added to two different molar ratios of additional glucose for greater back bone stability. The ratios were either 2:1 of 4:1 additional glucose to the original GT precipitate. The resulting solids were then pyrolyzed in a tube furnace under flowing argon. The materials were heated to 120ºC with a 1ºC/min ramp and held for 2 hours to ensure completion of the Maillard reaction before continued heating to 250ºC with an additional dwell time of 10 hrs. Following pyrolysis materials were ground into a fine powder using a cryomill with a 10 cps impact rate for three one minute cycles. Following milling, materials were activated by soaking in 5 M KOH and heated for 4 hours at 150 C, and then washed with 5M HCl followed by water until resulting liquid was no longer acidic. It was then dried overnight in an oven at 110ºC and used with no further modifications. These samples were labelled in accordance to the

ratio of extra glucose to the 1:1 glucose taurine precipitate and which ion was used in their synthesis (e.g. GT2:1K or GT4:1Na).

2.3 Synthesis of SBA-15

In a typical experiment, P123(BASF,7.0g) was dissolved in 274 g of 1.6M HCl and stirred for 1 hr under 55ºC. Then, 10.64g of TMOS(tetramethoxy silane) was quickly added and the resultant solution was stirred for another 24 hours. A milky solution was obtained and transferred to a autoclave for additional 24 hours of hydrothermal treating under 120ºC. After that, the solid was filtered and dried in air. To remove the surfactant, the SBA-15 materials was calcined under 550 ºC in the air for 6 hours.

2.4 Synthesis of the GT on SBA-15

After the SBA-15 was prepared a glucose and taurine solution with a 2:1 molar ratio of the glucose to taurine was added to the silica. Then a sufficient amount of water was added to cover the SBA-15. It was placed in a hood to evaporate at room temperature. After evaporation, the catalyst was placed in a drying oven (110ºC) to initiate the Maillard reaction. After overnight in the drying oven, it was calcined in a tube furnace at 250ºC in nitrogen for 9 1/3 hours. This material was used without further preparation. This samples was labeled "GT on SBA-15".

2.5 Mesoporous Carbon Nanoparticle (MCN) Synthesis

In a typical experiment, 4.0 g SBA-15 was mixed with 20g of an aqueous solution containing 5.0g of sucrose and 0.65g 98% sulfuric acid. The resultant mixture was treated under 100ºC for 6 hours, followed by another 6 hours under 160ºC. The process was repeated under the same condition but with 16 g of the same solution. Then the brownish solid as heated to 900ºC and kept for 10hr under nitrogen protection. The silica was removed from the hybrids using 10% HF in ethanol/water mixture(50:50, v:v). After copious filitering and then drying the solid, the MCN materials was obtained.

2.6 Synthesis of the GT on MCN

After the mesoporous carbon was prepared, it also was prepared in a way similar to the SBA-15. The mesoporous carbon was mixed with a glucose taurine solution in a 2:1 ratio. Then sufficient amount of water was added to cover the mesoporous carbon. The water was evaporated at room temperature and then the Maillard reaction was initiated by placing in an oven at 110ºC overnight. Then the materials was calcined at 250ºC in nitrogen for 9 1/3 hours. This samples was labeled "GT on MCN".

3. Characterization

Surface area characterization was performed by physisorption using Kr as the adsorbing gas in a Micromeritics ASAP 2020. Elemental analysis results for the carbon, hydrogen, nitrogen, and sulfur (CHNS) were acquired using a PE 2100 Series II combustion analyzer (Perkin Elmer Inc., Waltham, MA). The

chemical state of sulfur was analyzed using a Physical Electronics 550 Multitechnique XPS system employing a standard Al electron source. The samples were run at 10^{-9} Torr and mounted on double-sided tape. Charging was corrected for by adjusting the carbon peak to 284 eV. The number of sulfonic acid (R-SO_3H), carboxylic acid, and phenolic hydroxyl groups were measured using the titration method reported by Suganuma et al. [23]. One back titration measured all the acidic functionalities. It used a known amount of NaOH (~0.1g) dissolved in water with the catalytic material using sufficient time (~2 hours) to exchange the sodium ions with all the hydrogen ions from the acid groups on the material. Then, a simple acid titration using sodium hydroxide was used to exchange the acidic protons from the sulfonic acid and carboxylic acid groups. It was assumed that the sulfonic acid, carboxylic acid, and hydroxyl groups were measured. The sulfonic acid groups were measured by the elemental analysis of the sulfur and the other groups were determined by subtraction of these measurements. The carbon materials were imaged with scanning electron microscopy (FEI Quanta-250 SEM), to investigate their morphologies and compare with other sulfonated carbon catalysts carbons. Surface area characterization was performed by physisorption using with nitrogen as the adsorbing gas in a Micromeritics ASAP 2020. Analysis of the materials with a Perkin Elmer STA 6000 Simultaneous Thermal Analyzer (TGA), using a ramp rate of 10°C in flowing air was performed.

Esterification of acetic acid with methanol was used as the test reaction since it is sensitive to the number of acid sites and their pK_a [14]. The reactions were performed at 40 °C in an Alltech 10 mL reactor vial loaded (total volume 7 mL) with methanol (6 M) and acetic acid (3 M) in dioxane with the respective sulfonated carbon (10 mg). The reactions were run at low conversions (<5%) to allow comparison of initial rates. The reaction testing was performed at a range of stir rates so that it was determined that no mass transfer effects occurred as long as the stirring rate was above 200 rpm. The reaction product samples were analyzed on an Agilent 7890A GC equipped with a flame ionization detector. The sulfonated carbons were compared in terms of activity per mass of catalyst giving the units of mmol acetate formed min^{-1} (g catalyst)$^{-1}$.

Similar to the previous research [31], after full characterization of the fresh materials, the catalysts were subjected to three rounds of hydrothermal treatments. The treatment subjected the catalyst material (0.5 g) to 160°C DI water (7 mL) stirred in an Alltech reactor under autogenous pressure for 24 hours. The solid material was filtered and washed copiously (generally about 0.5 L of DI water) until the filtrate was clear and colorless. The hydrothermally treated sulfonated carbon was then characterized and subjected to two more hydrothermal treatments following the same protocol as the first treatment.

3.1 Solid State NMR

Quantitative solid state NMR was applied using a recently developed cross-polaization pulse sequence that utilized both a ramped 1H CP power level and multiple cross polarization periods to allow for full 13C magnetization equilibration as shown by previous work [40].

4. Results and discussion

These catalysts produced are fairly similar to previously created sulfonated carbon catalysts except for their significant amount of nitrogen as seen in the elemental analysis (see Figure 1). This nitrogen is expected from the Maillard reaction and the use of the taurine allows for aliphatic linkages seen to be important for hydrothermal stability to be connected to the carbon backbone [33]. The nitrogen and sulfur are in a one to one molar ratio which supports the idea that the linkage including the sulfur was not lost during the synthesis. The XPS data (not shown) confirmed the sulfur resided in the expected sulfonic acid with 168eV binding energy in the Sp2 of sulfur. This material has a significant amount of oxygen in it because of the low synthesis temperatures. The relative hydrogen poor results indicate significant amounts of aromaticity. This aromatic nature of the carbon support is what leads to the hydrothermal stability however the linkage must also remain for both the carbon support and the active group to ensure a hydrothermally stable catalyst.

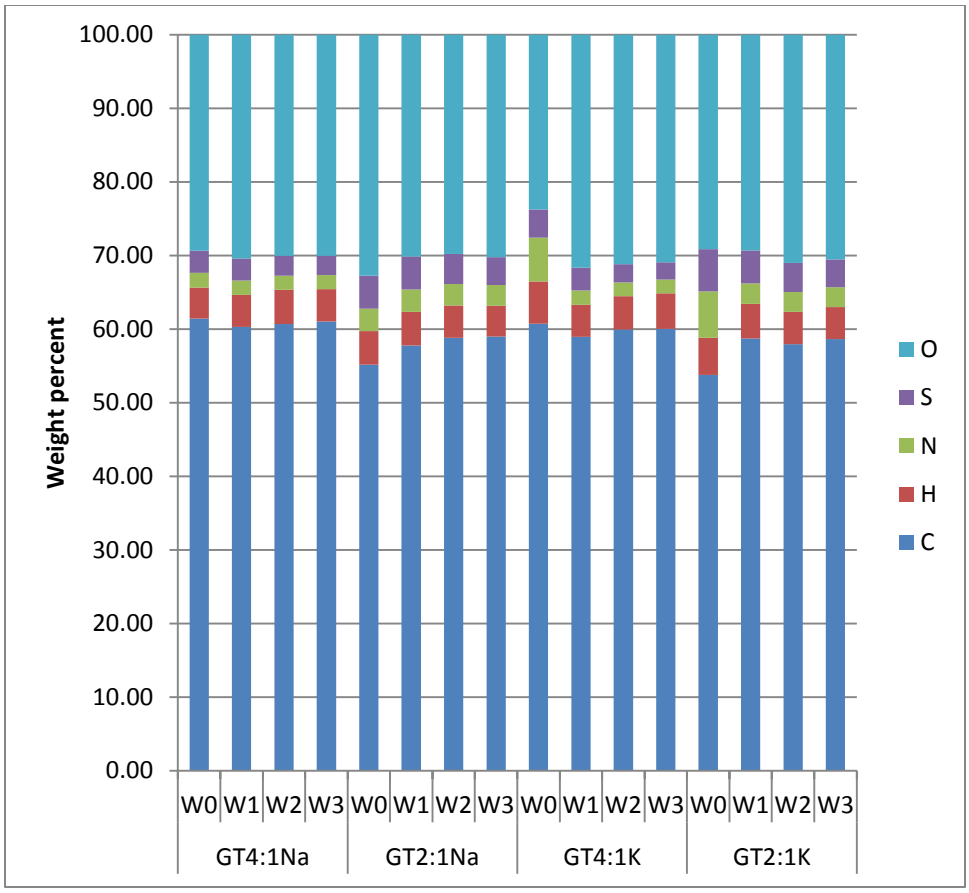

Figure 1. The CHNS analysis of the bulk GT catalysts. There are four sets of four catalysts types that are labeled with either W0, indicating the initial samples, or W1-W3, indicating how many hydrothermal treatments each samples has been through.

The BET data showed these materials to have low surface area of $<0.1 m^2/g$. From the analysis of the surface alone, it can be deduced that many of the sulfur active groups are in the bulk. This was further verified by titrations of the better two catalysts showing that only 2-8% of the total sulfur is accessible for

titration. This led to lower reaction rates than what previous research has reported for similar materials. If a better dispersion of the sulfonic acid groups could be achieved in a stable manner, then these catalysts could be even better.

As seen by the SEM images, these materials are similar to pyrolyzed materials as seen before (see Figure 2) [31, 41, 42]. The amorphous carbon resemble shards of glass. The supported GT catalysts had some long-ranged order associated with them as expected from the synthesis method (see Figure 3). The surface area of these catalysts was significantly higher with the GT on SBA-15 catalyst having 314 m^2/g and the GT on the MCN having 1110 m^2/g. The thermogravametric analysis showed that the GT on the SBA-15 had about 7 weight percent combustibles at 800ºC. This corresponds well with the sulfur it contained as the total combustibles times the expected weight percent of sulfur in the bulk 2:1GT samples give close to the value measured by the elemental analysis for the bulk samples.

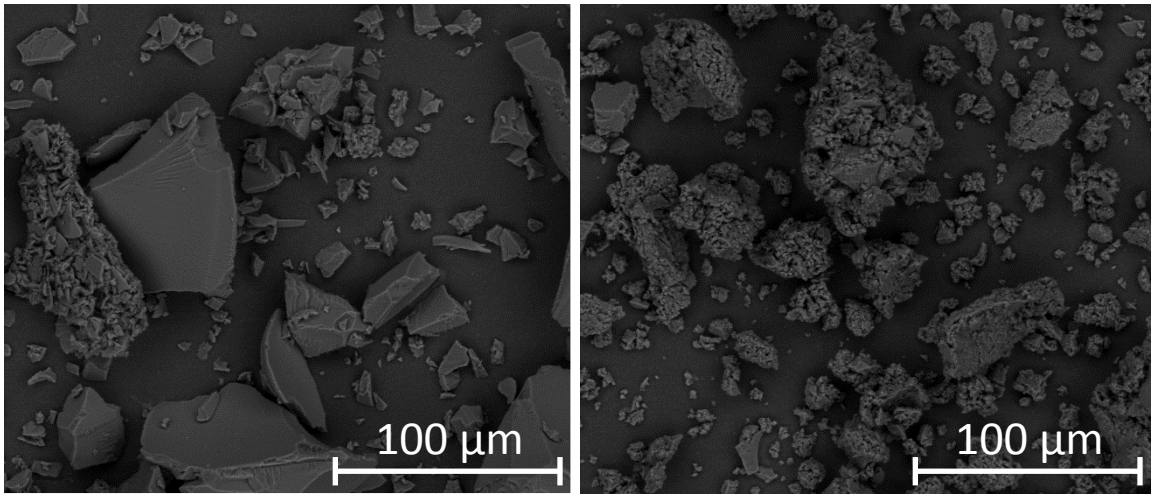

Figure 2. SEM pictures of GTK on left and GTNa on right. Both the 4:1 and 2:1 varieties looked the same, i.e. the left picture represents both the GT2:1K and GT4:1K.

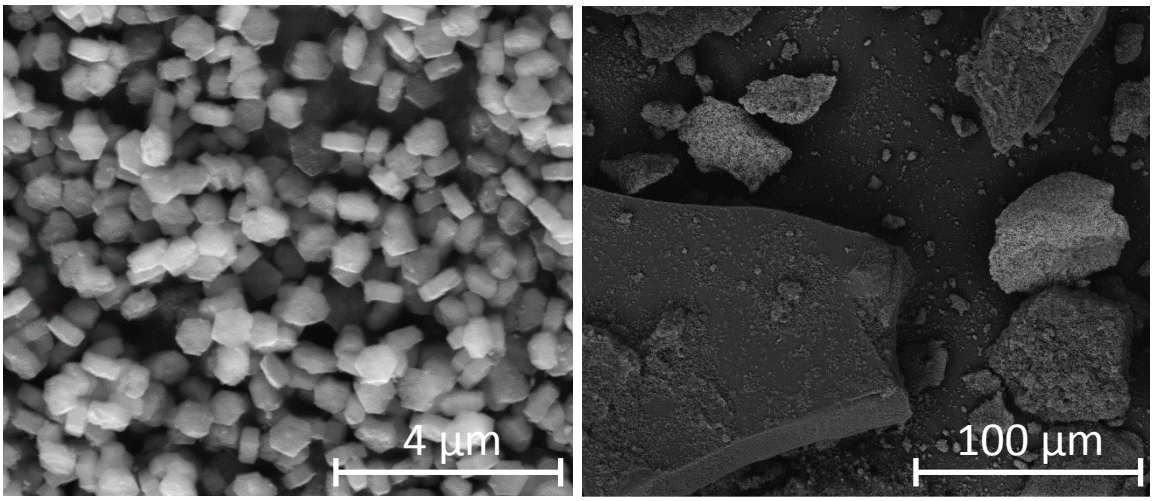

Figure 3. SEM pictures of GT on SBA-15 on left and GT on Mesoporous Carbon on right.

Solid state NMR was used to verify the presence of CH_2 groups characteristic of taurine incorporated into the carbon backbone. Shown in Figure 4, the characteristic CH2 groups on taurine are in the low 40 ppm (NCH_2) and 50 ppm (CH_2SO_3) range. We tried various combinations of glucose taurine ratios, addition of glucose to the colloid, followed by lyophilizing and pyrolysis, and found that the characteristic CH_2 peaks of the taurine fragments were present under all conditions. For a more complete description of the transformation occurring please see [4]. Shown in Figure 4 we can see the increase in glucose increases the peaks attributed to glucose carbon.

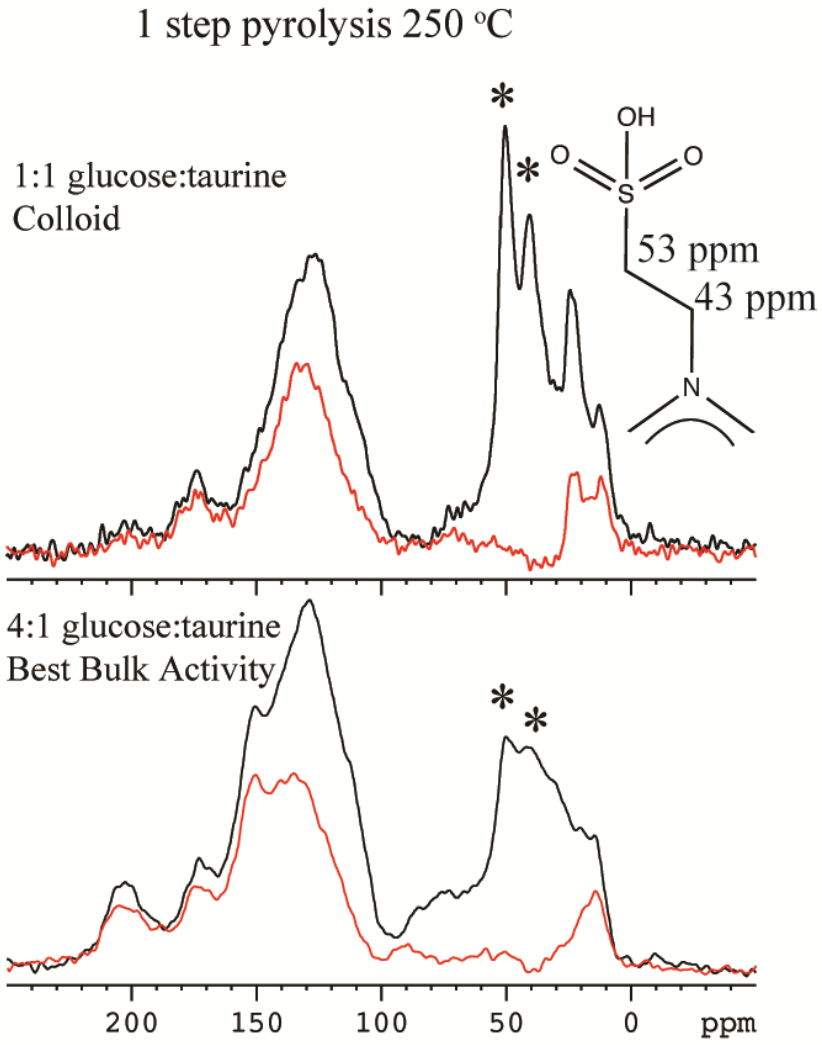

Figure 4. NMR of the 1:1 GT colloid on top and the 4:1GT catalyst on bottom. The two asterisks point to the two carbons in between the nitrogen and the sulfur. The upper line is total carbons, the lower line in each of the spectra is all the non-protonated carbons.

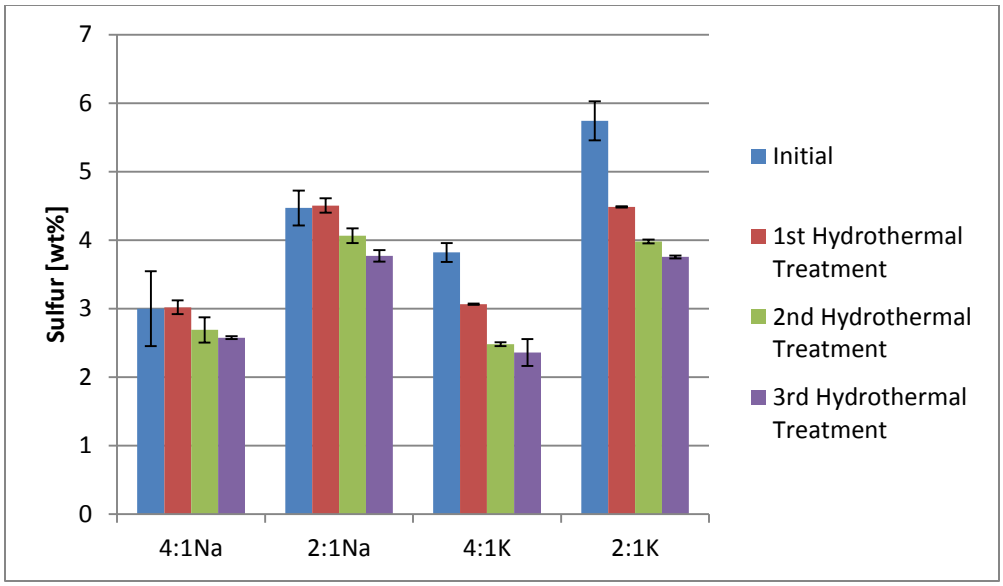

Figure 5. The sulfur retention data for the GT catalysts. Each hydrothermal treatment was 160ºC liquid water for 24 hours.

If the sulfur retention is compared to previous work, the increase of stability can be seen. Whereas previous carbon catalysts lost 60-90% of the sulfur loaded on them, these materials lost 20-40% of the sulfur loaded on them (see Figure 5). These materials also lost the nitrogen in the same amount as the sulfur indicating the whole linker was lost. If the whole linker is preserved as it leaches, then the C-S bond no longer is the weakest part in the hydrothermal stability of the sulfonated carbon catalysts. This sulfur retention represents a great improvement over previously researched materials.

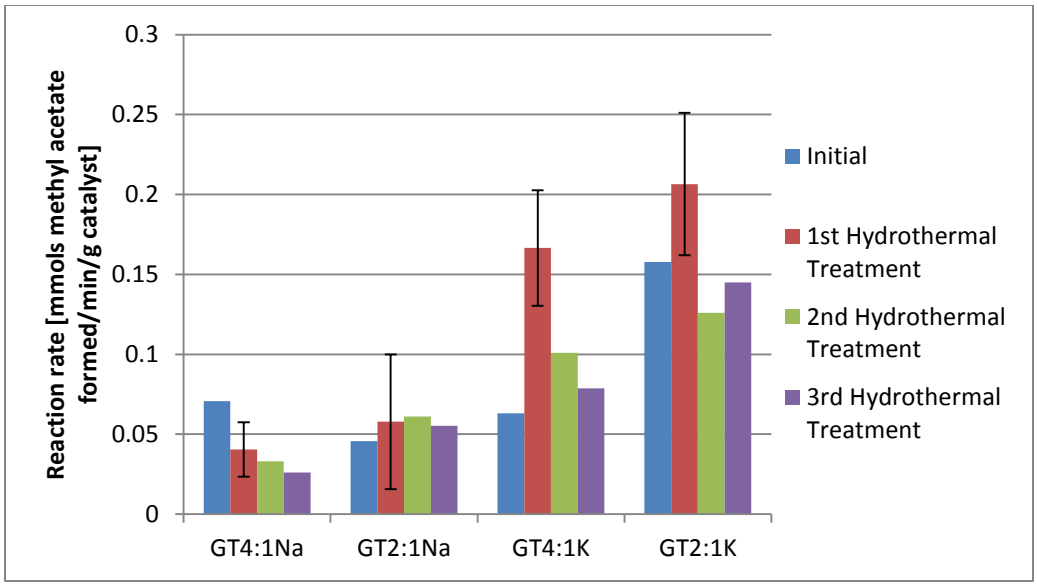

Figure 6. Reaction rates for the pyrolyzed GT catalysts throughout the hydrothermal treatments.

The reaction rate data (see Figure 6) shows an improvement in the stability of the reaction rates throughout the hydrothermal testings. While the data shows quite a bit of noise-a consequence of the low catalytic activity, it shows the relative consistency of the reaction rate even through the hydrothermal tests. This is in contrast to the previous materials that lost significant activity even after one hydrothermal test. These materials do have a lower overall activity than the aromatic sulfonic acid materials. This may be attributed to an acidity difference between the two materials the pK_a of aliphatic sulfonic acids is -1.9 and aromatic sulfonic acids is -2.8. This sensitivity of the pKa is expected from this reaction [14] and this is a tradeoff with the strength of the acid site with the hydrothermal stability of the catalyst.

As a precursor to supporting the catalysts on a support we verified that acid washing and cryomilling were important to the resulting reaction rates. Working with the GT4:1K sample, it was milled and/or acid washed. The BET surface areas did not change significantly with the milling but we saw rate improvement over materials that was not milled. Washing the solid with acetone to remove any loosely connected parts did not increase the reaction rate significantly and was not investigated further.

Table 1. Various improvements to the catalyst reaction rate.

Sample	Reaction rate [mmols methy acetate formed/min/(gcatalyst)]
GT4:1K no milling, no acid wash	No reaction
GT4:1K no milling, 5M HCl acid wash	0.2
GT4:1K milled, 0.5M HCl acid wash	0.23
GT4:1K milled, 5M HCl acid wash	0.37
GT2:1K milled, 5M HCl acid wash	0.26
GT4:1K milled, acetone washed, 5M HCL acid wash	0.41

Seen in Table 1 are the various improvements made to the catalysts via different means. The initial material is not catalytic unless the material is acid

washed. Both the milling and the acid wash have an effect on the catalytic activity and it seems to be additive as seen by the sample GT4:1K milled, 5M HCl acid wash. The 2:1GTK material does not seem to have such a favorable impact. Using acetone to remove any soluble parts of the material only has a minimally positive effect on the reaction rate. These are all initial rates that have not gone through hydrothermal treatment but it shows that these reaction rates can increase with better accessibility of the acid sites.

Since these materials needed more surface area and it was presumed that with better dispersion, the catalysts would have greater activity, we tested supporting the GT catalysts on SBA-15 and mesoporous carbon. Seen in Table 2, when the GT colloid was supported on SBA-15 and mesoporous carbon, it did better than the bulk catalysts on a per sulfur basis. Comparing the catalysts on the same mass basis of supported GT catalysts gave the comparison basis for the catalysts. If the supported catalysts are compared on the same mass basis of the GT material present on the catalyst (extracted from TGA data) then they have a reaction rate of 0.7 mmols/min/(g GT catalyst) for the 2:1 GT on SBA-15 and 0.56 mmols/min/(g GT catalyst) for the 2:1 GT on MCN. The turnover frequency for the 2:1 GT on SBA-15 was 0.46/min and for the 2:1 GT on MCN was 0.55/min. Both of these are in the same magnitude of sulfuric acid doing the same reaction.

Table 2. Details of the supported catalysts and the similar sulfur basis used for comparison of the supported catalysts.

	Units	2:1 GT on SBA-15	2:1 GT on MCN
Weight percent S	[% of the total mass]	0.35	0.24
Surface area	[m^2/g]	314	1110
GT weight (from TGA)	[weight %]	7.3	7.3
Measured reaction rate	[mmols methyl acetate formed/min/(g catalyst)]	0.041	0.051
Reaction rate on a similar weight basis	[mmols methyl acetate formed/min/(g of GT catalyst)]	0.7	0.56
Turnover frequency	[1/min]	0.458	0.548

Since these supported catalysts offer a great improvement in reaction rates with greater surface area, it greatly confirms the presumption of significant sulfur inclusion into the bulk of the catalyst where it is inaccessible to the reactants. The titration data showed 2-8% of the sulfur as accessible in the titration. Therefore, even the pyrolyzed catalysts' reaction rate would be in the same order of

magnitude as the supported catalysts if all of the sulfonic acid groups were accessible. If those TOF are compared with the best case bulk GT catalyst from above (the GT2:1K gives an initial TOF of 0.088/min) we see 5-6 time increase in specific rates as the GT catalysts is supported.

With either of these supports, it has not been specifically shown these supported catalysts is as stable as the bulk catalysts. However the mesoporous carbon is known to be stable under these conditions [43] and SBA-15 has had significant progress made in protecting it from the hot water [39]. Therefore, it is conceivable that the addition of the GT component would not adversely affect the hydrothermal stability of the supported catalyst.

5. Conclusion

This material is an extension of the colloidal material we made previously and with further addition of glucose, it becomes a heterogeneous acid catalyst. This provides greater advantageous in processability than a colloid as it is easier to separate and reuse than a colloid. This application of the Maillard reaction in a new way allows for a more hydrothermally stable connection of the sulfonic acid group to be produced in an easy method. We showed that even with minimal optimization, the new carbon catalysts retain sulfur better and have more consistent catalyst activity than similar catalysts in literature. The best catalyst from a sulfur stability standpoint was the catalysts made with sodium hydroxide

while the best catalysts for activity were the ones made from potassium hydroxide. Both had relatively low activities due to the embedded sulfonic acid groups that were inaccessible to the reactants. We explored ways to increase the limited surface area by supporting the GT material on SBA-15 and mesoporous carbon nanoparticles. These two gave good results on a similar sulfur basis. Either may have the hydrothermal stability required for biorenewable processing. This new way of creating a hydrothermally stable solid acid catalyst provides a good start into a broad group of materials that can have applications in several fields that require hydrothermally stable supports and active groups.

6. Acknowledgements

The authors would like to acknowledge NSF Award number EEC-0813570 for generously supporting this work. Purchase of the Perkin Elmer 2100 Series II CHN/S analyzer used to obtain results included in this publication was supported in part by the National Science Foundation under Grant No. DBI 9413969. We wish to thank ISU Chemical Instrumentation Facility staff members Stephen Veysey for training and assistance pertaining to the PE 2100 CHN/S elemental analysis. Keith Fritzsching developed the coding for transferring ACD NMR chemical shifts into MatLab. The authors would like to acknowledge Karl Aldreks that worked on the project. Jim Anderegg graciously ran and expertly helped interpret the XPS results. Any opinions, findings, and

conclusions, or recommendations expressed herein are those of the authors and do not necessarily reflect the views of the National Science Foundation.

References

1. Liang, X. and J. Yang, *Synthesis of a Novel Carbon Based Strong Acid Catalyst Through Hydrothermal Carbonization.* Catal. Lett., 2009. **132**(3-4): p. 460-463.
2. Rappold, T.A. and K.S. Lackner, *Large scale disposal of waste sulfur: From sulfide fuels to sulfate sequestration.* Energy, 2010. **35**(3): p. 1368-1380.
3. Kitano, M., et al., *Preparation of a Sulfonated Porous Carbon Catalyst with High Specific Surface Area.* Catal. Lett., 2009. **131**(1-2): p. 242-249.
4. Johnson, R., et al., *Engineering of Carbon Materials Produced from the Maillard Reaction to Produce a Colloid.* Carbon *Submitted,* 2014.
5. Peng, L., et al., *Preparation of sulfonated ordered mesoporous carbon and its use for the esterification of fatty acids.* Catalysis Today, 2010. **150**(1-2): p. 140-146.
6. Luque, R., et al., *Microwave-assisted preparation of amides using a stable and reusable mesoporous carbonaceous solid acid.* Green Chem., 2009. **11**(4): p. 459-461.
7. Luque, R., et al., *Glycerol transformations on polysaccharide derived mesoporous materials.* Appl. Catal., B, 2008. **82**(3-4): p. 157-162.
8. Hara, M., *Biodiesel Production by Amorphous Carbon Bearing SO3H, COOH and Phenolic OH Groups, a Solid Bronsted Acid Catalyst.* Top. Catal., 2010. **53**(11-12): p. 805-810.

9. Luque, R. and J.H. Clark, *Water-tolerant Ru-Starbon materials for the hydrogenation of organic acids in aqueous ethanol.* Catal. Commun., 2010. **11**(10): p. 928-931.

10. Xing, R., et al., *Active solid acid catalysts prepared by sulfonation of carbonization-controlled mesoporous carbon materials.* Microporous and Mesoporous Materials, 2007. **105**(1-2): p. 41-48.

11. Suganuma, S., et al., *Hydrolysis of cellulose by amorphous carbon bearing SO3H, COOH, and OH groups.* Journal of the American Chemical Society, 2008. **130**(38): p. 12787-12793.

12. Kitano, M., et al., *Adsorption-Enhanced Hydrolysis of β-1,4-Glucan on Graphene-Based Amorphous Carbon Bearing SO3H, COOH, and OH Groups.* Langmuir, 2009. **25**(9): p. 5068-5075.

13. Tang, Y., et al., *Bifunctional mesoporous organic-inorganic hybrid silica for combined one-step hydrogenation/esterification.* Appl. Catal., A, 2010. **375**(2): p. 310-317.

14. Miao, S. and B.H. Shanks, *Esterification of biomass pyrolysis model acids over sulfonic acid-functionalized mesoporous silicas.* Applied Catalysis A: General, 2009. **359**(1-2): p. 113-120.

15. Brown, R.C., *Biorenewable Resources: Engineering New Products from Agriculture*. 2003: Blackwell Publishing.

16. Akbar, J., et al., *Kinetics and mechanism of thermal degradation of pentose- and hexose-based carbohydrate polymers.* Carbohydrate Polymers, 2012. **90**(3): p. 1386-1393.

17. Yaylayan, V.A. and A. Keyhani, *Carbohydrate and Amino Acid Degradation Pathways in L-Methionine/D-[13C] Glucose Model Systems.* J. Agric. Food Chem., 2001. **49**(2): p. 800-803.

18. Adams, A., et al., *Characterization of Model Melanoidins by the Thermal Degradation Profile.* J. Agric. Food Chem., 2003. **51**(15): p. 4338-4343.

19. Clark, J.H., et al., *Catalytic performance of carbonaceous materials in the esterification of succinic acid.* Catalysis Communications, 2008. **9**(8): p. 1709-1714.

20. Budarin Vitaly, L., et al., *Versatile mesoporous carbonaceous materials for acid catalysis.* Chem Commun (Camb), 2007(6): p. 634-6.

21. Budarin, V., et al., *Towards a bio-based industry: benign catalytic esterifications of succinic acid in the presence of water.* Chem. - Eur. J., 2007. **13**(24): p. 6914-6919.

22. Hara, M., et al., *Sulfonated incompletely carbonized glucose as strong Bronsted acid catalyst.* Stud. Surf. Sci. Catal., 2007. **172**(Science and Technology in Catalysis 2006): p. 405-408.

23. Suganuma, S., et al., *Synthesis and acid catalysis of cellulose-derived carbon-based solid acid.* Solid State Sciences, 2010. **12**(6): p. 1029-1034.

24. Mo, X., et al., *Activation and deactivation characteristics of sulfonated carbon catalysts.* J. Catal., 2008. **254**(2): p. 332-338.

25. Radovic, L.R. and F. Rodriguez-Reinoso, *Carbon materials in catalysis.* Chem. Phys. Carbon, 1997. **25**: p. 243-358.

26. Mo, X., et al., *A Novel Sulfonated Carbon Composite Solid Acid Catalyst for Biodiesel Synthesis.* Catal. Lett., 2008. **123**(1-2): p. 1-6.

27. Hara, M., et al., *A Carbon Material as a Strong Protonic Acid.* Angewandte Chemie International Edition, 2004. **43**(22): p. 2955-2958.

28. Titirici, M.-M., A. Thomas, and M. Antonietti, *Back in the black: Hydrothermal carbonization of plant material as an efficient chemical process to treat the CO2 problem?* New J. Chem., 2007. **31**(6): p. 787-789.

29. Sevilla, M. and A.B. Fuertes, *Chemical and structural properties of carbonaceous products obtained by hydrothermal carbonization of saccharides.* Chem. - Eur. J., 2009. **15**(16): p. 4195-4203.

30. Li, M., W. Li, and S. Liu, *Control of the morphology and chemical properties of carbon spheres prepared from glucose by a hydrothermal method.* J. Mater. Res., 2012. **27**(8): p. 1117-1123.

31. Anderson, J., et al., *Chemical Structure and Hydrothermal Deactivation of Moderate-Temperature Carbon Materials with Acidic SO_3H Sites.* Carbon *Submitted*, 2014.

32. Johnson, R.L., et al., *Spectrally edited 2D 13C13C NMR spectra without diagonal ridge for characterizing 13C-enriched low-temperature carbon materials.* J. Magn. Reson., 2013. **234**: p. 112-124.

33. Anderson, J., et al., *Model Sulfonic Acid Compounds: Probing the Relative Sulfur-Carbon Bond Strength.* Applied Catalysts A *Submitted*, 2014.

34. Fang, X. and K. Schmidt-Rohr, *Alkyl and Other Major Structures in 13C-Labeled Glucose-Glycine Melanoidins Identified by Solid-State Nuclear Magnetic Resonance.* Journal of Agricultural and Food Chemistry, 2010. **59**(2): p. 481-490.

35. Fang, X. and K. Schmidt-Rohr, *Fate of the Amino Acid in Glucose-Glycine Melanoidins Investigated by Solid-State Nuclear Magnetic Resonance (NMR).* J. Agric. Food Chem., 2009. **57**(22): p. 10701-10711.

36. Maillard, L.C., *Action of Amino Acids on Sugars. Formation of Melanoidins in a Methodical Way.* Compt. rend., 1912. **154**: p. 66-8.

37. Hodge, J.E., *Dehydrated Foods, Chemistry of Browning Reactions in Model Systems.* Journal of Agricultural and Food Chemistry, 1953. **1**(15): p. 928-943.

38. Ames, J.M., R.G. Bailey, and J. Mann, *Analysis of furanone, pyranone, and new heterocyclic colored compounds from sugar-glycine model Maillard systems.* J Agric Food Chem, 1999. **47**(2): p. 438-43.

39. Pham, H.N., et al., *Improved Hydrothermal Stability of Mesoporous Oxides for Reactions in the Aqueous Phase.* Angewandte Chemie International Edition, 2012. **51**(52): p. 13163-13167.

40. Johnson, R.L. and K. Schmidt-Rohr, *Quantitative Solid-State 13C NMR with Signal Enhancement by Multiple Cross Polarization.* Journal of Magnetic Resonance, (0).

41. Torri, C., et al., *Preliminary investigation on the production of fuels and bio-char from Chlamydomonas reinhardtii biomass residue after bio-hydrogen production.* Bioresource Technology, 2011. **102**(18): p. 8707-8713.

42. Takagaki, A., et al., *Esterification of higher fatty acids by a novel strong solid acid.* Catalysis Today, 2006. **116**(2): p. 157-161.

43. Mesa, M., L. Hoyos, and L. Sierra, *Effect of the porosity and hydrothermal stability of SBA-16 type mesoporous silica on the characteristics of their carbon replicas.* Stud. Surf. Sci. Catal., 2008. **174A**(Zeolites and Related Materials): p. 361-364.

CHAPTER 5.

HYDROTHERMALLY SYNTHESIZED GT AS A HYDROTHERMALLY STABLE SOLID-ACID CATALYST

A paper to be submitted to Carbon

Jason M Anderson, Robert L Johnson, Klaus Friedel, Annette Trunschke, Robert Schlögl, Klaus Schmidt-Rohr, Brent H Shanks

Abstract

From previous research the Maillard reaction was successfully used to create hydrothermally stable carbon catalysts through pyrolysis synthesis. The Maillard reaction was used to create a new catalyst through a hydrothermal synthesis. The combination of glucose and taurine in a hydrothermal synthesis creates a solid that retains the sulfur-from the active group-even better than through pyrolysis synthesis. The synthesis temperatures ranged from 200-300ºC and it was found that the most stable catalysts were synthesized at 250ºC. The catalytic activity seemed insensitive to differences in the changes of the glucose to taurine ratio from 1:1 to 2:1 at the 250ºC synthesis. At the 200ºC synthesis temperature, the activity is not stable through the hydrothermal testing and at the 300ºC synthesis temperature; the sulfur retention is not as stable as the catalysts synthesized at 250ºC.

1. Introduction

New chemical synthesis especially focused on sustainability are needed in today's world [1]. Hydrothermal carbon is a hot topic in literature [2, 3]. It is a resurgence of interest in an old process [4]. The fundamentals of hydrothermal carbon are fairly well studied [5, 6]. Hydrothermal carbon interests researchers and industry alike with its relatively mild processing conditions (typically 160-220ºC with abundant biomass [7-10]) versus pyrolysis [11-13]. Hydrothermal carbon material has various precursors [10, 14-16] but glucose remains the most well studied [9]. The degradation pathways for glucose are well understood and begin to describe the resulting material [17-19]. Studies have gone further to describe the resulting physical and chemical structure [20]. Hydrothermal carbon remains a promising avenue toward more sustainable chemical synthesis.

Hydrothermal carbons have several different applications [14, 21-30] through surface modifications [31] and physical modifications [32]. Typical literature suggestions include adsorption [33-39], separation [40], stationary phases[41, 42], and water purification [16, 43]. Hydrothermal carbon may also be conductive depending on synthesis [44]. Therefore the electronic potential has also been explored and it has been suggested hydrothermal carbons may play a role in electro chemistry [45] and energy research[46-50]. Specific research has been focused with supercapacitors [51], fuel cells [52, 53], and electrodes [54-56].

Since hydrothermal carbon has such wide applications, it may be able to help make chemical synthesis more sustainable.

The hydrothermal materials can be tailored via a number of different methods, therefore they are also interesting materials for applications as solid catalysts. The straightforward synthesis method lends them towards industrial production and use. While these materials do not have extreme surface areas like activated carbons, the limited surface area can be overcome through templating [57]. Various supports and reactions schemes have been used-for example Clark's group used expanded starch and esterified succinic acid [22, 58]. Since the hydrothermal spheres' surface can be tailored via hydrophilic [31] or hydrophobic[59] coupling agents, adjustments can be made to encourage a wide variety of reactions. Because of their flexible chemical nature, facile synthesis, and renewable chemical precursors, hydrothermal materials are interesting as use as solid catalysts.

As the research in bio-based feedstocks increases, so does the need for heterogeneous catalysts that are stable and active in the aqueous phase. The common materials used for catalysts supports: alumina, silica, and zeolites degrade rapidly under hydrothermal conditions [22, 60, 61]. Carbon supports are the logical choice for hydrothermal stability and researchers have reported this hydrothermal stability [62, 63]. Hydrothermally synthesized catalysts can help

fill this need for hydrothermally stable catalysts because they are intuitively stable since the conditions that form it create a stable insoluble material.

This work focused on sulfonated carbons because of their applications as a solid acid catalyst. Previous research has created a various varieties of sulfonated carbon catalysts and variously tested those catalysts for their stability [64, 65]. Some were chosen to and systematically tested for stability to determine differences between the carbons [10, 20, 64, 66, 67]. It was shown that overall these materials could not handle the harshness of 160°C liquid water for several cycles however significant strides were made in characterizing these difficult carbons [20]. Further research was done to probe the immediate chemical nature of the active site with model compounds [68]. It was found that the carbons nearby the carbon linking the sulfur group to the backbone must be alkane to ensure the most hydrothermal stability. Therefore a new synthesis method must be used to create hydrothermally stable carbon catalysts.

From unrelated research a unique synthesis method was developed to create these alkane linkages desired in the catalyst [69, 70]. This has led to more hydrothermally stable carbon catalysts. This material was all pyrolyzed material and we set out to develop a hydrothermal method to create the stable acid catalysts in a different method. Previous research was undecided about the fate of the carbon linkage on the amine functionalized group-some thought it would break apart[71]-however our research has shown that the functionality largely

remains intact and catalytically active. Other research in this area pointed to heteroatom addition being possible-hydrothermal carbons have been researched before with nitrogen doping [72] and even with nitrogen and sulfur doping [73]. Sulfur doped carbon has been researched for waste metal removal [33], sulfur removal of crude oil [33, 34, 74], and fuel cells [75]. However, analysis is limited on the hydrothermal stability and the catalytic properties of these materials.

In this research the GT colloid is expanded on to be a useful catalyst with a different synthesis. At an even molar ratio, the resulting catalyst forms as a colloid resulting in poor handling characteristics versus those typically inherent of industrially used heterogeneous catalyst. A new synthesis method for this interesting group of carbons is developed in this research and new analysis done with NMR and TPD. These characterizations show the differences between the carbons and which ratio imparts the most hydrothermal stability and catalytic activity.

2. Experimental

2.1 Materials and synthesis

Glucose, 1,4 dioxane, glacial acetic acid, and methanol was purchased from Fisher Scientific. Taurine was purchased from Sigma-Aldrich. Glucose enriched with ^{13}C was purchased from Cambridge Isotopes. All chemical were used with without further purification. Nitrogen gas (99.995%) was purchased from Airgas.

2.2 Synthesis

The materials were prepared in batches based on 2 grams of glucose. The typical combination was 2 grams of glucose with 1.4 grams of taurine or about a 1:1 molar ratio of the two reactants. This was placed in a glass sleeve with 20 mL of DI water to solubilize the solution. This was placed in a stainless steel Parr reactor. The head space was pressurized with 500 psi of nitrogen and heated at 10ºC/min until the desired temperature was reached. The solution was stirred at 200 RPM. It was held at the desired temperature for 18.5 hours then cooled to room temperature. The resulting solid was filtered, dried, and crushed to yield the final catalyst. For the material with a 2:1 molar ratio of glucose to taurine, the amount of taurine was halved to end up at the desired ratio.

The catalysts were designated via the nomenclature as follows: the ratio of the glucose to taurine mixture with the letters GT, the synthesis temperature, and then if it has been subjected to hydrothermal treatment a W with a number of times (1-3). For example, sample 1:1GT250W2 is the 1:1 glucose to taurine ratio synthesized at 250ºC and it has been subjected to two rounds of hydrothermal treatment.

3. Characterization

3.1 Catalyst Characterization

The carbon materials were imaged with scanning electron microscopy (FEI Quanta-250 SEM), to compare their morphologies with carbons generated by similar synthesis methods in the literature. Surface area characterization was performed by physisorption using nitrogen as the adsorbing gas in a Micromeritics ASAP 2020. Analysis of the materials with a Perkin Elmer STA 6000 Simultaneous Thermal Analyzer (TGA), using a ramp rate of 10°C in flowing air was performed. Elemental analysis results for the carbon, hydrogen, nitrogen, and sulfur (CHNS) were acquired using a PE 2100 Series II combustion analyzer (Perkin Elmer Inc., Waltham, MA). The chemical state of sulfur was analyzed using a Physical Electronics 550 Multitechnique XPS system employing a standard Al electron source. The samples were run at 10^{-9} Torr and mounted on double-sided tape. Charging was corrected for by adjusting the carbon peak to 284 eV. Ion exchange titrations were run to measure the number of acidic groups present on the sulfonated carbons. The number of sulfonic acid ($R\text{-}SO_3H$), carboxylic acid, and phenolic hydroxyl groups were measured using the titration method reported by Suganuma et al. [76]. One back titration measured all the acidic functionalities. It used a known amount of NaOH (~0.1g) dissolved in water with the catalytic material using sufficient time (~2 hours) to exchange the sodium ions with all the hydrogen ions from the acid groups on the material.

Then, a simple acid titration using sodium hydroxide was used to exchange the acidic protons from the sulfonic acid and carboxylic acid groups. It was assumed that the sulfonic acid, carboxylic acid, and hydroxyl groups were measured. The sulfonic acid groups were measured by the elemental analysis of the sulfur and the other groups were determined by subtraction of these measurements.

3.2 TPD characterization

Temperature-programmed desorption was carried out in a home-built setup equipped with a gas chromatograph (Varian CP-4900 Micro-GC) and a mass spectrometer (Pfeiffer Omnistar) for on-line product analysis. Typically, 20 mg of sample were loaded into a fixed-bed quartz reactor, which was placed in a self-constructed furnace with an isothermal zone of 4 cm at the upper temperature limit. Weakly adsorbed water was effectively removed within 1 h at 373 K in a He stream passed at a flow rate of 25 mL/min. Experiments were started thereafter by linearly heating the reactor at 5 K/min to 1323 K. This temperature was maintained for 30 min before cooling to room temperature. The basis for the samples is compared as a per carbon mass of the remaining sample after the experiment.

3.3 Reaction Testing

Esterification of acetic acid with methanol was used as the test reaction since it is sensitive to the number of acid sites and their pK_a [77]. The reactions were performed at 40 °C in an Alltech 10 mL reactor vial loaded (total volume 7

mL) with methanol (6 M)and acetic acid (3 M) in dioxane with the respective sulfonated carbon (10 mg). The reactions were run at low conversions (<5%) to allow comparison of initial rates. The reaction testing was performed at a range of stir rates so that it was determined that no mass transfer effects occurred as long as the stirring rate was above 200 rpm. The reaction product samples were analyzed on an Agilent 7890A GC equipped with a flame ionization detector. The sulfonated carbons were compared in terms of activity per mass of catalyst giving the units of mmol acetate formed min^{-1} (g catalyst)$^{-1}$.

As developed in previous research [20], After full characterization of the fresh materials, the catalysts were subjected to three individual hydrothermal treatments. Each treatment placed the catalyst material (0.5 g), stirred in DI water (7 mL) at 160°C, in the Alltech reactors under autogenous pressure for 24 hours. The solid material was filtered and washed extensively (generally about 0.5 L of DI water) until the filtrate was clear and colorless. The hydrothermally treated sulfonated carbon was then characterized and subjected to two more hydrothermal treatments following the same protocol as the first treatment.

4. Results and discussion

The materials made by this method are similar to the previous pyrolyzed material from the Maillard reaction of glucose and taurine [70]. The materials seem to have minimal changes throughout the hydrothermal testings from the elemental analysis (see Figure 1). The 200ºC synthesis has the least amount of

carbon while the three other synthesis have similar weight percent of carbon. The sulfur and the nitrogen are in a one to one ratio as expected from the Maillard reaction. This indicated the linker was able to be retained during synthesis. Increasing the glucose to taurine ratio from 1:1 to 2:1 decreased the amount of sulfur by little over a half. Unexpectedly, the 200ºC material also had low weight percent of sulfur. Indicative of the strength of the linker on the nitrogen bond, as the sulfur is removed from the solid, so too is the nitrogen. The material is also relatively hydrogen poor which indicates aromaticity. It is this aromaticity that gives the carbon framework hydrothermal stability while the sulfonic acid must be attached via aliphatic linkages to ensure its hydrothermal stability.

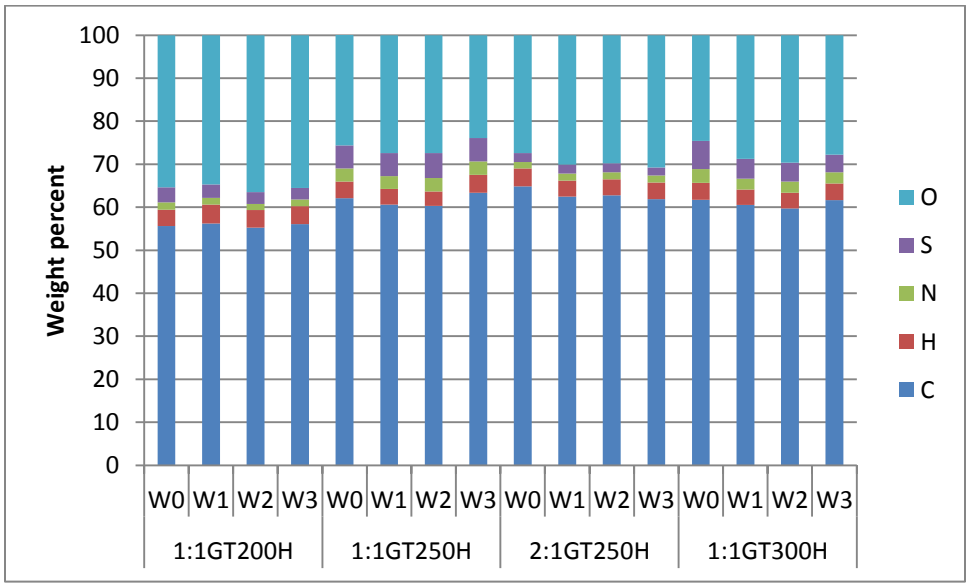

Figure 1. Elemental analysis data. There are four sets of four included with the W0 data points representing the initial samples and the W1-W3 represent the number of hydrothermal tests the sample was subjected to.

The BET data showed all these catalysts had <0.1m^2/g. From this data, sulfur must be incorporated into the bulk of the catalyst. Titrations were done and showed that only ~10% of the sulfur groups were accessible via titration. This means these catalysts would enjoy better reaction rates if they were better dispersed. Previous research showed the supported catalysts enjoyed greater activity on a similar sulfur basis than this bulk GT material [70]. This lower dispersal explains the lower reaction rates that previous materials made in literature. The SEM data (see Figure 2) shows these catalysts to look more like glass shards like particles from incompletely pyrolyzed glucose [20, 70, 78, 79] rather than spheres from hydrothermally formed glucose [20, 31, 80]. It was only necessary to include one SEM picture because all the other catalysts formed similar type particles.

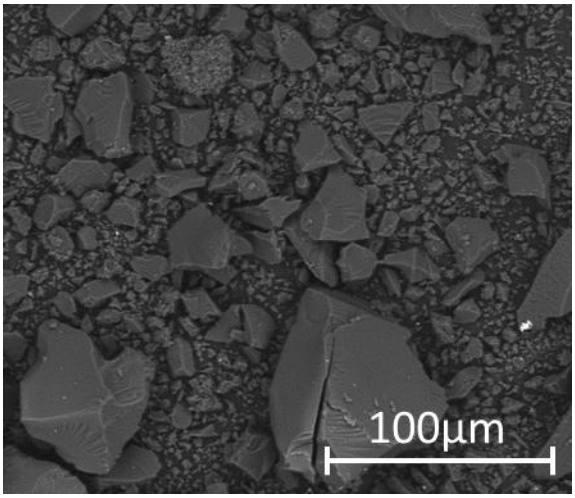

Figure 2. SEM of the 1:1GT200 sample. This is a representative picture as all had similar type particles.

4.1 Temperature-programmed desorption

Profiles of the volatile compounds detected in the course of TPD experiments contain valuable information about the structural state of a carbonaceous compound, the extent of functionalization and the thermal stability of heteroatomic species present in the material. Since the carbonyl group in glucose reacts with the amino group in taurine via the Maillard reaction, it can be expected that sulfonic acid entities are attached to the hydrothermally formed carbon via N-substituted alkyl chains. In view of this, SO_2 and NH_3 were monitored in addition to CO, CO_2, CH_4, H_2 and H_2O. Quantitative information gives a deeper insight into the thermally induced processes taking place. For this reason all aforementioned compounds, excepting hydrogen and water, were previously calibrated and analysed by means of gas chromatography.

Figure 4a shows the evolution of CO_2 of the hydrothermally prepared carbons. Three characteristic regions are observed in 1:1GT200. The broad region between 150°C and 460°C is an overlap of the contributions arising from the decomposition of carboxylic acids (~260°C) and anhydrides (~380°C). The most thermally stable species are lactones, whose presence is reflected by the shoulder centred at 560°C [81]. As observed by the CO_2 evolution of 1:1GT250, increasing the synthesis temperature to 250°C leads to almost a complete disappearance of the carboxylic acid feature and a significant reduction of the anhydride/lactone functionalities. According to the calculated amounts summarized in Table 1, 70% less CO_2 evolves from 1:1GT250 compared to 1:1GT200. An increase in the synthesis temperature from 250°C to 300°C decreases the CO_2 contribution by around 60%. This is associated with the gradual increase of condensation between the building blocks of the carbonaceous structure as further evidenced by the steady decrease in CH_4 formation (Figure 4g) from initially 1698 to finally 1003 µmol/g. Methane is linked to the thermal decomposition of aliphatic, hydroaromatic and aryl methyl groups [82, 83]. As expected from the nature of glucose, which is used as the carbon precursor, less CH_4 evolves with increasing aromatic character of the carbon. In addition, the methane peak maximum is shifted by 60°C to 570K for 1:1GT300, whereas the remaining samples have this feature located at 510°C. Interestingly, the amount of CO_2 detected during the TPD of 2:1GT250 is comparable to 1:1GT250. Evidently, doubling the molar ratio of glucose to taurine has no significant effect

on the CO_2 evolution. This agrees with the elemental analysis data which saw little increase in the amount C between the two samples. However, the amount of methane behaves in the same manner as the molar ratio changes, indicating that this volatile compound is in fact linked to the carbon precursor.

Table 1. Specific molar concentrations of CO, CO_2, CH_4, SO_2 and NH_3 derived from TPD experiments.

Sample	**CO [µmol·g_C^{-1}]**	**CO_2 [µmol·g_C^{-1}]**	**CH_4 [µmol·g_C^{-1}]**	**SO_2 [µmol·g_C^{-1}]**	**NH_3 [µmol·g_C^{-1}]**	**n_{SO2}:n_{NH3}**	**S:N ratio (CHNS)**
1:1GT200	24250	11484	1698	3548	3356	1.06	0.92
1:1GT250	10469	3496	1306	1676	2854	0.59	0.76
2:1GT250	18710	3580	2734	1206	1437	0.84	0.62
1:1GT300	8613	1445	1003	1888	3433	0.55	0.89

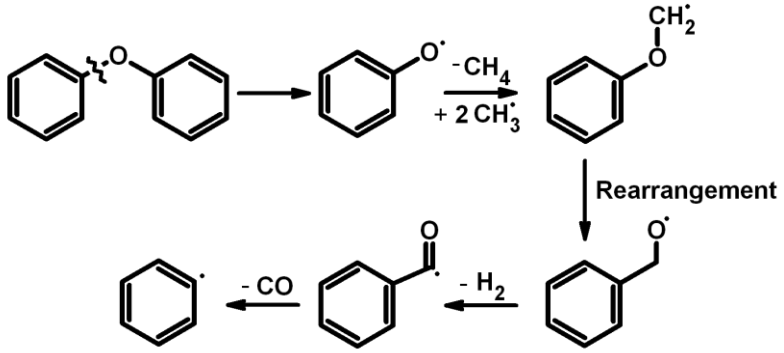

Figure 3. Carbon monoxide, hydrogen and methane formation during pyrolysis.

As can be observed in Figure 4a, CO profiles exhibit a broad feature with a peak maximum located at around 550°C. Oxygenated species present in carbon nanostructures decomposing to CO are anhydrides, phenols, ethers and carbonyl

groups [81]. In view of their structural and binding state differences, these functionalities are thermally decomposed over a wide temperature range. However, the building units of hydrothermally prepared carbons are prone to undergo further condensation reactions, which among others is reflected in the formation of CO. A plausible pathway as depicted in Figure 3 for this temperature regime involves the cleavage of diaryl ethers yielding phenoxy radicals that upon reacting with methyl radicals and subsequent methane elimination lead to methoxyphenyl radicals. After rearrangement and dehydrogenation, a benzene radical is formed via CO elimination [84, 85]. Growth of the aromatic system can subsequently proceed by recombination of benzene radicals. CO amounts calculated from the TPD profiles drastically drop from 24250 to 8613 µmol/g_{carbon} for the carbons synthesized with a glucose-to-taurine ratio of 1:1. Since the thermal decomposition of oxygen functional groups involved in the formation of carbon monoxide begins at values beyond the highest applied synthesis temperature of 300°C, the determined inversely proportional trend between CO evolution and synthesis temperature indicates that a significant amount of CO arises from the carbonization processes, reflecting different degrees of condensation between 1:1GT200, 1:1GT250 and 1:1GT300. Hence, merely a small fraction of CO is associated with the thermal depletion of O-containing surface species. These findings are in line with the CO amounts obtained for 1:1GT250 and 2:1GT250. Doubling the glucose-to-taurine ratio

increases the amount of released CO from 10469 to 18710 µmol/g_c, which corresponds to a rise of about 80%.

According to Figure 3, H_2 is formed prior to the decarbonylation step, which is in line with the lower temperature onset of hydrogen evolution in comparison to that of the CO formation. Figure 4f displays a shoulder at 550°C that has been attributed to this process. The main phenomenon represented by the peak located at around 750°C is related to the H_2 evolution as a consequence of polyaromatic condensation reactions taking place in various superimposed steps. This leads to the formation of large polycondensed units that represent the main building blocks of the pyrolyzed carbon [3]. No dehydrogenation is observed above 900°C, which is related to the homolytical cleavage of C-H bonds. From this it can be inferred that most likely only a negligible fraction of sites is saturated after heat treatment.

Evolution of H_2O is related to various processes. This is reflected in Figure 4e by the presence of several peaks. Weakly adsorbed water has no contribution since the samples were dried at 100°C for 1 h prior to the TPD experiments. The shoulder observed below 300°C can be attributed not only to the dehydration of adjacent carboxylic acid species yielding cyclic anhydrides [6], but also to condensation of neighbouring sulfonic acid entities. Glucose as the carbon precursor consists of five OH groups distributed over six carbon atoms. For this reason the hydrothermal carbons are expected to contain a large number

of phenolic species. As has been stated by Jakab et. al [86], the thermal decomposition of OH groups leads to the formation of pyrolysis water over a broad temperature range clearly evidenced by the H_2O evolution between 400°C and 800°C.

In addition to the changes observed to which the hydrothermal carbons are subjected in the course of the TPD experiments, the success of functionalization is evidenced by the evolution of sulfur dioxide (Figure 4c) and ammonia (Figure 4d). Sulfonic acid entities decompose to SO_2 at temperatures below 200°C, whereas the onset of NH_3 evolution is nearly 300°C. This finding implies that the thermal stability of the linker between the carbon backbone and the SO_3H groups is significantly more than the acid entities themselves. Furthermore, less sulfonic acid groups are attached to the hydrothermal carbon when increasing the synthesis temperature from 200°C to 250°C. This is evidenced by the reduction of SO_2 from 3548 to 1676 $\mu mol/g_{carbon}$. Interestingly, the effect is reversed when the temperature is further increased to 300°C. Ammonia behaves in a similar manner. However, more ammonia evolves from sample 1:1GT300 than 1:1GT200, meaning that 300°C is beneficial for the Maillard reaction, but at the same time detrimental for the attached sulfonic acid groups. Increasing the glucose-to-taurine ratio from 1:1 to 2:1 leads to a lower specific molar concentration of sulfonic acid groups. As evidenced by the arrows in Figure 4c, all the samples exhibit the presence of two or even three types of sulfonic acid groups differing in terms of thermal stability. A more heterogeneous character is

observed in the case of ammonia, since 1:1GT200 and 2:1GT250 show one broad peak centred below 400°C, whereas 1:1GT250 releases ammonia in two different stages with the second maximum located below 600°C. In the case of 1:1GT300 three different steps are observed. The calculated SO_2-to-NH_3 molar ratio of 1:1GT200 corresponds to the expected nitrogen and sulfur molarity found in taurine. On the contrary, all other samples exhibit values below 1. This is in contrast to the results from elemental analysis where all of the samples contained more nitrogen on a molar basis than sulfur. The trend from the TPD and the CHNS also do not agree on which sample is the lowest revealing the limitation of this analysis. It only measures the volitilized molecules and does not analyse the whole solid like elemental analysis does under oxidizing conditions. A reason for the low S:N ratio might be the degradation of sulfonic acid groups under hydrothermal conditions. While the linker remains attached to the carbonaceous framework, the acid group is decomposed. Furthermore, NH_3 may be formed in the course of the hydrothermal synthesis via deamination of taurine. Under these conditions, ammonia is capable of reacting with oxygen functional groups available in the carbon compound leading to nitrogen species that decompose to ammonia during the TPD experiments. To a certain extent, both processes could overlap, enhancing the deamination route with increasing temperature.

The TPD experiments were excellent at confirming with NMR with the carbons that are detected. However, only about 50% of the material was volatilized which leaves a considerable amount not analysed by this method. This

is especially evident with the discussion on the S:N molar ratio. The main conclusion from the TPD analysis was the linker we put on the carbon is stronger than the desired sulfonic acid. Since the linkage is stronger than the sulfonic acid, the hydrothermal instability inherent from these materials is not from the addition of the linker itself.

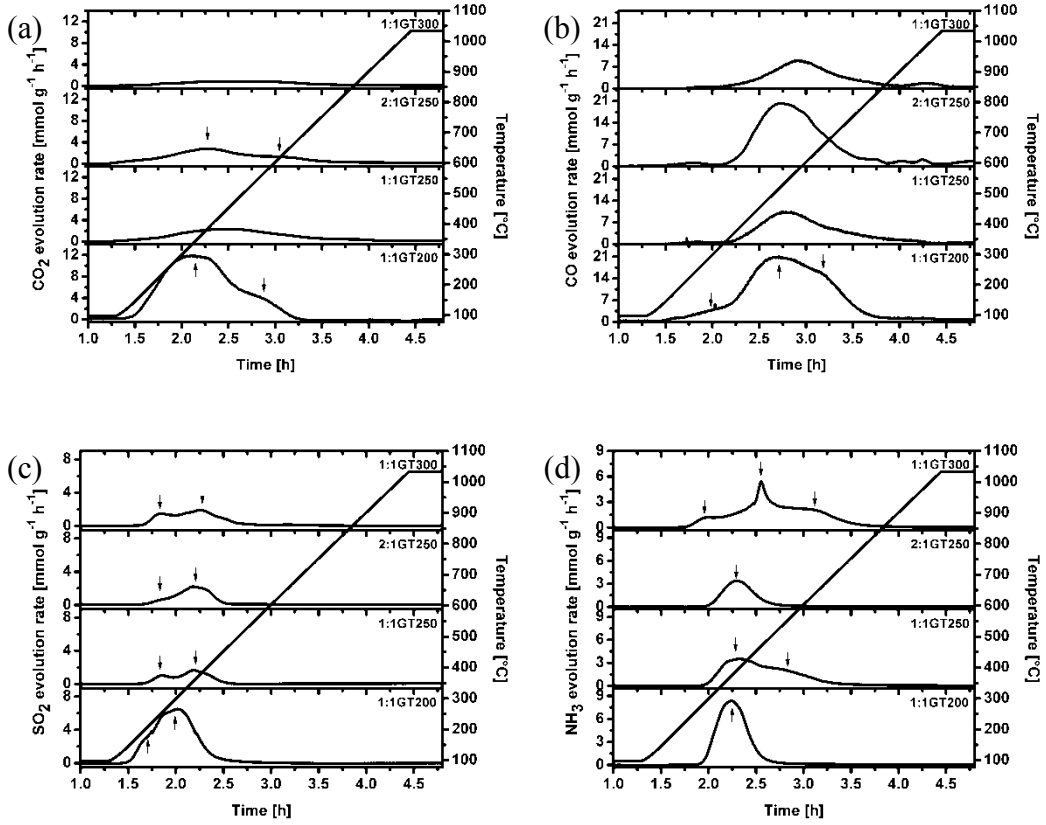

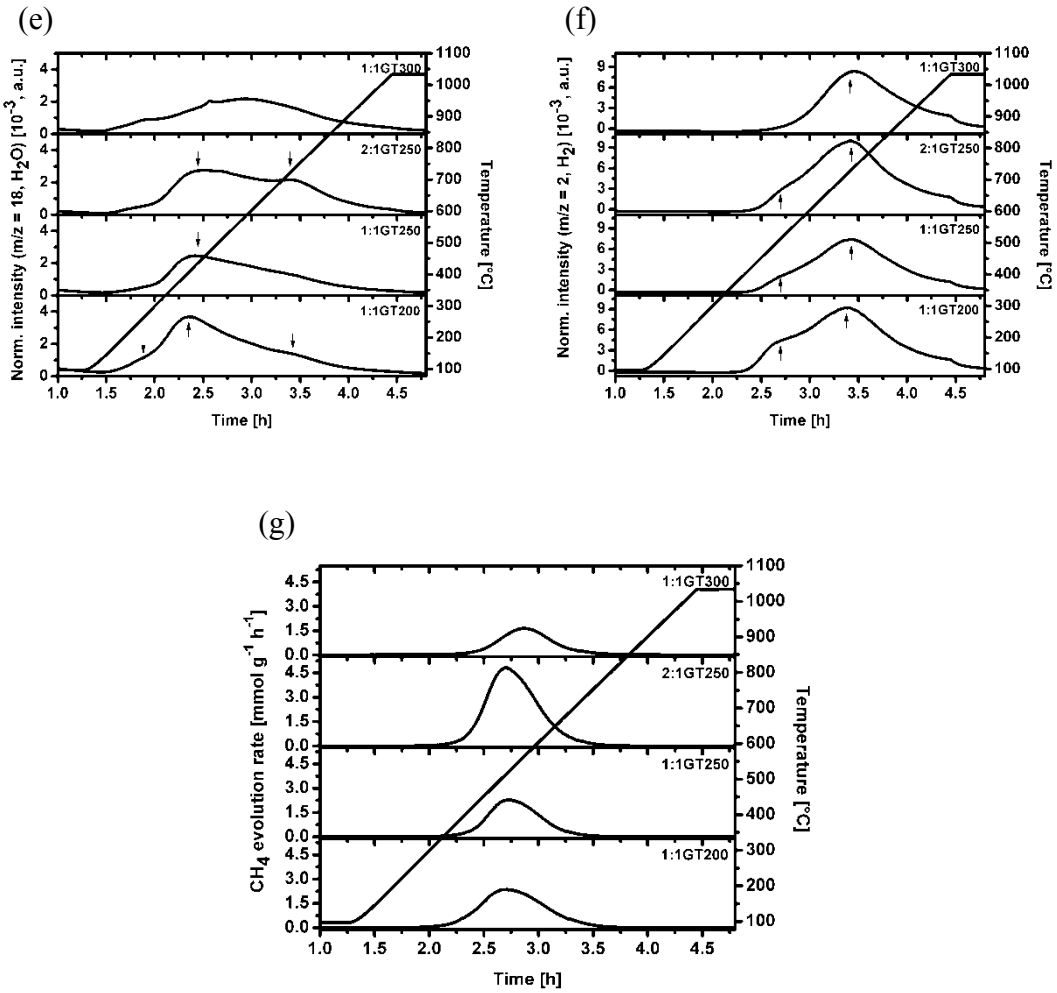

Figure 4: Evolution of (a) CO_2, (b) CO, (c) SO_2, (d) NH_3, (e) H_2O, (f) H_2, and (g) CH_4 during TPD analysis of aminoethanesulfonic acid containing hydrothermal carbons.

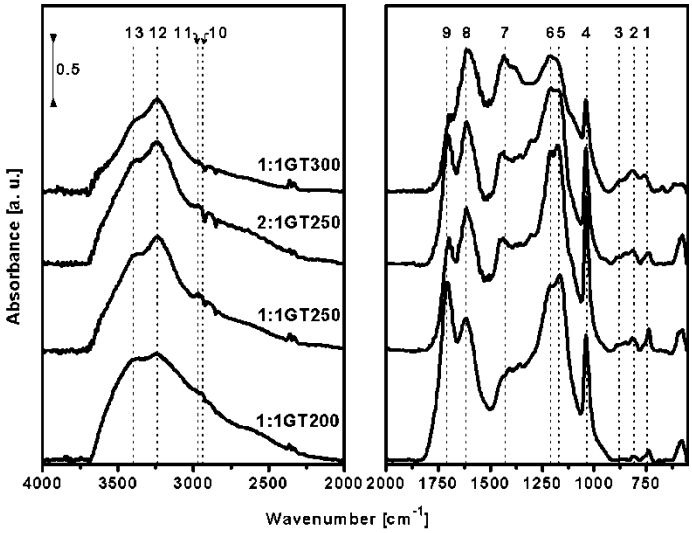

Figure 4: ATR-FTIR spectra of sulfonated hydrothermal carbons

4.2 ATR-FTIR

Spectroscopic methods are suitable for monitoring the hydrothermal transformation of glucose into carbonaceous products and the concomitant modification with sulfonic acid entities via the Maillard reaction. Figure 5 displays the ATR-FTIR spectra of the obtained hydrothermal carbons. The presence of aromatic domains is confirmed by the band located at 1614 cm^{-1} (**8**), which corresponds to the C=C stretching vibrations of aromatic and furanic rings. This is further evidenced by the feature at 1436 cm^{-1} (**7**), attributed to C-C stretching vibrations of aromatic rings [87]. Aromatic C-H out-of-plane bending vibrations encountered in the region between 900 and 700 cm^{-1} (**1**-**3**) underpin the aromatic character of the samples [80]. As expected from the structure of glucose and from the results derived from the TPD experiments, phenolic species exist on the carbon compounds as suggested by the broad band at 3400 cm^{-1} (**13**) [87].

The presence of further oxygen functional groups can be confirmed by the feature at 1703 cm^{-1} (**9**), which are ascribable to C=O vibrations of carbonyl, quinone, ester or carboxyl moieties [80]. Differences in terms of carbonization degree can be encountered among 1:1GT200, 1:1GT250, and 1:1GT300. The relative intensity between the C=O (**9**) and the aromatic C=C stretching vibrations (**8**) clearly decreases with increasing synthesis temperature, suggesting a higher extent of condensation between the building blocks constituting the carbonaceous compounds accompanied by a loss of oxygen. These observations are in line with the changes observed for CH_4 and CO during TPD. Sulfonic acid groups give rise to the bands at 1209 cm^{-1} (**6**) and 1039 cm^{-1} (**4**) that can be respectively attributed to the antisymmetric and symmetric SO_3 stretching vibrations [88]. Bands at 3241 cm^{-1} (**12**) and 1174 cm^{-1} (**5**) indicate the presence of nitrogen species as expected from the employment of taurine during hydrothermal synthesis. The former is ascribable to N-H stretching vibrations of aliphatic secondary amines, whereas the latter may be assigned to C-N stretching vibrations of secondary amines [89]. The carbon materials also possess aliphatic structures as evidenced by the bands in the region between 3000 and 2900 cm^{-1} (**10, 11**), which arise from the stretching vibrations of aliphatic C-H bonds [80]. These findings suggest the covalent binding of the sulfonic acid entities to the carbon backbone through an alkyl linker, underpinning the success of the Maillard reaction for functionalization purposes.

4.3 Solid-State NMR

Solid state NMR of the 2:1GT250, shows the presence of strong methylene peaks which are consistent with what would be expected from this Maillard reaction synthesis. Additionally, many of the spectral features present in rigorously characterized GT materials produced in dry pyrolysis are present [70]. Although this spectra was collected using standard cross polarization, it is very likely that the aromatic groups are underrepresenting with respect to the methylene groups. The dipolar dephased spectra which removed most of the signal of carbons that have strong 1H-13C dipolar coupling, shows that the resonance between 40-60ppm are likely CH and CH_2's and the peaks below 30 ppm are predominantly CH_3's, which is consistent with levulinic and acetic acid derived from glucose breakdown. Further, little dephasing in the aromatic region is consistent with the aromatic units being heavily substituted and therefore crosslinked. The aromatic section of the spectra (150-100 ppm) looks very similar to the typical hydrothermal material [20] with the qualifier of the overrepresentation of the carbon attached to hydrogen. Not observed is the strong levulinic acid ketone and CH_3 peaks observed with hydrothermal char produced from carbohydrate only feedstocks. This is an indication that the reactions of pure glucose during hydrothermal carbonization have been significantly altered when starting with a glucose-taurine mixture. These results can also be seen by the SEM picture showing amorphous shards morphology rather than the expected spherical morphology.

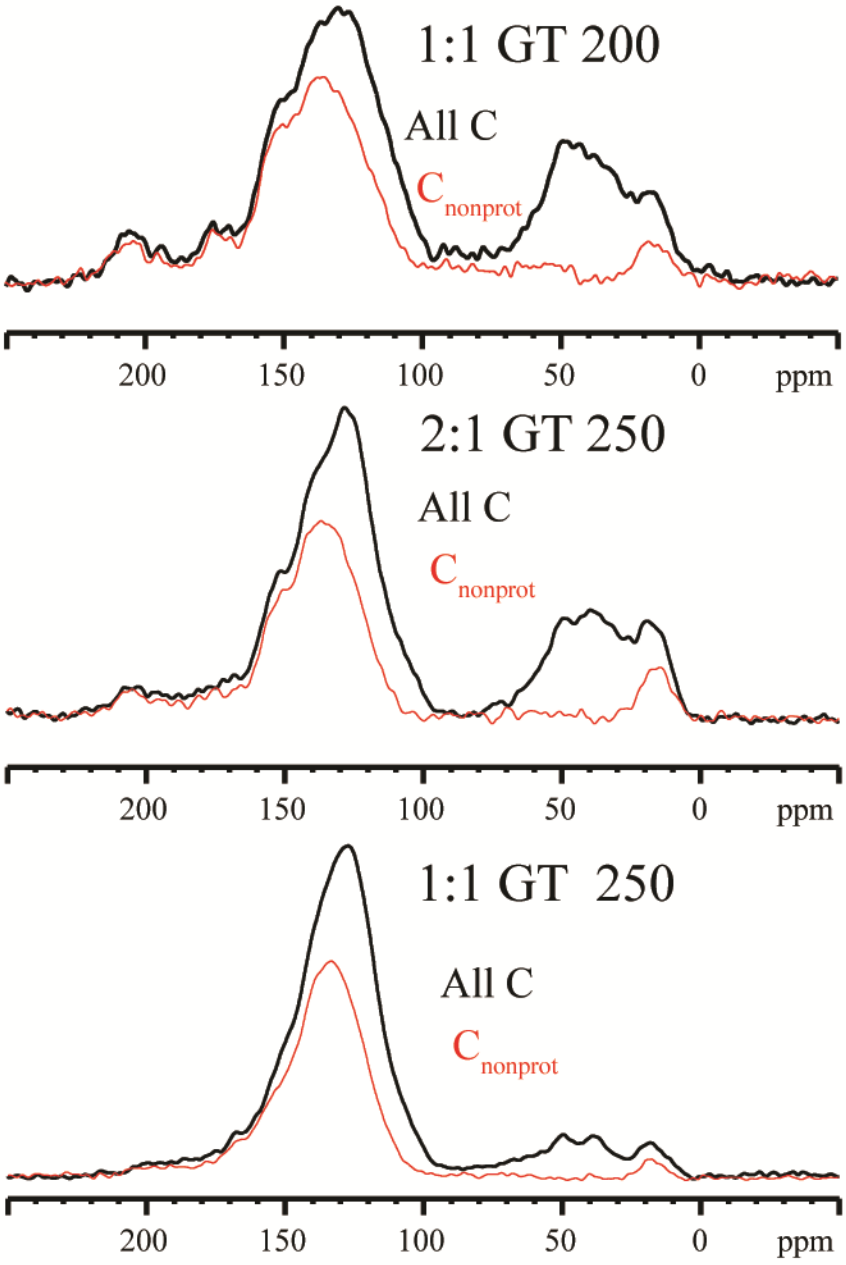

Figure 6. NMR of three of the hydrothermal GT catalysts. The upper line is total carbons, the lower line in each of the spectra is all the non-protonated carbons.

4.4 Sulfur Retention and Reaction Rates

This synthesis method created the most stable catalysts yet of the glucose taurine materials. The sulfur loss of the 1:1GT300H was the most significant at 36% while the 1:1GT200H lost 23% and the 2:1GT250H lost 12%. The 1:1GT250H was the best at retaining the sulfur throughout the hydrothermal treatments as it had no significant loss of sulfur. Especially when compared to the previous sulfonated carbon materials in literature [20, 70], these catalysts are excellent at retaining their sulfur.

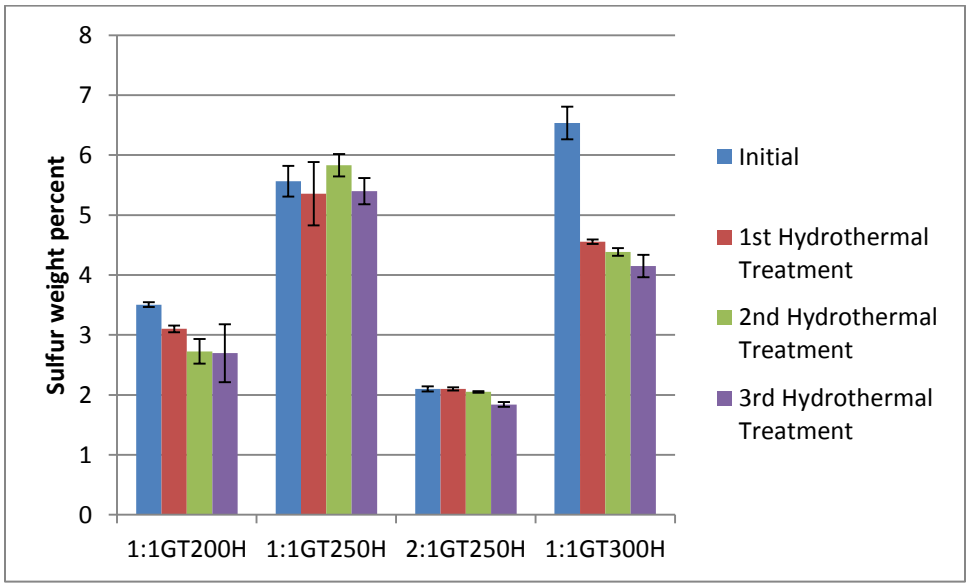

Figure 7. The sulfur retention data for the hydrothermal GT catalysts. Each hydrothermal test was 24 hours in 160ºC liquid water.

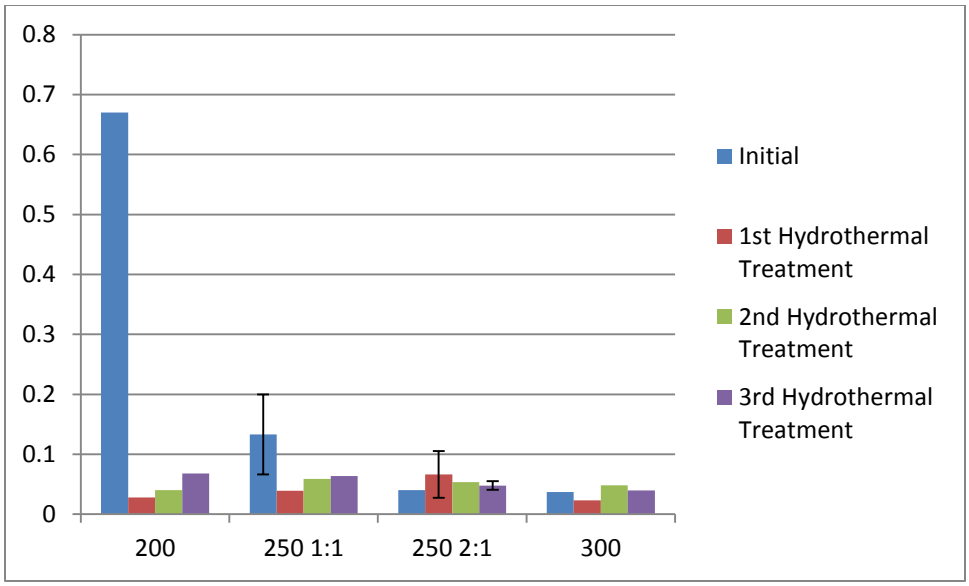

Figure 8. Reaction rate date for the hydrothermal GT catalysts throughout the hydrothermal treatments.

The reaction rate data tells the story of stability for the materials synthesized above 200ºC. As a result of the low activity of most of the catalysts, the data are noisy. In those materials, the differences in the activity are insignificant throughout each of the hydrothermal tests. There were not significant reaction differences in the 1:1GT250 sample and the 2:1GT250 sample. As seen from elemental analysis, the sulfur was a little over twice as in the sample not enriched in glucose but this did not significantly affect the reaction rates. As shown with previous research, supporting this material on high surface area material promotes better reaction rates which also could be used for this material as well.

5. Conclusion

These materials represent an additional improvement in the glucose taurine catalysts. They have excellent retention of their initial sulfur loading. The 1:1GT250 retained its sulfur the best with only an insignificant amount of loss. The reaction rates are stable throughout the hydrothermal treatments provided the synthesis temperature is high enough. Extensive characterization showed the material to be a successful use of the Maillard reaction to create a sulfonic acid attached with an alkyl linker through a nitrogen atom. The characterization also showed higher temperatures increased the incorporation of the nitrogen atom into the matrix at the cost of sulfur incorporation. This suggests a maximum effective synthesis temperature to incorporate both the linker and the sulfonic acid. The Maillard reaction, as studied for this catalyst synthesis, is an effective way to incorporate the linkages needed for a hydrothermally stable acid catalyst.

6. Acknowledgements

The authors would like to acknowledge NSF Award number EEC-0813570 for generously supporting this work. Purchase of the Perkin Elmer 2100 Series II CHN/S analyzer used to obtain results included in this publication was supported in part by the National Science Foundation under Grant No. DBI 9413969. We wish to thank ISU Chemical Instrumentation Facility staff members Stephen Veysey for training and assistance pertaining to the PE 2100 CHN/S elemental analysis. The authors would like to acknowledge

undergraduates that worked on the project: Ashley Leitner, Scott Nauert, and Karl Alderks. Jim Anderegg graciously ran and expertly helped interpret the XPS results. Any opinions, findings, and conclusions, or recommendations expressed herein are those of the authors and do not necessarily reflect the views of the National Science Foundation.

References

1. Corma, A., S. Iborra, and A. Velty, *Chemical Routes for the Transformation of Biomass into Chemicals.* Chem. Rev. (Washington, DC, U. S.), 2007. **107**(6): p. 2411-2502.
2. Liang, C., Z. Li, and S. Dai, *Mesoporous carbon materials: synthesis and modification.* Angew. Chem., Int. Ed., 2008. **47**(20): p. 3696-3717.
3. Wildgoose, G.G., C.E. Banks, and R.G. Compton, *Metal nanoparticles and related materials supported on carbon nanotubes. Methods and applications.* Small, 2006. **2**(2): p. 182-193.
4. Bergius, F., *The formation of coal.* Naturwissenschaften, 1928. **16**: p. 1-10.
5. Baccile, N., et al., *Structural Characterization of Hydrothermal Carbon Spheres by Advanced Solid-State MAS 13C NMR Investigations.* The Journal of Physical Chemistry C, 2009. **113**(22): p. 9644-9654.
6. Sevilla, M. and A.B. Fuertes, *Chemical and structural properties of carbonaceous products obtained by hydrothermal carbonization of saccharides.* Chem. - Eur. J., 2009. **15**(16): p. 4195-4203.
7. Titirici, M.-M., A. Thomas, and M. Antonietti, *Back in the black: Hydrothermal carbonization of plant material as an efficient chemical process to treat the CO2 problem?* New J. Chem., 2007. **31**(6): p. 787-789.

8. Falco, C., et al., *Hydrothermal Carbons from Hemicellulose-Derived Aqueous Hydrolysis Products as Electrode Materials for Supercapacitors.* ChemSusChem, 2013. **6**(2): p. 374-382.

9. Titirici, M.-M., M. Antonietti, and N. Baccile, *Hydrothermal carbon from biomass: a comparison of the local structure from poly- to monosaccharides and pentoses/hexoses.* Green Chem., 2008. **10**(11): p. 1204-1212.

10. Titirici, M.-M. and M. Antonietti, *Chemistry and materials options of sustainable carbon materials made by hydrothermal carbonization.* Chem. Soc. Rev., 2010. **39**(1): p. 103-116.

11. Thess, A., et al., *Crystalline ropes of metallic carbon nanotubes.* Science (Washington, D. C.), 1996. **273**(5274): p. 483-487.

12. Gherghel, L., et al., *Pyrolysis in the Mesophase: A Chemist's Approach toward Preparing Carbon Nano- and Microparticles.* J. Am. Chem. Soc., 2002. **124**(44): p. 13130-13138.

13. Jose-Yacaman, M., et al., *Catalytic growth of carbon microtubules with fullerene structure.* Appl. Phys. Lett., 1993. **62**(6): p. 657-9.

14. White Robin, J., et al., *Tuneable porous carbonaceous materials from renewable resources.* Chemical Society Reviews, 2009. **38**(12): p. 3401-18.

15. Hu, B., et al., *Functional carbonaceous materials from hydrothermal carbonization of biomass: an effective chemical process.* Dalton Trans., 2008(40): p. 5414-5423.

16. Hu, B., et al., *Engineering Carbon Materials from the Hydrothermal Carbonization Process of Biomass.* Adv. Mater. (Weinheim, Ger.), 2010. **22**(7): p. 813-828.

17. Lourvanij, K. and G.L. Rorrer, *Reactions of aqueous glucose solutions over solid-acid Y-zeolite catalyst at 110-160 °C.* Ind. Eng. Chem. Res., 1993. **32**(1): p. 11-19.

18. Antal, M.J., Jr., W.S.L. Mok, and G.N. Richards, *Kinetic studies of the reactions of ketoses and aldoses in water at high temperature. 1. Mechanism of formation of 5-(hydroxymethyl)-2-furaldehyde from D-fructose and sucrose.* Carbohydr. Res., 1990. **199**(1): p. 91-109.

19. Lourvanij, K. and G.L. Rorrer, *Dehydration of glucose to organic acids in microporous pillared clay catalysts.* Appl. Catal., A, 1994. **109**(1): p. 147-65.

20. Anderson, J., et al., *Chemical Structure and Hydrothermal Deactivation of Moderate-Temperature Carbon Materials with Acidic SO_3H Sites.* Carbon *Submitted*, 2014.

21. Yao, C., et al., *Hydrothermal Dehydration of Aqueous Fructose Solutions in a Closed System.* J. Phys. Chem. C, 2007. **111**(42): p. 15141-15145.

22. Budarin, V.L., et al., *Tunable mesoporous materials optimized for aqueous phase esterifications.* Green Chem., 2007. **9**(9): p. 992-995.

23. Budarin Vitaly, L., et al., *Versatile mesoporous carbonaceous materials for acid catalysis.* Chem Commun (Camb), 2007(6): p. 634-6.

24. Cui, X., M. Antonietti, and S.-H. Yu, *Structural Effects of Iron Oxide Nanoparticles and Iron Ions on the Hydrothermal Carbonization of Starch and Rice Carbohydrates.* Small, 2006. **2**(6): p. 756-759.

25. Yu, S.-H., et al., *From starch to metal/carbon hybrid nanostructures: Hydrothermal metal-catalyzed carbonization.* Adv. Mater. (Weinheim, Ger.), 2004. **16**(18): p. 1636-1640.

26. Tusi, M.M., et al., *Preparation of PtRu/carbon hybrids by hydrothermal carbonization process.* Mater. Res. (Sao Carlos, Braz.), 2007. **10**(2): p. 171-175.

27. Sevilla, M., G. Lota, and A.B. Fuertes, *Saccharide-based graphitic carbon nanocoils as supports for PtRu nanoparticles for methanol electrooxidation.* J. Power Sources, 2007. **171**(2): p. 546-551.

28. Qian, Z., et al., *Manufacture of chemical products by continuous fermentation*. 2010, (Toray Industries, Inc., Japan). Application: JP JP. p. 32pp.

29. Sun, X., J. Liu, and Y. Li, *Use of carbonaceous polysaccharide microspheres as templates for fabricating metal oxide hollow spheres.* Chem. - Eur. J., 2006. **12**(7): p. 2039-2047.

30. Zhu, K., K. Egeblad, and C.H. Christensen, *Mesoporous carbon prepared from carbohydrate as hard template for hierarchical zeolites.* Eur. J. Inorg. Chem., 2007(25): p. 3955-3960.

31. Demir-Cakan, R., et al., *Carboxylate-Rich Carbonaceous Materials via One-Step Hydrothermal Carbonization of Glucose in the Presence of Acrylic Acid.* Chemistry of Materials, 2009. **21**(3): p. 484-490.

32. Falco, C., N. Baccile, and M.-M. Titirici, *Morphological and structural differences between glucose, cellulose and lignocellulosic biomass derived hydrothermal carbons.* Green Chem., 2011. **13**(11): p. 3273-3281.

33. Petit, C., et al., *The effect of oxidation on the surface chemistry of sulfur-containing carbons and their arsine adsorption capacity.* Carbon, 2010. **48**(6): p. 1779-1787.

34. Seredych, M., M. Khine, and T.J. Bandosz, *Enhancement in Dibenzothiophene Reactive Adsorption from Liquid Fuel via Incorporation of Sulfur Heteroatoms into the Nanoporous Carbon Matrix.* ChemSusChem, 2011. **4**(1): p. 139-147.

35. Wu, Z. and D. Zhao, *Ordered mesoporous materials as adsorbents.* Chem. Commun. (Cambridge, U. K.), 2011. **47**(12): p. 3332-3338.

36. Jia, Y.F., B. Xiao, and K.M. Thomas, *Adsorption of Metal Ions on Nitrogen Surface Functional Groups in Activated Carbons.* Langmuir, 2002. **18**(2): p. 470-478.

37. Hulicova, D., M. Kodama, and H. Hatori, *Electrochemical Performance of Nitrogen-Enriched Carbons in Aqueous and Non-Aqueous Supercapacitors.* Chemistry of Materials, 2006. **18**(9): p. 2318-2326.

38. Shao, Y., et al., *Nitrogen-doped carbon nanostructures and their composites as catalytic materials for proton exchange membrane fuel cell.* Applied Catalysis B: Environmental, 2008. **79**(1): p. 89-99.

39. Plaza, M.G., et al., *CO2 capture by adsorption with nitrogen enriched carbons.* Fuel, 2007. **86**(14): p. 2204-2212.

40. Steel, K.M. and W.J. Koros, *Investigation of porosity of carbon materials and related effects on gas separation properties.* Carbon, 2003. **41**(2): p. 253-266.

41. West, C., C. Elfakir, and M. Lafosse, *Porous graphitic carbon: A versatile stationary phase for liquid chromatography.* J. Chromatogr. A, 2010. **1217**(19): p. 3201-3216.

42. Muna, G.W., et al., *Electrochemically modulated liquid chromatography using a boron-doped diamond particle stationary phase.* J. Chromatogr. A, 2008. **1210**(2): p. 154-159.

43. Kubo, S., et al., *Porous Carbohydrate-Based Materials via Hard Templating.* ChemSusChem, 2010. **3**(2): p. 188-194.

44. Paraknowitsch, J.P., et al., *Ionic Liquids as Precursors for Nitrogen-Doped Graphitic Carbon.* Adv. Mater. (Weinheim, Ger.), 2010. **22**(1): p. 87-92.

45. Zhao, Q., Z. Gan, and Q. Zhuang, *Electrochemical sensors based on carbon nanotubes.* Electroanalysis, 2002. **14**(23): p. 1609-1613.

46. Iijima, T., K. Suzuki, and Y. Matsuda, *Electrodic characteristics of various carbon materials for lithium rechargeable batteries.* Synth. Met., 1995. **73**(1): p. 9-20.

47. Wu, Y.P., et al., *Effects of doped sulfur on electrochemical performance of carbon anode.* J. Power Sources, 2002. **108**(1-2): p. 245-249.

48. Lota, G., et al., *Effect of nitrogen in carbon electrode on the supercapacitor performance.* Chem. Phys. Lett., 2005. **404**(1-3): p. 53-58.

49. Frackowiak, E., *Carbon materials for supercapacitor application.* Phys. Chem. Chem. Phys., 2007. **9**(15): p. 1774-1785.

50. Demir, C.R., et al., *Hydrothermal carbon spheres containing silicon nanoparticles: synthesis and lithium storage performance.* Chem. Commun. (Cambridge, U. K.), 2008(32): p. 3759-3761.

51. Hulicova, D., M. Kodama, and H. Hatori, *Electrochemical Performance of Nitrogen-Enriched Carbons in Aqueous and Non-Aqueous Supercapacitors.* Chem. Mater., 2006. **18**(9): p. 2318-2326.

52. Paraknowitsch, J.P., A. Thomas, and M. Antonietti, *Carbon Colloids Prepared by Hydrothermal Carbonization as Efficient Fuel for Indirect Carbon Fuel Cells.* Chem. Mater., 2009. **21**(7): p. 1170-1172.

53. Shao, Y., et al., *Nitrogen-doped carbon nanostructures and their composites as catalytic materials for proton exchange membrane fuel cell.* Appl. Catal., B, 2008. **79**(1): p. 89-99.

54. Gong, K., et al., *Nitrogen-Doped Carbon Nanotube Arrays with High Electrocatalytic Activity for Oxygen Reduction.* Science (Washington, DC, U. S.), 2009. **323**(5915): p. 760-764.

55. Kurak, K.A. and A.B. Anderson, *Nitrogen-Treated Graphite and Oxygen Electroreduction on Pyridinic Edge Sites.* J. Phys. Chem. C, 2009. **113**(16): p. 6730-6734.

56. Matter, P.H., et al., *Oxygen Reduction Reaction Catalysts Prepared from Acetonitrile Pyrolysis over Alumina-Supported Metal Particles.* J. Phys. Chem. B, 2006. **110**(37): p. 18374-18384.

57. Kubo, S., et al., *Ordered Carbohydrate-Derived Porous Carbons.* Chemistry of Materials, 2011. **23**(22): p. 4882-4885.

58. Clark, J.H., et al., *Catalytic performance of carbonaceous materials in the esterification of succinic acid.* Catalysis Communications, 2008. **9**(8): p. 1709-1714.

59. Titirici, M.-M., A. Thomas, and M. Antonietti, *Aminated hydrophilic ordered mesoporous carbons.* J. Mater. Chem., 2007. **17**(32): p. 3412-3418.

60. Xing, R., et al., *Active solid acid catalysts prepared by sulfonation of carbonization-controlled mesoporous carbon materials.* Microporous and Mesoporous Materials, 2007. **105**(1-2): p. 41-48.

61. Petrus, L., E.J. Stamhuis, and G.E.H. Joosten, *Thermal deactivation of strong-acid ion-exchange resins in water.* Industrial & Engineering Chemistry Product Research and Development, 1981. **20**(2): p. 366-371.

62. Zaiku, X.i.e., Xie, and Z. Xie, *An overview of recent development in composite catalysts from porous materials for various reactions and processes.* International journal of molecular sciences, 2010. **11**(5): p. 2152.

63. Onda, A., T. Ochi, and K. Yanagisawa, *Hydrolysis of Cellulose Selectively into Glucose Over Sulfonated Activated-Carbon Catalyst Under Hydrothermal Conditions.* Top. Catal., 2009. **52**(6-7): p. 801-807.

64. Hara, M., *Biodiesel Production by Amorphous Carbon Bearing SO3H, COOH and Phenolic OH Groups, a Solid Bronsted Acid Catalyst.* Top. Catal., 2010. **53**(11-12): p. 805-810.

65. Suganuma, S., et al., *Hydrolysis of cellulose by amorphous carbon bearing SO3H, COOH, and OH groups.* Journal of the American Chemical Society, 2008. **130**(38): p. 12787-12793.

66. Toda, M., et al., *Green chemistry: Biodiesel made with sugar catalyst.* Nature, 2005. **438**(7065): p. 178-178.

67. Hara, M., et al., *Sulfonated incompletely carbonized glucose as strong Bronsted acid catalyst.* Stud. Surf. Sci. Catal., 2007. **172**(Science and Technology in Catalysis 2006): p. 405-408.

68. Anderson, J., et al., *Model Sulfonic Acid Compounds: Probing the Relative Sulfur-Carbon Bond Strength.* Applied Catalysts A *Submitted*, 2014.

69. Johnson, R., et al., *Engineering of Carbon Materials Produced from the Maillard Reaction to Produce a Colloid.* Carbon *Submitted*, 2014.

70. Anderson, J., et al., *Engineering of Carbon Materials Produced from the Maillard Reaction to Produce Hydrothermally Stable Acid Catalyst.* Carbon *Submitted*, 2014.

71. Ames, J.M., R.G. Bailey, and J. Mann, *Analysis of furanone, pyranone, and new heterocyclic colored compounds from sugar-glycine model Maillard systems.* J Agric Food Chem, 1999. **47**(2): p. 438-43.

72. Baccile, N., et al., *Structural Insights on Nitrogen-Containing Hydrothermal Carbon Using Solid-State Magic Angle Spinning 13C and 15N Nuclear Magnetic Resonance.* The Journal of Physical Chemistry C, 2011. **115**(18): p. 8976-8982.

73. Wohlgemuth, S.-A., et al., *A one-pot hydrothermal synthesis of tunable dual heteroatom-doped carbon microspheres.* Green Chem., 2012. **14**(3): p. 741-749.

74. Paraknowitsch, J.P., A. Thomas, and J. Schmidt, *Microporous sulfur-doped carbon from thienyl-based polymer network precursors.* Chem. Commun. (Cambridge, U. K.), 2011. **47**(29): p. 8283-8285.

75. Choi, C.H., S.H. Park, and S.I. Woo, *Heteroatom doped carbons prepared by the pyrolysis of bio-derived amino acids as highly active catalysts for oxygen electro-reduction reactions.* Green Chem., 2011. **13**(2): p. 406-412.

76. Suganuma, S., et al., *Synthesis and acid catalysis of cellulose-derived carbon-based solid acid.* Solid State Sciences, 2010. **12**(6): p. 1029-1034.

77. Miao, S. and B.H. Shanks, *Esterification of biomass pyrolysis model acids over sulfonic acid-functionalized mesoporous silicas.* Applied Catalysis A: General, 2009. **359**(1-2): p. 113-120.

78. Torri, C., et al., *Preliminary investigation on the production of fuels and bio-char from Chlamydomonas reinhardtii biomass residue after bio-hydrogen production.* Bioresource Technology, 2011. **102**(18): p. 8707-8713.

79. Takagaki, A., et al., *Esterification of higher fatty acids by a novel strong solid acid.* Catalysis Today, 2006. **116**(2): p. 157-161.

80. Sevilla, M. and A.B. Fuertes, *The production of carbon materials by hydrothermal carbonization of cellulose.* Carbon, 2009. **47**(9): p. 2281-2289.

81. Figueiredo, J.L., et al., *Modification of the surface chemistry of activated carbons.* Carbon, 1999. **37**(9): p. 1379-1389.

82. Arenillas, A., F. Rubiera, and J.J. Pis, *Simultaneous thermogravimetric–mass spectrometric study on the pyrolysis behaviour of different rank coals.* Journal of Analytical and Applied Pyrolysis, 1999. **50**(1): p. 31-46.

83. *A comparative Tg-Ms study of the carbonization behavior of different pitches : Garcia, R. et al. Energy & Fuels, 2002, 16, (4), 935–943.* Fuel and Energy Abstracts, 2003. **44**(3): p. 147.

84. Hodek, W., J. Kirschstein, and K.-H. van Heek, *Reactions of oxygen containing structures in coal pyrolysis.* Fuel, 1991. **70**(3): p. 424-428.

85. Schlosberg, R.H., et al., *Pyrolysis studies of organic oxygenates: 3. High temperature rearrangement of aryl alkyl ethers.* Fuel, 1983. **62**(6): p. 690-694.

86. Jakab, E., F. Till, and G. Várhegyi, *Thermogravimetric-mass spectrometric study on the low temperature oxidation of coals.* Fuel Processing Technology, 1991. **28**(3): p. 221-238.

87. Brun, N., et al., *Hydrothermal synthesis of highly porous carbon monoliths from carbohydrates and phloroglucinol.* RSC Advances, 2013. **3**(38): p. 17088-17096.

88. Freire, P.T.C., F.E.A. Melo, and J. Mendes Filho, *Polarized Raman and Infrared Spectra of Taurine Crystals.* Journal of Raman Spectroscopy, 1996. **27**(7): p. 507-512.

89. Coates, J., *Interpretation of Infrared Spectra, A Practical Approach*, in *Encyclopedia of Analytical Chemistry*. 2006, John Wiley & Sons, Ltd.

CHAPTER 6.

GENERAL CONCLUSIONS AND FUTURE CONSIDERATIONS

The sulfonic acid catalyst has great potential for increased hydrothermal stability compared to traditional solid acid catalysts used in the petroleum industry. Several catalysts taken from literature were tested in harsher conditions -160ºC for 24 hours- than had been done by prior researchers. They turned out not to be as stable as previously thought. Therefore new catalysts were needed to develop catalysts that could be stable in hydrothermal conditions.

Next the catalyst active site was investigated via several model compounds that showed differences in their immediate chemical environment. They were tested at three different temperatures (100, 130, 160ºC) and time dependent samples were taken out (up to 24 hours). The compounds were identified via liquid NMR. This testing in hydrothermal conditions showed the important result that the linkage to the carbon backbone needs to be aliphatic rather than aromatic. The presumption in literature claimed aromatic nature would be better but we found evidence to the contrary. Therefore the catalyst that would be most hydrothermally stable would include aliphatic carbon connecting the sulfonic acid group to the backbone rather than the sulfonic acid directly bonded to aromatic carbons.

From unrelated research, we developed a method for a synthesis of the carbon with aliphatic sulfonic acid linkages. Using the Maillard reaction-typically avoided in biological research-we incorporated both more sulfonic acid

than previously possible and did so with a linker that was aliphatic. We showed that while there is considerable ways to go with this material, it can be made both in a dry or wet synthesis. It also can be placed on a high-surface area support to overcome the activity problems inherent with the bulk material. Since the National Science Foundation engineering research Center for Biorenewable Chemicals (CBiRC) is researching chemical transformations of sugar to chemicals. Reactions with sugar require condensed phase processing and CBiRC has identified hydrothermal stability as a barrier to overcome. With better knowledge of the fundamentals of sulfonated carbon catalysts, the transformations CBiRC wants with sugars transformed to biorenewable chemicals are possible.